Dino Emanuel Santos Matias

Human Neurons Derived from Induced Pluripotent Stem Cells: A Platform for Screening Compounds to Treat Gaucher's Disease and Parkinson's Disease

2020

Dino Emanuel Santos Matias

Human Neurons Derived from Induced Pluripotent Stem Cells: A Platform for Screening Compounds to Treat Gaucher's Disease and Parkinson's Disease

PhD Program in Mechanisms of Disease

and Regenerative Medicine

Work developed under the supervision of:

Prof. Doctor Gustavo Tiscornia

2020

Human Neurons Derived from Induced Pluripotent Stem Cells: A Platform for Screening Compounds to Treat Gaucher's Disease and Parkinson's Disease

Declaração de autoria de trabalho

Declaro ser o autor deste trabalho, que é inédito e original. Autores e trabalhos consultados estão devidamente citados no texto e constam da listagem de referências incluída.

.

This work has been performed at:

Centre for Biomedical Research, University of Algarve

CBMR Molecular and Regenerative Medicine Lab, University of Algarve

Departamento de Ciências Biomédicas e Medicina – Universidade do Algarve

Campus Gambelas, 8005-139 Faro, Portugal

This work was supported by National Portuguese funding through FCT – Fundação para a Ciência e a Tecnologia, scholarship PD/BD/52423/2013 and Genzyme Young Investigator Award 2012, with the title: Development of an induced pluripotent stem cell model of neuronopathic Gaucher's Disease for investigating mechanisms of pathogenesis and small molecule testing.

This page is intentionally left blank

Acknowledgements

I would like to thank Prof. Gustavo Tiscornia, for his support, teachings, adventures, and misadventures throughout these years. It has been a long journey, and honestly quite rough at times, but I wouldn´t have had it any other way. More than teaching me to think like a scientist, you´ve showed how to live like one, to persist even when it's too dark to see clearly, never to bow down, never surrender. May this be the beginning of a new chapter and, who knows, future collaborations. Thank you.

Quero agradecer ao Prof. José Belo e a toda a direção do Programa Doutoral pelo suporte e compreensão durante esta longa caminhada. Agradeço também à Universidade do Algarve e ao CBMR por me acolher durante estes anos.

À minha família, sem os quais não teria chegado aqui. Como dizia o velho poeta, "a minha mãe deu-me um coração para amar e meu pai uma terra pela que lutar". Obrigado por serem o meu porto seguro. Aos meus avós, a verdadeira encarnação do amor mais puro, obrigado por todo o carinho. À minha irmã que me atura desde o primeiro choro e pesar das diferenças está para mim incondicionalmente. Ao Ricardo pela presença, suporte e alegrias. E a ambos, por me darem as coisas mais preciosas da minha vida, os meus pequeninos, Diana e Simão.

To Rae, my dear, I have no words to thank you enough for all the support and love. For being there when I needed and when I didn´t. There are things to which the words of Men cannot yet truly describe. This journey would have been much harder without you. Thank you for everything.

Aos meus velhos amigos, Ariana e Prata, pelos anos e intimidade que não se dissipa pela distância ou ausência. Que assim seja, e que de cada vez que nos voltarmos a encontrar seja como se fosse ontem. Ao Titi, Janita e Maia, pelos longos anos de amizade. Por onde quer que a vida me leve estarão sempre comigo.

À minha família de Faro: Pedro, Vera e Mariano. Obrigado por me adotarem quando ainda não entendia nada do que diziam quando falavam mediquês, e por esta amizade que ainda recente já é tão velha.

Aos meus companheiros de armas: Gil, Om, Diogo, Ignasi, Susana M., Marta, Gonçalo, Daniel, Susana R., e ProRegeM. Obrigado por estarem a meu lado nos altos e baixos desta jornada.

Aos meus irmãos espalhados pelo mundo que tantos são e a quem tanto quero. Que sintam como vosso também este meu pequeno contributo para as ciências e para alumiar este nosso mundo.

A todos os cientistas do mundo que apesar das dificuldades financeiras e falta de reconhecimento continuam a dar o melhor de si e a desbravar o caminho do progresso.

A todos vós muito obrigado.

Fiat lux!

Resumo

A doença de Gaucher (*Gaucher disease* – GD) é a doença lisossomal com maior taxa incidência em todo o mundo (Mistry et al., 2017). As doenças de armazenamento lisossomal, são um grupo de doenças metabólicas hereditárias caracterizadas pela redução de atividade ao longo de uma via metabólica, levando à acumulação de um ou mais dos seus substratos, e consequente desregulação celular. GD é causada por níveis reduzidos de atividade da hidrolase β-glucocerebrosidase (GCase), o que pode ocorrer por mutações no centro ativo, alterações no processamento, no ativador ou nos transportadores. A doença transmite-se quase exclusivamente de por transmissão autossómica recessiva de mutações no gene da GCase, *GBA1*. Ainda que raro, alguns casos de GD causados por mutações no gene *PSAP*, que codifica para o cofator da GCase, Saposin C (Kang et al., 2018). Até à data, mais de 300 mutações *GBA1* foram descritas como causadoras de GD e, apesar da grande maioria poupar o centro ativo da enzima, tendem a alterar drasticamente a estrutura tridimensional, estabilidade e transporte da GCase (Dvir et al., 2003; Manoj Kumar Pandey, Rani, Zhang, Setchell, & Grabowski, 2012). Produção de GCase com uma estrutura tridimensional errada ativa o sistema de controlo de qualidade do reticulo endoplasmático que, através do uso de chaperones do sistema UPR (*Unfolded Protein Response*), tenta promover uma conformação correta. Após vários ciclos falhados de remodelação molecular, o UPR despoleta apoptose através da via mitocondrial (Bendikov-Bar & Horowitz, 2012; Grabowski, Zimran, & Ida, 2015).Para além da pressão exercida sob o Retículo Endoplasmático (ER), a baixa atividade da GCase leva a uma acumulação intralisossomal de substratos glucosilceramida (GlcCer) e glucosilsesfingosina (Awad et al., 2015; Choi et al., 2011). Apesar desta ser expressa ubiquamente, devido à sua natureza e função fisiológica com altos níveis de remodelação e atividade lisossomal, as células do sistema reticuloendotelial e neuronal são primordialmente afetadas. Nos macrófagos, GlcCer acumula-se em vesículas que ocupam grande parte do citoplasma, formando as características células de Gaucher, identificáveis por histologia, que mantêm um estado de inflamação sistémica constante (Hollak, van Weely, van Oers, & Aerts, 1994; Klein & Futerman, 2013). Neurónios, por outro lado, são especialmente sensíveis a baixos níveis de GCase devido à alta taxa de processamento de gangliósidos por processos associados à sinapse, entrando em apoptose e gerando um ciclo de inflamação e morte neuronal (Grabowski, 2008; Mencarelli & Martinez–Martinez,

2013). O modo como cada mutação ou genótipo afeta estes dois tipos celulares explica a panóplia de sintomas que são geralmente associados a GD e são comumente divididos em sintomas viscerais ou sistémicos que afetam fígado, baço, pulmões e ossos, e sintomas neurológicos, com afeção de áreas específicas do cérebro e sistema nervoso central.

Apesar de algumas mutações apresentarem um fenótipo predominantemente sistémico ou neurológico, a vasta maioria das mutações, não está diretamente associada a um padrão sintomático ou severidade. Atualmente, num contexto académico reconhece-se que a dispersão dos sintomas e sua severidade formam um gradiente, das formas neurológicas congénitas mais agudas até formas mais leves de envolvimento somático exclusivamente detetadas numa fase mais tardia de vida ou que não são detetadas de todo (Aureli et al., 2012). No contexto clínico, a sintomatologia é classificada em três tipos de acordo com as necessidades terapêuticas e prognóstico: tipo 1 (não neuropático); tipo 2 (neuropático agudo); e tipo 3 (neuropático crónico). As manifestações sistémicas mais comuns incluem inflamação generalizada, hepatomegalia, esplenomegalia, pancitopenia e osteoporose, e tendem a estar presentes em todos os tipos de GD ao passo que as manifestações neurológicas incluem espasticidade, nistagmo, défice cognitivo e neurodegeneração e manifestam-se nos tipos 2 e 3 (Butler, 2001; McNeill et al., 2012).GD tipo 1 é a forma mais frequente da doença, afetando mais de 90% dos pacientes, ao passo que o tipo 2 é a forma mais severa, apresentando um prognóstico muito reservado com uma degeneração neurológica rápida e acentuada, resultando numa esperança média de vida de 9 meses. O tipo 3 encontra-se entre o tipo 1 e 2 em termos de severidade, apresentando tanto sintomas viscerais como neurológicos crónicos (Ozlem Goker-Alpan et al., 2003).

Ainda que não haja cura para GD, existem presentemente várias alternativas de tratamento e gestão de sintomas, dependendo da sintomatologia e apresentação fenotípica da doença. O primeiro tratamento desenvolvido foi o transplante de medula óssea (*bone marrow transplantation* - BMT) através da transfusão de progenitores hematopoiéticos de dadores saudáveis. Se feito correta e precocemente, BMT pode prevenir tanto manifestações viscerais como neurológicas da doença, no entanto este efeito terapêutico é perdido com a idade (Platt & Jeyakumar, 2008). Para além disso BMT não tem efeito nas formas neuropatológicas mais agudas de GD tipo 2 pela rápida progressão e deterioração (Platt & Jeyakumar, 2008; Shawky & Elsayed, 2016). Durante vários anos, a única alternativa a BMT foi, a suplementação endovenosa de GCase, num sistema terapêutico de substituição enzimática (*enzyme replacement therapies* – ERT). Terapias ERT são ainda a primeira linha de tratamento de GD, com melhorias

como a marcação de GCase com resíduos de manose para facilitar a sua captação por macrófagos (Grabowski, 2008; McEachern et al., 2007). No entanto, apesar de aliviar a grande maioria dos sintomas sistémicos, uma vez que GCase não atravessa a barreira hematoencefálica, ERT não tem qualquer efeito nas manifestações neuronais da doença (R Kornfeld & Kornfeld, 1985). A classe de fármacos mais recente na prática clínica, aposta numa diminuição da acumulação de GlcCer através da inibição a montante da via catabólica, numa abordagem denominada terapia de redução de substrato (*substrate reduction therapy* - SRT). Esta abordagem tem foco na inibição da glucosilceramida sintetase, reduzindo a concentração intracelular dos seus produtos, glucose e ceramida (Rao Vunnam & Radin, 1980). Apesar de apresentarem um potencial terapêutico mais baixo do que ERT para sintomas viscerais, as terapias por SRT, ao serem baseadas em pequenas moléculas glicomiméticas são capazes de atravessar a barreira hematoencefálica e aliviar os sintomas neuronais. Contudo, apesar do baixo custo, os efeitos secundários e o baixo efeito terapêutico relegam SRT para uma segunda linha de tratamento.

Inspirados na terapia SRT, uma nova classe de fármacos tem vindo a ganhar a atenção da comunidade científica: chaperones farmacológicas (*pharmacological chaperones* – PC). Estes compostos atuam como inibidores reversíveis da GCase e, ligando-se ao centro ativo da enzima melhoram a sua conformação, ajudando-a a iludir o Sistema de Controlo de Qualidade do Retículo Endoplasmático, aumentando a quantidade de Gcase e permitindo que exerça a sua função com a capacidade hidrolítica remanescente.

Recentemente, investigação e desenvolvimento de novas abordagens para compensar ou suplementar défices de atividade de GCase no sistema nervoso central têm ganho novo fôlego devido a uma série de associações entre mutações em *GBA1* e desenvolvimento de patologias neurológicas degenerativas. Apesar de GD tipo 1 ser, por definição, ausente de qualquer manifestação neurológica ao longo dos anos, uma série de casos esporádicos de manifestações semelhantes à sintomatologia clássica da doença de Parkinson (PD) começaram a ser notadas. Apesar de inicialmente episódica, a incidência mais elevada de bradicinesia, demência, défice cognitivo, hiposmia e depressão levaram a que fossem feitos os primeiros estudos genéticos de associação ente PD e GD (Sidransky & Lopez, 2012; Yang, Lee, Lee, Kim, & Lee, 2013). Estudos recentes apontam para uma sobre representação de pacientes PD com mutações *GBA1*, 5 a 7 vezes superior quando comparado a um grupo controlo, com uma idade média no momento do diagnóstico 4 a 6 anos inferior (Aharon-Peretz , Rosenbaum , & Gershoni-Baruch 2004; Sidransky & Hart, 2012; Toft, Pielsticker, Ross, Aasly, & Farrer,

2006). No entanto, apesar da correlação estatística, o mecanismo subjacente à relação entre GCase e α-sinucleína ainda é pouco claro. O primeiro modelo mecanístico foi desenvolvido em Mazzulli et al em 2011, no qual é proposta a existência de uma relação inversamente proporcional entre a atividade de GCase e os níveis de α-sinucleína, na qual reduzida atividade de GCase resulta em elevados níveis de α-sinucleína, que, por sua vez, diminuem o transporte de GCase para o lisossoma, reduzindo os níveis de hidrólise e aumentando o numero de fibrilas de α-sinucleína (Mazzulli et al., 2011). GCase tornou-se, deste modo, não apenas o alvo terapêutico para GD, mas também para PD (Aflaki et al., 2016).

O presente trabalho teve como objetivos: I) Estabelecer um modelo neuronal *in vitro* a partir de iPSc para os genótipos de GD tipo 2 L444P/L444P (clone A), L444P/P415R (clone B), G325R/C342G (clone C), L444P/G202R (clone D), e controlo (*wild type* - WT), e corroborar a relação entre a atividade de GCase e os níveis de α-sinucleína; II) testar um grupo de 12 chaperones farmacológicas em neurónios de pacientes GD2 e caracterizá-los quanto ao seu efeito na Gcase, quer na quantidade de proteína, quer na sua atividade; III) testar o efeito de retroalimentação positiva proposto por Mazzulli et al., através da medição dos níveis de α-sinucleína e da relação destes com a atividade de GCase e quantidade de proteína (Mazzulli et al., 2011). Para tal, fibroblastos de 3 genótipos GD tipo 2 (Clones A, B e C) foram reprogramados ao estado de pluripotência através de transdução e expressão dos fatores de reprogramação Oct4, Sox2, Klf4 e C-Myc (OSKM) (Takahashi et al., 2007). Um controlo sem mutação *GBA1* (WT) e um outro genótipo GD tipo 2 (clone D) previamente reprogramados e testados foram também usados durante este trabalho. O conjunto dos clones iPSc WT, A, B, C e, D foram então diferenciados em neurónios através de um protocolo de diferenciação em camada única adaptado e otimizado por nós. Culturas confluentes de neurónios foram tratadas com um conjunto de chaperones pertencentes a iminoaçucares, piperidinas monocíclicas (MTD131, TMB69, TMB65 e TMB84); piperidinas bicíclicas (MTD106, MG174, MTD132 e RV21); e nortropanos (MG235, CVI62, DW43 e DW45), com os seguintes resultados:

I) No modelo estabelecido, os níveis de GCase estão de acordo com o que foi descrito para neurónios GD2, com níveis de atividade hidrolítica inferiores 20% aos observados para o controlo. Simultaneamente, com níveis reduzidos de GCase, estes clones apresentavam níveis aumentados de α-sinucleína.

II) Ainda que a maioria dos compostos tenha afetado os níveis de proteína GCase, o efeito foi pouco consistente nos diferentes genótipos, apresentando variações consideráveis consoante as mutações *GBA1* pressentes. Não obstante, alguns compostos demonstraram um efeito potencialmente terapêutico num ou mais genótipos:

Clone A (L444P/L444P) apresentou um aumento dos níveis proteicos de GCase e redução dos níveis de α-sinucleína na presença dos chaperones TMB69, TMB65, MTD132, RV21, MG235 e CVI62; Clone B (L444P/P415R), aumentou os níveis proteicos de GCase por um fator de 3 quando tratado com TBM69, com concomitante redução de α-sinucleína em 70%. Neste mesmo genótipo, TMB65, reduziu α-sinucleína em 90% apesar de não ter nenhum efeito observável na GCase; para o Clone C (G325R/C342G), o chaperone MTD106 elevou a atividade de GCase e reduziu em 50% os níveis de α-sinucleína ; relativamente ao Clone D (L444P/G202R), apesar de nenhum dos compostos reduzir efetivamente os níveis de α-sinucleína, um aumento da atividade de GCase foi alcançado quando tratado com MTD106.

III) Apesar do efeito positivo de alguns chaperones seja na quantidade ou atividade de GCase, como na redução dos níveis de α-sinucleína, esse efeito não é consistente. Esta observação pode ser causada por vários fenómenos como o efeito inibitório do composto, a afinidade e resistência de alguns dos compostos usados aos métodos de extração e desnaturação usados. Novos estudos serão necessários de modo a clarificar a interação entre os diferentes alelos de GD e chaperones de modo a garantir não só um aumento da atividade de GCase, mas também a segurança quanto aos níveis de α-sinucleína.

Palavras chave: Doença de Gaucher, Doença de Parkinson, GCase, α-sinucleína, chaperones

This page is intentionally left blank

Abstract

Gaucher Disease (GD) is the most common lysosomal storage disease. It is caused by mutations in *GBA1* which lead to dysfunctional β-glucocerebrosidase (GCase) activity and an accumulation of its substrates, glucosylceramide and glucosylsphingosine. Reticuloendothelial system cells and neurons are especially affected by high glucosylceramide levels, generating multiple symptoms. According to the distribution and severity of the symptoms, and degree of neuronal involvement, GD can be classified as systemic (GD1), severe acute neuropathic (GD2) or chronic neuropathic (GD3). Presently, none of the available therapies are effective at alleviating neuronopathic forms of the disease. Recent studies have pointed to *GBA1* mutations as the most frequent genetic risk factor for Parkinson Disease. In 2011, Mazzulli et al. proposed a feed-forward mechanistic loop model explaining the inverse correlation between GCase activity and α-syn levels. In the present work, we developed an optimized differentiation protocol to test iPSc derived neurons from four GD2 genotypes (L444P/L444P, L444P/P415R, G325R/C342G and L444P/G202R). Each clone was treated with a set of 12 chaperone compounds regarding their effect on GCase protein levels, and activity. Simultaneously, α-syn levels were measured for each sample to test Mazzulli's hypothesis. Our results identified some compounds which effectively enhanced GCase and decreased α-syn, which can be considered and explored as novel therapies for GD and PD. Our results indicate that chaperone treatment does not affect GCase levels/activity and the relation with α-syn levels in a way consistent with Mazzulli's proposed model. This might be due to the multiple variable at play in our experimental system and suggests the need for follow-up studies.

Keywords: Gaucher Disease, Parkinson Disease, α-synuclein, chaperones

This page is intentionally left blank

Publications and Communications

Publications

Santos, D., & Tiscornia, G. (2017). Induced Pluripotent Stem Cell Modeling of Gaucher's Disease: What Have We Learned? International Journal of Molecular Sciences, 18(4), 888. doi: 10.3390/ijms18040888;

Mena-Barragán, T., Narita, A., **Matias, D.**, Tiscornia, G., Nanba, E., Ohno, K., Suzuki, Y., Higaki, K.,Garcia Fernández, J. M. and Ortiz Mellet, C. (2015). pH-Responsive Pharmacological Chaperones for Rescuing Mutant Glycosidases. Angew. Chem. Int. Ed., 54: 11696– 11700. doi:10.1002/anie.201505147.

Posters

Santos Matias, D., Tiscornia, G. (2017) Modelling Gaucher disease using induced pluripotent stem cells. CBMR 2nd Annual Meeting.

This page is intentionally left blank

Table of Contents

This page is intentionally left blank

List of Figures

List of Tables

This page is intentionally left blank

Abbreviations

BDNF	Brain-derived neurotrophic factor
bFGF	Basic fibroblast growth factor
BMP	Bone morphogenetic protein
cAMP	Cyclic adenosine monophosphate
CBE	Conduritol-β-epoxide
CM	Conditioned Media
CNS	Central nervous system
DA	Dopaminergic
DAPT	N-[N-(3, 5-difluorophenacetyl)-L-alanyl]-S-phenylglycine t-butyl ester
db-cAMP	Dibutyryl-cAMP
DMEM	Dulbecco's Modified Eagle Medium
DMSO	Dimethyl sulfoxide
DNA	Deoxyribonucleic acid
DPBS	Dulbecco's Phosphate-Buffered Saline
EB	Embryoid bodies
ER	Endoplasmic reticulum
ERAD	ER Associated Degradation
ERQC	ER quality control system
ERT	Enzyme replacement therapy
ESc	Embryonic stem cell
FGF	Fibroblast Growth Factor
FOXA2	Forkhead class A2 gene
GBA1	Acid β-glucocerebrosidase gene
GBAP1	GBA1 pseudogene
GCase	β-Glucocerebrosidase
GD	Gaucher Disease
gDNA	Genomic DNA
GDNF	Glial cell line-derived neurotrophic factor
GFAP	Glial fibrillary acidic protein
GFP	Green fluorescent protein
GlcCer	Glucosylceramide
GlcSph	Glucosylsphingosine

GSK3	Glycogen synthase kinase 3
HEK	Human Embryonic Kidney 293 cells
HFF	Human foreskin fibroblasts
hiPSc	Human Induced Pluripotent Stem Cells
HLA	Human leukocyte antigen
HRP	Horseradish peroxidase
IL	Interleukin
iPSc	Induced Pluripotent Stem Cells
KO	Knockout
KSR	Knockout serum replacement
LB	Lewy bodies
LIMP-2	Lysosomal integral membrane protein 2
LSD	Lysosomal storage disease
mDA	Midbrain dopaminergic
MEM	Minimum Essential Medium
MG	Matrigel®
micHDF	Mitomycin-C treated human dermal fibroblasts
mitcHFF	Mitomycin-C treated human foreskin fibroblasts
MOI	Multiplicity of infection
NDM	Neural Differentiation Medium
NEAA	Non-Essential Amino Acids
nGBA	GBA null
NIM	Neural Induction Medium
NPM	Neural Proliferation Medium
NURR1	Nuclear receptor related 1 protein
OSKM	Factors Oct4, Sox2, Klf4 and C-Myc
PCT	Pharmacological Chaperone Therapy
PD	Parkinson’s disease
PFA	Paraformaldehyde
PGK	Phosphoglycerate kinase promoter
RA	Retinoic acid
RIPA	Radioimmunoprecipitation assay buffer
RNA	Ribonucleic acid
SHH	Sonic Hedgehog signalling molecules
SNCA	Alpha-synuclein gene
SRP	Signal recognition particle

SRT	Substrate reduction therapy
Syn	Synuclein
TFEB	Transcription factor EB
TGF-b3	Transforming growth factor, beta 3
TH	Tyrosine hydroxylase
TUJ1	Class III beta-tubulin
UPR	Unfolded protein response
Wnt	Wingless pathway
WT	Wild type
Y-27632	Y-27632 dihydrochloride

This page is intentionally left blank

1. Introduction

1.1 Gaucher disease

Gaucher disease (GD) is the most frequent lysosomal storage disease (LSD), a group of rare inborn metabolic disorders. The syndrome was first reported by Philippe Gaucher in his medical doctorate, in 1882. Gaucher reported a 34-year old woman suffering from hepatosplenomegaly with lipid-filled macrophages. In 1934, the French chemist Henriette Aghion identified the accumulated lipid as GlcCer (Mistry et al., 2017). However, the mechanism underlying GlcCer accumulation was only discovered by Brady et al in 1965 (R. O. Brady, Kanfer, Bradley, & Shapiro, 1966; Roscoe O. Brady, Kanfer, & Shapiro, 1965; Grabowski, Bendikov-Bar, Maor, & Horowitz, 2013). The metabolic defect was shown to be caused by deficiency of the hydrolase β-glucocerebrosidase (GCase) or through alterations in its respective activator or transporter. In the case of GD, the syndrome is transmitted in an almost exclusive autosomal recessive manner and leads to deregulation of normal lysosomal function of β-glucocerebrosidase (GCase) or, very rarely, in its co-factor, saposin C (Kang et al., 2018). With over 300 described mutations known to cause GD, inherited alterations in *GBA1* are the main cause for GD. These alterations can affect one or more aa. which can alter the final tridimensional structure and change enzyme's stability, trafficking efficiency and/or hydrolytic activity (Dvir et al., 2003; Manoj Kumar Pandey et al., 2012).

The high number of mutations is thought to be partly due to recombination events with a pseudogene (GBAP1) only 16Kb downstream of the functioning gene. With over 96% homology to the functional gene, GBAP1 is thought to be a relatively recent duplication of *GBA1* which has undergone several insertions of Alu repeats in its sequence (Horowitz et al., 1989; Straniero et al., 2017). *GBA1* is located in the long arm of chromosome 1 and is ubiquitously expressed throughout the adult human body. It has 11 exons and 10 introns, Figure 1. The mature transcript has two equally efficient ATG start sites at the beginning of exons 1 and 2. Depending on where translation begins, the emerging protein will contain either a 39 or 19 aa. signal peptide residue. Upon synthesis in the polyribosomes, the peptide enters the lumen of the endoplasmic reticulum, where it's recognized by the signal recognition particle (SRP) and cleaved by Sec61 into the final 497 aa. protein that composes the mature enzyme (Ozlem Goker-Alpan et al., 2003; Grabowski et al., 2013; Hruska, LaMarca, Scott, & Sidransky, 2008; Ron & Horowitz,

2005). In normal conditions, GCase enters the ER lumen and undergoes N-linked glycosylation in 4 asparagine residues by glucosidase I and II. At this point, the enzyme is exposed to the ER quality control system (ERQC) and to the chaperones HSP homologues, lectins and thiol oxidoreductases. Correctly folded proteins are transported to the Golgi in COPII-coated vesicles and finally to the lysosome in a LIMP-2 dependent manner (Bendikov-Bar & Horowitz, 2012; Maor, Filocamo, & Horowitz, 2013; Zhao, Ren, Padilla-Parra, Fry, & Stuart, 2014). In the case of a mutation which alters the enzyme's folding, the ERQC halts the secretory pathway and moves the misfolded proteins to Sec61 and Derlin membrane channels where they are retrotranslocated via AAA-ATPase p97 to the cytoplasm, targeted by ubiquitination and degraded in the proteasome (Bendikov-Bar & Horowitz, 2012).

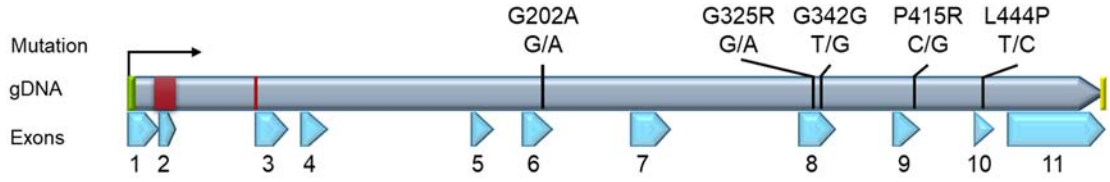

Figure 1. Schematic representation of *GBA1* gene flanked by the start (green box and black arrow) and stop (yellow box) codons and containing the signaling peptide sequence (red boxes), as well as the location of each of the studied mutations in the genomic sequence (gDNA). Bellow the gDNA sequence, numbered blue arrows represent the location and size of each exon.

Prolonged expression of faulty protein can lead to accumulation of misfolded protein in the ER. This further activates the stress mechanism known as Unfolded Protein Response (UPR), in which, consecutive cycles of recognition and folding attempts by UPR chaperones occur (Grabowski et al., 2013). UPR is an intricate signal transduction pathway with three functions: adaptation to increasing levels of unfolded protein, alarm and, if the stress response persists, apoptosis. The UPR has three main membrane receptors as interactors: the double-stranded RNA-activated protein kinase (PKR)-like endoplasmic reticulum kinase (PERK), the activating transcription factor 6 (ATF6), and inositol requiring kinase 1 (IRE1). The complex functions to reestablish protein folding and homeostasis through the expression of chaperones. In parallel, translation is attenuated to decrease the ER protein load. Failure to resolve the problem triggers mitochondrial mediated apoptosis (Bendikov-Bar & Horowitz, 2012).

In addition to the ER stress, the decreased hydrolytic activity of the mutated forms of GCase leads to intra-lysosomal accumulation of its substrates, glucosylceramide (GlcCer) and glucosylsphingosine (GlcSph) (Awad et al., 2015; Choi et al., 2011). Despite being ubiquitously expressed throughout the organism there are two cell types which are specially affected by GlcCer accumulation. Due to their physiological function, cells belonging to the reticuloendothelial and nervous system are especially affected in

GD. Among cells belonging to the reticuloendothelial lineage, macrophages are primarily responsible for phagocytosis. Besides their own products of autophagy, macrophages also accumulate exogenously derived lipids from phagocytosed cells and debris (Hein, Meikle, Hopwood, & Fuller, 2007). In macrophages, the increasing amounts of GlcCer accumulate in large intracellular vacuoles which grow to eventually 'clog' the cytoplasm, forming the characteristic lipid laden "Gaucher cells" (Hollak et al., 1994; Klein & Futerman, 2013; Willemsen et al., 1995). Neurons, on the other hand, are particularly sensitive to decreased levels of GCase, as, in brain development and function, neurons process vast amounts of gangliosides either as structural elements or involved in synapses physiology (Grabowski, 2008; Mencarelli & Martinez–Martinez, 2013).

GD can manifest itself in an array of symptoms which can be generally divided in systemic, affecting visceral organs (such as liver and spleen, and other systems such as lungs and bone), or, neurological, affecting neurons in specific brain areas. The symptoms have been recognized to follow a severity continuum, from acute neuropathological congenital forms to mild forms with exclusively visceral involvement appearing late in life, or indeed, going undetected (Aureli et al., 2012). Increased attention and registry protocols are revealing an increase in intra-type variations with new symptomatology increasingly more evident (Grabowski et al., 2015). The origin of this degree of variability is still poorly understood. Nevertheless, it's thought to be a combination between the residual hydrolytic activity of each mutation with other genetic, epigenetic or environmental interactions. (O. Goker-Alpan et al., 2005; Grabowski et al., 2015). In the clinical context, however, a simplified prognosis-based system is still preferred in the treatment decision making. Thus, GD is classified according to the severity of its visceral and neuronal involvement in Type 1 (non-neuronopathic), Type 2 (acute-neuronopathic) and Type 3 (chronic/ subacute neuronopathic), as summarized in Table 1. Systemic manifestations include gammopathy, generalized inflammation, hepatosplenomegaly, pancytopenia and osteoporosis. The neurological problems can range from spasticity, seizures, eye movement to cognitive problems and neurodegeneration (Butler, 2001; McNeill et al., 2012).

Type 1 is responsible for over 90% of GD cases worldwide. It is the mildest form of the disease and it lacks any kind of primary neuronal affection. Type 2 is the most severe form of the disease. GD type 2 carries a poor life expectancy prognosis with early onset, acute neuropathology and life expectancy of 9 months. Type 3 is situated, in terms of severity, between type 1 and type 2. Patients with this form of the disease also have the visceral presentations of the disease and a chronic neuronal manifestation (Ozlem Goker-Alpan et al., 2003).

Table 1. Phenotypic and prognostic comparison of Gaucher disease Type 1, Type 2 and Type 3. Adapted from (Lu et al., 2010; Santos & Tiscornia, 2017).

Feature	Type 1	Type 2	Type 3
Age at diagnosis	Adolescence to old age;	Early infancy	Infancy / childhood
Prevalence	General population: 1 in 100.000; Ashkenazi Jewish population: 1 in 450	General population: $1:10^6$	General population: $5:10^6$; Swedish Norrbottian Population: 2 in 100 000
Systemic symptoms	Hepatosplenomegaly, Thrombocytopenia, Anemia, Bone disease, Interstitial lung disease,	Hepatosplenomegaly, Anemia, Thrombocytopenia Interstitial lung disease	Hepatosplenomegaly, Anemia, Bone disease, Thrombocytopenia, Interstitial lung disease
Neurologic symptoms	None (higher risk to develop synucleinopathies)	Acute neurologic, seizures, convulsions, spasticity, neurodegeneration	Chronic neurologic problems, seizures, eye movement disorders, poor coordination, cognitive problems
Disease progression	Asymptomatic/slow progression	Rapid progression	progressive
Residual GCase activity*	<42-32%	<18.9%	<32-18.9%
Average lifespan	6-80 years	<2 years	2-60 years

*measured in fibroblasts

The disease has, on average, a worldwide prevalence of 1.5 patients per 100,000 individuals in the general population. Nevertheless, the incidence can be significantly higher in some populational groups, reaching 1 in 47 000 in the Swedish Norrbotten population and 1 in 855 live births in the Ashkenazi Jewish population (Nalysnyk, Rotella, Simeone, Hamed, & Weinreb, 2017; Westbroek, Gustafson, & Sidransky, 2011). Despite being classified as a rare disease, its relatively high prevalence, along with the fact that it still is the best described LSD has made GD the reference model for all LSDs.

1.2 Visceral phenotype

Until recently, the widespread distribution of cells from the macrophagic lineage was thought to account for all the pleotropic and multisystemic manifestations of the disease (Elleder, 2006; Grabowski et al., 2015). Nevertheless, recent studies have unveiled a strong participation of mesenchymal stem cells (MSCs) in macrophage activity and chronic inflammation. MSCs are bone marrow adult multipotent cells which have the ability to differentiate in several cell types, mainly from the mesodermal origin, like chondroblasts, osteoblasts and adipocytes. Besides their progenitor-like function in bone

development and maintenance, they have recently also proven to possess a strong immunoregulatory role. In normal situations, they function as a local sensor for inflammation, activating and suppressing both innate and adaptative immune responses according to the local biochemical cues. In GD, the high levels of GlcCer seem to destabilize both MSCs and Gaucher cells into of a pro-inflammatory state (Figure 2 – step 1). MSCs produce chemoattractant Chemokine (C-C motif) ligand 2 (CCL2) and inflammatory proteins like COX-2, prostaglandin E2, interleukin-8; lipid filed macrophages enter a pro-inflammatory state.

The simultaneous proinflammatory stimulus on the reticuloendothelial cells leads to a generalized state of inflammation with high serum levels of inflammatory interleukins (IL)-1, IL-2, IL-6, IL-8, IL-10 and IL-18, tumor necrosis factor (TNF-β), Interferon-γ, Macrophage colony-stimulating factor (M-CSF) and macrophage-inflammatory protein-1 (MIP-1) and unspecific inflammatory agents like prostaglandins E2 and COX2 activators (Bernardo & Fibbe, 2013; Campeau et al., 2009). Even though in GD low activity of GCase leads to GlcCer accumulation virtually in all somatic cells, cells with immunological functions seem to be especially sensitive. High GlcCer in MSCs and macrophages seem to trigger a pro-inflammatory state of activation. Independently of which cell type initiates this inflammatory state, both cell types seem to end up in a potent inflammatory feedback loop (Figure 2). GlcCer rich MSCs produce chemoattractant Chemokines (C-C motif) ligand 2 (CCL2) and inflammatory proteins like COX-2, prostaglandin E2 and interleukin-8 recruiting and activating macrophages and neutrophils along with a Th2 and B-cell mediated response. These stimuli lead to massive tissue infiltration by activated reticuloendothelial cells which respond with interleukin (IL) production, phagocytosis and bone resorption. Histologically, the most distinctive cells in this process are GD characteristic lipid-laden macrophage cells or Gaucher cells. These cells seem to have lost typical macrophage morphology, along with the typical CD11b macrophage marker. Nevertheless, they maintain other macrophage specific markers such as CD14, CD68, CD163 and HLA II, allowing their origin to be track. They also present scavenger receptors, mannose and galactose-type receptors. Presence of these markers, along with high activity levels of chitotriosidase.

This generalized state of inflammation leads to high serum levels of inflammatory interleukins like IL-1, IL-2, IL-6, IL-8, IL-10 and IL-18, tumor necrosis factor (TNF-β), Interferon-γ, macrophage colony-stimulating factor (M-CSF), macrophage-inflammatory protein-1 (MIP-1) and unspecific inflammatory agents like prostaglandins E2 and COX2 activators and chitotriosidase, a serum enzyme which degrades chitin present in the outer shell of some coated pathogens (Bernardo & Fibbe, 2013; Campeau et al., 2009;

Kadali, Kolusu, Sunkara, Gummadi, & Undamatla, 2016; Manoj K. Pandey & Grabowski, 2013; White, Iqbal, & Greaves, 2012). The inflammatory cascade molecularly mimics a parasitic response and leads to a chronic state of inflammation and tissue destruction. In essence, the process starts with tissue resident macrophages which accumulate GlcCer due to lack of GCase activity (Figure 2 – 1). These cells continuously release part of the accumulated GlcCer into the extracellular space, where it is recognized by B cells. This has two main effects. First, it triggers B cell differentiation into plasmocytes which synthesize IgG anti-GlcCer antibodies; second, activated B-cells activate T-cell response through epitope presentation (Figure 2– 2 and 6). Eventually, aggregation of anti-GlcCer IgG antibodies activate the complement system cascade, culminating in C5 cleavage and production of the major inflammation mediator, C5a. Simultaneously, the anti-GlcCer antibodies also activate local macrophages through FcγR inducing C5 and C5a production (Figure 2– 3 and 4). Finally, high levels of C5a and its receptor C5aR1 lead to an increase of glucosyl ceramide synthase (GCS), the enzyme responsible for GlcCer synthesis from glucose and ceramide, perpetuating the cycle (Figure 2 – 5) (Ginzburg, Kacher, & Futerman, 2004; Hollak et al., 1994; Manoj K. Pandey & Grabowski, 2013).

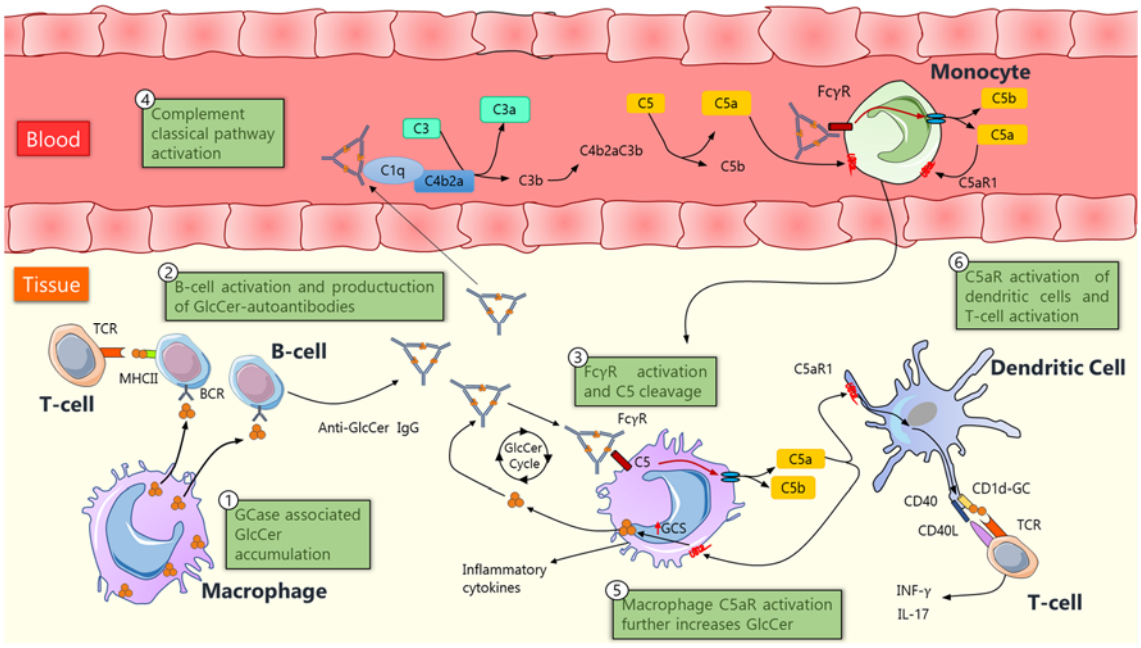

Figure 2. Main GlcCer driven inflammation events. 1- low GCase activity leads to GlcCer aggregates which extravasate to the extracellular media; 2- Circulating B-cells are activated by free GlcCer aggregates and respond with production of anti-GlcCer antibodies and MHCII-GlcCer presentation to T-cells; 3- GlcCer-antibody aggregates activate FcγR on macrophage's membrane; 4- simultaneous to macrophage activation, antibody-GlcCer complexes activate the complement classical pathway which activates circulating monocytes; Macrophage FcγR activation leads to C5a production which acts on the macrophage (5), leading to an increase in GSC activity and GlcCer production; and dendritic cells (6), increasing GlcCer presentation to T-cells and release of inflammatory factors. increases GCS activity and GlcCer synthesis. Adapted from (Manoj K. Pandey et al., 2017).

1.3 Neuronal phenotype

The origin of the neuronal phenotype is less understood. Research into the neuropathological phenotype has resulted in reports that are not in total agreement and, in some cases, are even contradictory. The difficulty of access to patient samples and the complexity of this pathological system has resulted in a considerably slower progress in this area. Only recently conditional mouse models were able to reproduce the neuronopathic forms of Gaucher's disease. These models have been profoundly helpful in uncovering the process of neurodegeneration in GD. Neuronopathic forms of Gaucher disease are characterized by GlcCer accumulation in the brain with infiltration of Gaucher macrophages, followed by inflammation, neuronal loss, astrocytosis and microgliosis (Enquist et al., 2007; Vitner, Farfel-Becker, Eilam, Biton, & Futerman, 2012). Contrary to the visceral manifestations of the disease, there seems to be neuronal affection even when presence of Gaucher cells is not yet evident. Thus, it is not clear if inflammation is a cause or consequence of neuronal death. Involvement of multiple cell types seem to indicate the existence of a complex system. On the one hand, studies in GD *GBA1* flox/flox; Nestin-Cre mice model show an increase in levels of inflammatory mediators like interleukin-1β, tumor necrosis factor-α and nitric oxide; on the other hand, myelin and cell debris produced by dying or senescent cells activate microglia which are the main mediators of brain inflammation, perpetuating the system (Gegg & Schapira, 2016; Mencarelli & Martinez–Martinez, 2013; Tantawy, 2015).

An important contribution to understand what triggers of the inflammatory loop was given by Vitner et al., who described an increase in expression levels of receptor-interacting protein kinase-3 (Ripk3) in GCase null mice with a caspase-8 independent neuronal necrosis. Ripk3 increased significantly in neuron's nuclei from *GBA1*$^{flox/flox}$ Nestin-Cre mice. This peak in Ripk3 level was more predominant in the more severely affected areas and preceded any neuropathological manifestation or detectable inflammation. This data, along with a previous report from the same group, which demonstrated a 10-fold increase in cathepsin levels in a mouse neuropathic model of the disease, suggests the existence of a stress point in the protein degradation pathway which culminates with activation of a necroptotic pathway (Vitner et al., 2010). Ripk3 can be expressed in response to stress and acts as an activator of programmed necrosis and coordinates astrocytosis and microgliosis, perpetuating neuronal death and inflammation cycle (Vitner et al., 2014).

1.4 Therapies

While there is still no cure for GD, there are presently several alternatives for symptomatology management. Depending on the clinical presentation of the disease clinicians have several tools available to slow down progression of the disease or improve life quality. From a therapeutic point of view, research in GD suffered from a succession of long periods where no advance was achieved. During this period, GD management was restricted to symptom control. Patients who developed secondary systemic problems such as clotting disorders, abnormal iron levels, liver cirrhosis, portal hypertension, esophageal and gastric varices, or even orthopedic surgery for avascular necrosis, would be tended for those problems. In the most acute forms of the disease, hepatosplenomegaly may reach volumes that compromise the respiratory function. In those cases, some relief is necessary, making partial splenectomy the only option (Grabowski et al., 2013; Mistry et al., 2017; Nagral, 2014).

In the meantime, bone marrow transplantation (BMT) through the intravenous delivery of hematopoietic cell progenitors to repopulate the marrow function was approved as a therapeutic option for storage diseases in 1980 (Lange et al., 2006). Heterologous bone marrow transplantation from a healthy donor is still the only way to permanently cure the visceral symptoms of GD. Correctly engrafted transplants repopulate the macrophages in the visceral tissues. If done early in life, BMT can prevent some neurological manifestations. Nevertheless, this effect is lost in older patients, despite bone marrow macrophages being found in the brain of transplanted macrophages, there has no benefit to the neurological phenotype. The risk of rejection and infection means that BMT has a higher cost-benefit ratio when comparing with ERT (Platt & Jeyakumar, 2008; Shawky & Elsayed, 2016). Furthermore, improvements in stem-cell development and transplantation, along with gene therapy, maintain the hope for a BMT curative alternative (Grabowski, 2008; McEachern et al., 2007).

1.4.1 Enzyme Replacement Therapy

The first effective treatment for GD was conceptually developed and tested by Brandy's group. They developed the first enzyme replacement therapy (ERT) treatment approach by intravenous supplementation of human placental purified GCase in GD patients (Brady , Pentchev , Gal , Hibbert , & Dekaban 1974). Notwithstanding, that treatment was never commercialized due to the high costs of production and scale up difficulties. Patients would have to wait for *GBA1* to be fully sequenced before the first commercial GD treatment would become available (Ginns et al., 1984; Sorge, West, Westwood, &

Beutler, 1985). Only in 1991 did the first GCase therapy, Ceredase® (alglucerase, Genzyme Corp), become an option in GD management (Bennett & Mohan, 2013). Since Brady's first proposal of infusible GCase as a clinical approach, some improvements have been made to the procedure. One improvement came from the elucidation of glucocerebrosidase post-translational modification through glycosylation with mannose-6-phosphate residues. This development led to the generation of mannose tagged GCase molecules which are largely up taken by macrophages, the target cell cause of most visceral symptoms(R Kornfeld & Kornfeld, 1985).

To date, ERT is the first line of treatment for GD patients. Early diagnosis and treatment with ERT is essential to prevent irreversible complications, especially in the musculoskeletal and respiratory systems (Beaton, Monzón, Hughes, & Pastores, 2017; Wenstrup, Roca-Espiau, Weinreb, & Bembi, 2002). There are 3 main treatment options (Table 2) which consist of intravenous infusions every 2-4 weeks with 60 international units (IU) per Kg of bodyweight. The systemically injected enzyme is recognized by α-mannosyl receptors on the macrophage cell surface and is internalized by endocytosis. These endocytic vesicles are fuse with the lysosome, liberating the recombinant enzyme into the lysosomal lumen where it catabolizes the existing GlcCer (Grabowski et al., 2013; Shawky & Elsayed, 2016). Regular treatments greatly improve life quality, preventing and reversing most visceral affections like bone disease, thrombocytopenia as well as hepatic and splenic disease (Beaton et al., 2017; Shawky & Elsayed, 2016).Nevertheless, ERT has some important limitations. Firstly, lymph nodes and lungs seem to be refractory to the treatment; secondly, the enzyme's inability to cross the blood-brain barrier means that it has no effect in the neurological forms of the disease that affect type 2 and type 3 patients. Furthermore, lifelong intravenous treatments are a burden for patients and some patients develop an immune response to the exogenous GCase. Importantly, the cost of the treatment, yearly between 100 to 400 thousand dollars per patient is unaffordable for most patients and healthcare systems (Beutler, 2006; Patnaik et al., 2012).

Table 2. Currently commercialized ERT treatments. Adapted from (Bennett & Mohan, 2013).

Drug name	***Provider***	***Produced in***	***Mechanism***
Imiglucerase	Genzyme	Chinese hamster ovary cell line	Mannose-tagged ERT: Alleviate mostly visceral symptoms
Velaglucerase alfa	Shire HGT	Carrot cells	
Taliglucerase alfa	Protalix/Pfizer	Human fibrosarcoma cells	

1.4.2 Substrate Reduction Therapy

A more recent therapeutic approach takes advantage of the residual GCase activity found in many mutations. First postulated by Radin in 1996, the first alternative treatment to ERT focuses on release of GlcCer cumulative pressure through inhibition of its upstream effectors in the catabolic pathway. This substrate reduction therapy (SRT) strategy is currently centered in partial or complete inhibition of glucosylceramide synthase, the enzyme responsible for the GlcCer synthesis from UDP-glucose and ceramide (Radin, 1996).

While ERT is favored as the primary therapy to treat the visceral affections of GD, there is still the need to treat patients who do not benefit from it. Despite the new versions of injectable GCase, velaglucerase alfa and taliglucerase alfa being considerably less immunogenic than the first available version (imiglucerase), a percentage of patients develop immune responses to the recombinant enzyme. Moreover, some patients, due to their physical condition, do not tolerate long term regular IV infusions. Finally, the inability of the infused GCase to cross the BBB renders it ineffective to treat the neuropathological forms of the disease. Alternative treatments for GD such as SRT must take into account individual parameters such as genotype, renal function and GCase residual activity. Presently, 2 compounds are clinically approved for SRT: Miglustat, based on the iminosugar N-butyldeoxynojirimycin and Eliglustat tartrate (Table 3), a ceramide analog based on PDMP (D-*threo*-1-Phenyl-2-decanoylamino-3-morpholinepropanol) (Nagral, 2014; Shayman, 2010), but other candidates of each class are under development.

Table 3. Currently commercialized SRT treatments. Adapted from (Bennett & Mohan, 2013).

Drug name	Provider	Produced in	Mechanism
Miglustat	Actelion Corp	Chemical synthesis	SRT by Glucosylceramide synthase inhibition, decreases Ceramide synthesis. Ameliorates visceral symptoms. Not proven neurological improvement
Eliglustat	Genzyme/Sanofi	Chemical synthesis	
Velaglucerase alfa	Shire HGT	Carrot cells	

Despite a delayed temporal response when compared with ERT, SRT has proved efficient in improving most visceral symptoms (see Table 4). In addition to their affordability, these compounds also offer the practicality of oral administration and the possibility of being used in combination with ERT. Furthermore, due to their small size, these compounds do not trigger acquired immunity and, more importantly, are able to

cross the blood-brain barrier, giving it the potential to improve the neuropathological variants of the disease. Nevertheless, there has been no significant enhancement of the neuronal phenotype prognosis with the currently available molecules. Important disadvantages of SRT include its side effects which can span from diarrhea and weight loss to tremor and burning paresthesia (Abian et al., 2011; Bennett & Mohan, 2013; Platt & Jeyakumar, 2008; Shayman, 2010).

Table 4. Comparison of the advantages and disadvantages of ERT and SRT. Adapted from (Bennett & Mohan, 2013)

	ERT	**SRT**
Pros	Effective and with over 20 years of use Reduces intracellular GlcCer Alleviates visceral symptoms: anemia, thrombocytopenia, bone disease, spleen and liver volumes	Administered orally Does not require weekly intravenous administration Cheaper Not antigenic Crosses BBB Reduces GlcCcer storages Improves biochemical, blood, liver and spleen affections
Cons	Requires bimensal intravenous infusion Does not cross BBB and has no effect in the neuropathic GD Limited effect on lung and bone symptoms Does not revert pre-existing lesions Expensive (>200 000 $ year)	Extensive side effects like diarrhea, vomiting, weight loss, tremors and peripheral neuropathy Possible effect on cognition Mild effect on GlcCcer reduction Contraindicated in children, adolescents and during pregnancy Affects male fertility

1.4.3 Pharmacological Chaperones

For the best part of the last-four decades, ERT has been the primary line of treatment for GD. More recently, inhibition of the upstream enzyme glucosylceramide synthase by glycomimetics like iminosugar N-(n-butyl)-1-deoxynojirimycin (miglustat, Zavesca) has proven to have therapeutic effect. This approach has been used as a second line of treatment for patients with neurological forms of the disease, and also for those who do not tolerate chronic enzyme infusions. The objective of this approach is to decrease the synthesis of the accumulated toxic substrate, GlcCer, allowing the remaining GCase activity to break down GlcCer. Nevertheless, SRT compounds can have serious side

effects that negatively impact patient's quality of life. More importantly, neither approaches have proven to effectively treat the neuropathic forms of the disease.

Recently, a new approach was discovered, inspired by the somewhat unexpected effect of the specific enzymatic inhibitor, N-(n-butyl)-1-deoxynojirimycin (NN-DNJ), which increased GCase activity by 2-fold in N370S and 1.7-fold in L444P GD genotypes. These inhibitors were able to bind to the target enzyme, promote the correct three-dimensional conformation and stabilize it enough to pass the ERQC system (Benito, García Fernández, & Mellet, 2011; Fan, Ishii, Asano, & Suzuki, 1999). Since most *GBA1* mutations lead to a decrease in enzyme levels than enzyme activity, using pharmacological chaperones that ease GCase's folding, and stabilize it enough to reach the lysosome, could prove to be an effective therapy. This new approach, termed Pharmacological Chaperone Therapy (PCT) could be useful for mutations that change protein conformation but not for mutations that severely abolish activity. PCT's first-generation consisted of modified sugars that mimicked GCase's substrate glycosidic component (D-glucopyranose) and could thus bind to the active site. The most successful compounds to decrease GlcCer levels were iminosugar derived 1-deoxynojirimycin (DNJ), 1-azasugar isofagomine and their N-alkyl derivatives. Iminosugars are sugar analogs composed of a stable piperidine ring in which the oxygen atoms present in sugars are substituted by nitrogen. In preliminary tests, isofagomine increased GCase trafficking to the lysosome and increased GCase activity 300% in N370S mutants while -dodecyl DNJ did not surpass 95% activity increase. Nevertheless, the compound had little effect on L444P variants and did not pass to phase III of clinical trials due to lack of improvement in GD markers in patients and relative unspecificity of the glycone radical which is recognized by several isoenzymes, leading to several undesired side effects (Alfonso et al., 2013).

Some alternatives with structural variations to the sugar moiety were promptly developed to circumvent this specificity problem. C-substituted iminosugars (Bergeron-Brlek, Meanwell, & Britton, 2015) and aminocyclitol glycomimetic (Trapero, González-Bulnes, Butters, & Llebaria, 2012) are more specific and effective, but their synthesis involves a sequence of expensive reactions. Surprisingly, GCase activity of L444P homozygous fibroblasts increased by 230% when treated with calystegines, a naturally occurring nortropane derived iminosugars. Little is known about their effect on human neurons or why they have such an effect on the usually refractory L444P homozygous mutation, but it has been postulated that other factors like net charge and hydrophobicity play an important rule not only in membrane crossing but also in intracellular transport.

These concerns concerning chaperone bioavailability, membrane permeability and selectivity are central to a new class of PC: bicyclic sp2- iminosugars. Induction of an sp2 conformation to the piperidine ring of the compound forces the endocyclic nitrogen's external electron pair from its sp3 orbital to an axial p orbital, reinforcing the anomeric effect. Having a bridgehead nitrogen further increases the inhibitory effect on glycosidases and enables fine tuning selectivity. Addition of lipophilic radicals such as 5-N,6-O-(N'-octyliminomethylidene) nojirimycin (NOI-NJ) or its 6-thio derivative 6-S,5-N,6-O-(N'-octyliminomethylidene) nojirimycin (6S-NOI-NJ) to the nojirimycin derived bicyclic sp2- iminosugars creates β-glucosidases specific inhibitors for GCase which was maintained for in N370S, F213I and L444P mutants.

Moreover, the inhibitory effect was stronger at neutral pH (ER) than at acidic lysosomal like 5.2, facilitating folding at the ER and unbinding at the lysosome, and leaving the active site free to hydrolyze GlcCer (Benito et al., 2011). Unfortunately, bicyclic sp2- iminosugar compounds show only a modest chaperone effect in the following genotypes: N188S/G193W (TMB65 -1.2x) and V230G/R296X (TMB65 -1.5x) (Mena-Barragán et al., 2015), 3x for N370S (DW45 and DW43), and around 4x for L444P (3.8x - DW45 and 4.98x- DW43) for (Alfonso et al., 2013). The best result so far came from reprogrammed G202R/L444P GD iPSc treated with 6S-ADBI-NJ increased GCase activity by 6-fold (Tiscornia et al., 2013).

1.5 Connection between Parkinson's Disease and Gaucher's Disease

Parkinson's disease (PD) is the second most common neurodegenerative disease, amounting to approximately 7 million patients worldwide. It is estimated to affect 2-3% of the population over 65 years of age, reaching 4% by the age of 85. The disease is caused by a largely unknown mix of factors, ranging from inherited polygenic susceptibility, to what is thought to be largely lifestyle and environmental contributions. In fact, only 27% of the PD cases can be attributed to familiar monogenic inheritance (Mullin & Schapira, 2015). The disease is caused by loss of dopaminergic (DA) neurons in the *substantia nigra* with consequent deficiency in striatal dopamine. The other hallmark of PD is the presence of α-syn amyloid Lewy body inclusions in the *substantia nigra*. It is thought that neuronal death and the presence of fibrillar forms of α-syn result in a sustained inflammatory reaction led by activated microglia and astrocytes. The inflammatory environment foments, and, in turn leads to stress and a progressive depletion of dopaminergic neurons in the *substantia nigra pars compacta*.

PD is primarily a movement disorder, death of DA neurons and consequent lack of dopamine in the *striatum* results in rigidity, bradykinesia and resting tremor. Additionally, continuous neuronal death leads to non-motor manifestations such as cognitive impairment, sleep disorders, autonomic system dysfunction, hyposmia and depression. As a matter of fact, PD is not the only pathology where α-synuclein inclusions can be found; the synucleinopathies are a group of disorders characterized by existence of α-synuclein aggregates in neuronal tissue. This group comprehends PD, Dementia with Lewy bodies, Lewy body variant of Alzheimer's disease, multiple system atrophy, and neurodegeneration with brain iron accumulation (Codolo et al., 2013; Galvin, Lee, & Trojanowski, 2001; Norris, Giasson, & Lee, 2004; Sardi et al., 2011). Lewy bodies (LB) are, in essence, large eosinophilic (acidic) protein inclusions in the neuronal cell's cytoplasm. Microscopic evaluation of these structures shows morphological variations depending on their location (whether they are in the brainstem, limbic system or neocortex), stage of maturation and the patient's specific genetic background. Postmortem proteomic studies of the LB composition identified over 300 different proteins forming part of this structure. Nevertheless, despite the high variability in composition, LB's share α-synuclein as their most abundant component (Shahmoradian et al., 2017; Weil, Lashley, Bras, Schrag, & Schott, 2017). The pathophysiology leading to LB formation and its relation to DA specific neuronal degeneration are still poorly understood. The main current working hypothesis is that LB formation is caused by α-syn imbalance and accumulation in the neuronal cytoplasm. This accumulation is thought to trigger a pathogenic loop which culminates in neuronal death. Due to its association with Parkinson's disease, as well as other neurodegenerative disorders in the synucleinopathy family, a great effort has been made in order to understand the variables which condition synuclein, and specially α-syn aggregation. The synuclein family is composed by α-, β- and γ-synucleins which are closely related and highly expressed peptides composing up to 1% of the neuronal proteome. Within the nervous system, a- and b- synuclein have a broader expression pattern, being present in most pre-synaptic and synaptic termini, while γ-synuclein presents higher specificity for glial and particular neuronal populations, predominantly in DA neurons. α-syn is a small acidic protein encoded by the *SNCA* gene. The final protein is composed of three main regions, weighs 14.5 kDa and is 140 amino acids length. The first N-terminal initial 60 aa. contain a series of hexameric repetitive amphipathic motifs similar to the ones present in apolipoproteins. This domain is thought to be involved in the interaction of with membrane components. Mutations in this region, like A30P, E46K and A53T, might interfere with the ability to bind membranes and have been associated with early onset and familial forms of PD. The intermediate region, between aa. 61 and 95, has a non-amyloid component (NAC),

a highly hydrophobic region known to fold into a secondary β-sheet conformation and form amyloid fibrils. The C-terminus of the protein is composed of several acidic residues containing negative charges. This terminal region has a Serine at position 129 which is typically phosphorylated in Lewy bodies. This region is thought to be responsible for the labile behavior of α-syn peptide and is known to participate in the aggregation process (Flagmeier et al., 2016; Gallegos, Pacheco, Peters, Opazo, & Aguayo, 2015).

The biological function of α-synuclein has been an object of debate for the last 30 years, and only recently have some of its functions in the normal brain been elucidated. As a result of its ability to bind to lipids, when present, α-syn is found in most intracellular membranes in association with phospholipids and sphingolipids (Galvagnion, 2017). In neurons, α-syn has been implicated in vesicle modulation and release during synaptic activity (Bendor, Logan, & Edwards, 2013; Zaltieri et al., 2015). α-syn has also been proved to participate in vesicle trafficking and chaperoning SNARE's assembly and modulation of dopamine release through simultaneous binding to the phospholipidic membrane and c-terminal of synaptobrevin-2 (Abeliovich et al., 2000; Bonini, 2005; Burré et al., 2010; Diao et al., 2013). As a result, α-syn monomers are thought to be essential for correct interactions between membranes in synapse function. Nevertheless, in pathological conditions α-syn is known to aggregate and form insoluble amyloid bodies. This aggregation can occur in response to α-syn overexpression, pH changes, prolonged exposure to oxidative stress and through interaction with dopamine. Additionally, post-translational modifications like nitration or extensive oxidation can lead to molecular stabilization and increase in cytoplasmic levels of monomeric α-syn levels. When intracellular levels of α-syn reach critical levels, they interfere with normal cellular functions and disrupt vesicle trafficking, lipid biosynthesis, and calcium storage and inhibit normal lysosomal enzymatic activity. Furthermore, stable monomeric forms tend to aggregate and form nonfunctioning oligomers and long polymeric β-sheet rich amyloid fibrils which are the main component of LB (Marques & Outeiro, 2012; Norris et al., 2004). The other two members of the synuclein family, β- and α-synuclein, have long been thought not to aggregate and even at some level protect against amyloid formation both *in vivo* and *in vitro*. Nonetheless, recent studies have been changing that perspective, showing the presence of α-β-synuclein heterodimers as well as β-syn aggregates. γ-syn aggregation is still unclear but seems to be rare or very context specific (Bendor et al., 2013; Galvin et al., 2001; Tenreiro et al., 2016). Interestingly, regardless of the initial trigger for aggregation, amyloid forms of synucleins have been found to contain consistent post-translational modifications. These usually take the form of phosphorylation, ubiquitination nitration in serine and tyrosine or carboxyl-terminal

truncation. The most common of these modifications is the Serine 129 phosphorylation. Presence of these modifications is associated with disease progression and poor prognosis, albeit the causality and effect on disease progression is still unclear (Gallegos et al., 2015; Tenreiro et al., 2016).

Despite constant and progressive α-syn accumulation in the brain being known to accompany neuronal degeneration, the extent to which aggregation of α-syn or its intermediates lead to neuronal death is still not clear (Bekris, Mata, & Zabetian, 2010; Blanz & Saftig, 2016; Galvagnion, 2017; Poewe et al., 2017; Yang et al., 2013). Recent results point to the lipophilic character and conformational flexibility of α-syn along with the widespread presence in the cell as the major causes for α-syn toxicity. Due to its nature, α-syn can take part in a multiplicity of interactions amongst a wide range of membranes and proteins. Four main mechanisms for synuclein induced cell death have been proposed based on damage of different intracellular structures: a) mitochondria, b) proteasome, c) ER, and d) cellular membrane:

a) Mitochondria have long been regarded as one of the most commonly damaged organelles in early neurodegeneration events. Alterations to mitochondrial membranes may cause the release of cytochrome C and trigger apoptosis. This has been proved in *in vitro* where neuronal cells overexpressing α-syn triggered release of cytochrome C and consequent Caspase 3/9 activation and apoptosis (Parihar, Parihar, Fujita, Hashimoto, & Ghafourifar, 2008). Nevertheless this hypothesis has recently been contested, by data that point to α-syn as a mitochondrial protector against oxidative stress and delaying apoptosis (Menges et al., 2017).
b) Deterioration of proteasome function has been reported as a consequence of A53T mutated α-syn expression and consequent oxidative stress (Gallegos et al., 2015). In a pathological context α-syn inhibits chaperone mediated autophagy (CMA) which results in an increase of macroautophagy in an effort to clear up α-syn aggregates (Macedo et al., 2018). Oxidative stress triggers lead-to cellular damage and α-syn aggregation which increases the mitochondrial and proteasome dysfunction (Macedo et al., 2018; Scudamore & Ciossek, 2018);
c) High levels of misfolded protein can lead to ER stress and activate the unfolded protein response (UPR) disturbing calcium homeostasis and activating apoptosis. α-syn also blocks ER-to-Golgi trafficking by blocking the activity of ortholog Rab1, which results in accumulation of immature proteins (Cooper et al., 2006; Mercado, Valdés, & Hetz, 2013; Patel & Witt, 2018);

d) α-syn's ability to bind to membranes can, when in high quantities, interfere with the cellular wall's functions, including porosity, provoking protein or ionic unbalances, which can lead to lysis or degeneration and programmed cell death (Tosatto et al., 2012; Tsigelny et al., 2012; Ysselstein et al., 2015).

Analysis of PD progression revealed that Lewy bodies form in an ascending prion-like manner starting from the lower brain stem or olfactory bulb towards the neocortex. This progression was even more evident in post-mortem analysis of PD patients who had received bilateral intrastriatal transplants of healthy DA neurons. One to two decades after graft transplantation, LB were present and positive for ubiquitin and Ser129 phosphorylated α-syn in the transplanted neurons (Angot et al., 2012; Brundin & Melki, 2017). Different mechanisms have been proposed for α-syn propagation *in vivo*. The first and most common is an alternative exocytic pathway present in neuronal cells. When in stress, neuronal cells encapsulate in vesicles more α-syn both in the monomeric and aggregated form. The origin of these vesicles is still not clear but it's thought that at least a part of them result from a failure in intracellular clearance pathways of which autophagy is the primary example. These vesicles accumulate in the cytoplasm and eventually are released to the exterior. Alternatively, dying cells can extravasate their intracellular contents into the extracellular matrix. Extracellular α-syn is easily internalized due to its small size and membrane affinity and is able to move antero- and retrogradely along the axon (Costanzo & Zurzolo, 2013; Freundt et al., 2012). Finally, the last known method of cell-to-cell α-syn propagation is through the formation of tunneling nanotubes (TNTs). TNTs are intercytoplasmic bridges mainly composed of filamentous actin between adjacent neurons. Recent studies show α-syn moving between TNFs in both neurons and astrocytes (Bieri, Gitler, & Brahic, 2018; Rostami et al., 2017). Withal, the extent to which each type of transmission, frequency and conditions of acquisition of the pathological phenotype in the receptor cell is still largely unknown (Costanzo & Zurzolo, 2013).

Since its original characterization, GD has been thought to be primarily a disease of the reticuloendothelial system, with clear distinction between its visceral and neuronal symptoms. Hence, GD type 1, by definition, was thought to be free of any neuronal manifestations. Nevertheless, throughout the years an association pattern between GD and PD has gradually but forcefully developed. In human genetic studies, the contribution of a particular gene to a disease or phenotype is usually found directly by sequencing large numbers of patients. However, the association between GD and PD has come to us straight from the Medical Genetics clinic. A predisposition for neurological problems in patients that suffered from GD1 has been known for over two decades. This was stated

in sporadic case reports of GD1 patients developing PD-like symptoms such as bradykinesia and dementia, cognitive impairment, autonomic dysfunction, disorders of sleep, depression and hyposmia. Moreover, these symptoms were surprisingly similar to the ones seen in PD, defying the frontiers of what was considered the etiology of GD1. (Sidransky & Lopez, 2012; Yang et al., 2013). These observations of epidemiologic studies were first performed by Neudorfer et al. in 1996 by comparing the phenotype of six GD1 patients regarding their parkinsonian symptomatology. The authors reported a correlation between GD and development of PD. In these patients, PD symptoms developed typically before the 60th year, with frequent onset during their 40th decade of life; furthermore, these patients were more severe and refractory to anti-Parkinson therapy using levodopa. Subsequent populational cohort studies compared the frequency of *GBA1* mutation carriers within PD patients. A large and careful study of PD and Alzheimer patients with Ashkenazi Jewish ancestry revealed a systematic over representation of *GBA1* mutation carriers (N370S, L444P, 84GG, IVS+1, V394L, and R496H) within the PD group only. In fact, consecutive studies determined that, despite the variation between populations, patients carrying *GBA1* mutations represented 2.3% to 9.4% of PD patient group. That value could reach between 10.7 and 31.3% if the patient had Ashkenazi Jewish ancestry. Taking into account that the prevalence of *GBA1* mutations is 5.55% to 7.14% in the Ashkenazi Jewish groups, while in the general population it is estimated to be between 0.6% and 1%, the difference results in a 5 to 7 times higher prevalence in GD patients compared to non GD aged-matched controls (Aharon-Peretz et al., 2004; Sidransky, 2012; Toft et al., 2006). In addition to this data, studies on post-mortem brains of GD1 patients showed presence of a severe form of Lewy body disease extending from *substantia nigra* to the cortex and hippocampus, concomitant with GCase presence. Interestingly, this was true even in the case of *GBA1* mutation carriers which had no manifestation of GD (Lopez, Monestime, & Sidransky, 2016).

Notwithstanding, despite the statistical data and causality regarding the correlation between low GCase activity and accumulation of α-syn, a mechanistic model which explained the predisposition and installment of the disease had to wait until 2011 with the work of Mazzulli et al. In this seminal work, the authors created the first mechanistic model for GD. By knocking out *GBA1* expression in a neuroglioma cell line (H4), the authors of this paper showed accumulation of α-syn. Moreover, iPSc derived neuronal cells from N370S/84GG insertion GD patient reproduced the *in vivo* phenotype with low GCase levels. Interestingly these neuros showed a specific four-fold increase α-synuclein when compared with a WT genotype for *GBA1*. Other neuronal proteins

which are known to aggregate (Tau, huntingtin) did not show any differences (Mazzulli et al., 2011). These results were promptly expanded, first by Panicker et al in 2012, with the reprogramming and differentiating GD Type 1 (N370S/N370S), type 2 (L444P/RecNcil) and type 3 (L444P/L444P) lines onto the neuronal fate. Besides the expected low levels of GCase and increased GlcCer and GSph, these cells showed autophagic impairment (Panicker et al., 2012). Furthermore, even in heterozygosis, *GBA1* mutations RecNcil, L444P and N370S led to both ganglioside and α-syn accumulation as well as autophagic flux blockage and ER-stress with increased calcium levels in the cytoplasm. Indicating that even in the cases which are usually asymptomatic, harboring one *GBA1* mutation can predispose to neurodegeneration (Schöndorf et al., 2014). The effect of a single *GBA1* mutation in the neuronal membrane potential is still not clear since, when submitted to patch clamp experiments, GD type 2 (L444P/P415R; G325R/C342G; L444P:E326K/L444P:E326K) iPSc derived neurons and CBE treated neurons did show a potential difference, but this was not the case in the presence of a WT allele (Sun et al., 2015). More recently Aflaki et al, derived GD iPSc lines (N370S/N370S; N370S/84GG; IVS2+1G>T/L444P) but the derived neurons showed to be electrophysiologically normal. This correlation made *GBA1* mutations the most common risk factor for the development of PD with a 4-to-6year earlier onset and drew a considerable amount of attention. Nevertheless, despite the increased risk, only a small percentage of carriers develop PD. So far, less than 10% of the GD registry show some degree of PD associated symptoms (Rosenbloom et al., 2011). With an overall prevalence of 1% within the general population and as high as 7% among Ashkenazi Jewish populations, mutations in *GBA1* are now considered the most frequent risk factor for PD (Sidransky, 2012). The consistency and degree of this inverse relationship between WT GCase levels and α-synuclein intracellular levels has paved the way for the development of new therapeutic strategies to prevent or halt the progression of PD through increase of GCase intracellular levels and activity in neurons (Aflaki et al., 2016; Sidransky, 2012).

Despite the statistical data and *in vitro* modelling, the mechanism behind the GCase-α-syn connection is still poorly understood. The first mechanistic proposal regarding α-syn accumulation in GD cells came from Mazzulli et al in 2011. In this paper, the authors proposed a positive feedback loop between α-syn levels and GCase activity. Low GCase activity would lead to GlcCer accumulation which would prompt α-syn aggregation. In turn the α-syn fibrils reduce GCase trafficking to the lysosome, further decreasing active GCase, resulting in further GlcCer and α-syn accumulation and amyloid fibril formation (Mazzulli et al., 2011). In 2013, Yap et al, built on this model.

Having proven that α-syn assumes an intralysosomal localization due to it's a-helical structure conferred by its amphipathic repeats, Yap et al proved the existence of a site-specific relation between α-syn and GCase. According to their results, α-syn assumes predominantly an open horseshoe helix conformation on the membrane with its two anti-parallel helices (residues 3-37 and 45-92). GCase's catalytical region lies immediately above the internal membrane-water interface, where it's lipid accessible and active. Structural alterations of α-syn towards a a-helical conformation, changes alters the membrane subtract accessibility and turn over either by occluding GCase's active site or by displacing it away from the interface (T. Yap et al., 2015; T. Yap, Velayati, Sidransky, & Lee, 2013).

Another way in which α-syn was proven to change GCase activity was in its connection to cytoplasmatic GCase. GCase adopts multimeric structures when not associated to a membrane. Sap C is able to stabilize GCase and impede multimerization, enabling docking to lysosomal membrane. Monomeric α-syn competes with Sap C for cytosolic GCase nevertheless does not block multimerization, decreasing the total availability of monomeric GCase able to bind to the lysosomal membrane. The present model thus, would include a direct inhibition of GCase by α-syn at the level of vesicular trafficking, GCase cytosolic availability and activity. Consequently, low GCase level results in a decrease in autophagy and accumulation of GlcCer, GSph and α-syn (Gruschus et al., 2015).

1.6 Human Neurons Derived from Pluripotent Cells as a New *In vitro* Model

Advances in healthcare in the last century have led to a great increase in longevity and consequently, to progressive population ageing specially in the western world. With that, the prevalence of age-related neurological diseases such as dementia, Parkinson's and Alzheimer's have skyrocketed. Contrary to the biggest killers, the available therapeutic options for neurological diseases have little or no influence in the outcome of such diseases, rendering degenerative neurological diseases as some of the most incapacitating. These facts have spurred a massive investment in early diagnostic methods and well as pharmacological models to test new therapeutic drugs (Association, 2015; Reeve, Simcox, & Turnbull, 2014).

Organized in multiple physical and functional layers, the human brain is the most complex system in the human body. Due to the difficulty of obtaining and culturing human brain samples, research in neurobiology has been typically performed in animal or cell models. Primary human neurons are not readily available and when obtainable, difficult

to culture due to their post-mitotic nature. Neuronal cell lines can be obtained by culturing cells from neuronal tumors, or by immortalization of primary neuronal cultures. These cultures allow for large expansions with low variability and virtually unlimited cells numbers. Nevertheless, due to their transformed origin these models have important physiological differences with normal cells, and typically accumulate further genetic alterations while in culture. Animal models allow *in vivo* experiments to be performed and offer a more abundant source of primary cells. However, they also present important disadvantages. Primary cultures of neuronal cells from animals suffer from low expansion and high variability. Importantly, species specific differences between animals and humans can limit the translatability of result obtained with animal cells to the human system (Gordon, Amini, & White, 2013; Korhonen, Malm, & White, 2018). In sum, despite the difficulties of sample procurement and culture, human cell neuronal cultures offer the best experimental option to study human neuron biology, drug screening and species-specific pathophysiological studies. Human or humanized neurons are able to provide disease-specific and genetically contextualized measurable cellular phenotypes. Pathophysiological phenotypes can be observed at a cellular level even in situations in which the phenotype is transient or neuroimaging is inconclusive. Variations in soma size, neurite length, neuronal spine density, potential deficiency can be measured in culture. Additionally, increase in sample input enables the use of biochemical tests like protein levels, enzymatic activity and gene expression and immunohistochemistry as readouts (Adegbola, Bury, Fu, Zhang, & Wynshaw-Boris, 2017; Xu & Zhong, 2013).

In 1998, the first human embryonic stem cell lines were derived from which many types of differentiated cells, including neurons, could be obtained. In the last decade, with the development of human induced pluripotent stem cells (hiPSc), it is now possible to reprogram virtually any adult somatic cell type to a state of pluripotency (Itskovitz-Eldor, 2018). ESc and hiPSc cells can then be indefinitely expanded and guided to differentiate towards the neuronal cell type. Hence, abundant numbers of healthy and patient-specific neurons encompassing several genotypes can be obtained (Mazzulli et al., 2011; Santos & Tiscornia, 2017; Tiscornia, Vivas, & Belmonte, 2011; Tiscornia et al., 2013). The advantages of this system have made it an excellent model for complex or late onset neurological and neuropsychiatric diseases. iPSc based models avoid using animal models with simpler CNS, post-mortem samples which are frequently at the end stage of the disease, or immortalized cell cultures which show a fixed phenotype. Additionally, as the differentiation process mimics human neuronal development *in vitro*, iPSc-derived neuronal cultures offer the possibility of studying development and disease progression (Adegbola et al., 2017; Li et al., 2005; Torrent et al., 2015). Despite the

overall advantages of the system, it is not without technical challenges. Differentiation is usually achieved by extended culture in a multistep procedure involving inhibition and stimulation of biochemical pathways in a temporally defined manner which ultimately induces the cell population towards the intended fate. These protocols may last several weeks and are both cost and labor intensive. The degree of differentiation, purity of the resulting population and the yield of the process introduce considerable noise and variability in the results.

The first protocols to obtain neuronal cells were based on the spontaneous tendency of embryonic stem cells to differentiate to the neuronal lineage in the absence of signaling that maintains the pluripotent state, due to the fact that one mechanism of maintenance of pluripotency is the inhibition of neurogenic differentiation pathways. Culture a suspension of ESc in non-pluripotent favoring conditions (constant agitation of cell suspensions on low adherence plates or the 'hanging drop' method) produce an embryo like structure (embryoid body) which induces exit of the pluripotent state and differentiation to the three germ layers. Pro-neurogenic media formulations result in preferential differentiation to neuronal lineage cell types. However, efficiency is low and mixed populations usually result. Gradually, more efficient protocols were developed. ESc grown on specific stromal cell layers (such as S2, MS5 or PA6) in absence of bFGF (a crucial ingredient of pluripotency maintenance media) resulted in neuronal cultures relatively high percentages (~50-90%) of neuronal cells. Nevertheless, the efficiency was still variable and undesired cell types were present in considerable percentages (Mizuseki et al., 2003; Perrier et al., 2004). Gradually, initial cues, signaling pathways and mechanisms underlying differentiation to the neurogenic fate were worked out by empirical trials inspired in knowledge obtained from studies in developmental biology.

1.7 Neurodifferentiation of hiPSc

The incidence of neurological diseases such as dementia, Parkinson's and Alzheimer's increases with age. Along with the increase in longevity and progressive population aging, the prevalence of these diseases is expected to greatly increase in the next decades. Despite presently being surpassed by cardiovascular diseases and cancer as the main causes of death, its numbers are rapidly growing to the topmost frequent causes of death. Furthermore, the available therapeutic options for neurological diseases have little or no influence in the outcome of such diseases. These diseases tend to severely incapacitate patients and have slow time courses, resulting in high burdens for families, healthcare systems and society at large. This has spurred a

massive investment in early diagnostic methods and well as pharmacological models to test new therapeutic drugs (Association, 2015; Reeve et al., 2014).

Organized in multiple physical and functional layers, the human brain is the most complex system in the human body. Due to the difficulty to obtain and culture human brain samples, research in neurobiology has been typically performed in animal or cancer cells models. Culture of mature neurons is exceptionally hard due to their post-mitotic nature. Neuronal cell lines can be obtained by culturing cells from neuronal tumors, or by immortalization of primary neuronal cultures. These cultures allow for large expansions with low variability and virtually unlimited cells numbers. Nevertheless, these models have important physiological differences and accumulate aberrant genetic alterations while in culture. Animal models, on the other hand, despite more complex and complete, also present important disadvantages such as inter-specific differences and higher variability. Animals can be used for *in vivo* experiments, or as source of neuronal material for primary brain cultures. In the last, neonatal brains are harvested, set in culture and subjected to a specific experimental procedure. Unfortunately, these culture systems suffer from low expansion and high variability. *In vivo* models, complex as they are, simply do not reflect the complexity and uniqueness of the human brain. This has led to the present low degree of prediction and translatability (Gordon et al., 2013; Korhonen et al., 2018). Furthermore, for these reasons, despite lacking the systemic context provided by animal models, cell-based models have been preferred for drug screening and species-specific pathophysiological studies. Human or humanized neurons are able to provide disease-specific and genetically contextualized measurable cellular phenotypes. Pathophysiological phenotypes can be observed at a cellular level even in situations in which the phenotype is transient or neuroimaging is inconclusive. Variations in soma size, neurite length, neuronal spine density, potential deficiency can be measured in culture. Additionally, increase in sample input enables the use of biochemical tests quantifying protein levels, enzymatic activity or gene expression and immunohistochemistry as readouts (Adegbola et al., 2017; Xu & Zhong, 2013).

With the development of hiPSc it is now possible to reprogram virtually any adult somatic cell type to a state of pluripotency. hiPSc cells can then be indefinitely expanded and guided to differentiate towards the neuronal cell type. Hence, abundant numbers of healthy and patient-specific neurons encompassing several genotypes can be obtained (Santos & Tiscornia, 2017). Moreover, the possibility to target differentiation to a concrete brain region, generating cell cultures representative of specific areas of human brain, with its, biochemical and physiological idiosyncrasies, has propelled it to the first line of research as the best alternative for complex or late onset neurological and

neuropsychiatric diseases. Thus, surpassing animal models with simpler CNS, post-mortem samples which are frequently at the end stage of the disease, or immortalized cell cultures which show a fixed phenotype. Finally, since the differentiation process mimics the human neuronal development *in vitro*, iPSc-derived neuronal cultures offer the possibility not only of studying disease progression but also the biochemical and mechanistic forces during human development (Adegbola et al., 2017; Li et al., 2005; Torrent et al., 2015). Nonetheless, despite all the advantages, differentiation is a long and intricate process which through inhibition and stimulation of signaling pathways in a temporally defined manner guides the cell towards a given fate. The final degree of differentiation and the purity of the final neuronal population greatly influences the reproducibility and transferability of the results. The first protocols to obtain neuronal cells were based on default tendency of stem cells to differentiate to the neuronal fate in the absence of pluripotency promoting factors. For example, simply removing bFGF from adherent cultures of hES cells, neuronal phenotypes appear. This can be combined with formation of embryoid bodies (EB) (embryoid body). EBs can be formed by simply dissociating a monolayer culture of pluripotent cells and culturing them either in low attachment conditions or in hanging drop. These floating cells will form an embryo-like spheroid structure which when cultured without pluripotency factors initiates stochastic differentiation into the three germ layers. Nevertheless, the yield of these protocols is very low, and the number of neuronal progenitors is very variable. Plus, extended culture leads to large colonies or EBs with internal necrosis which may result in poor quality cultures. Since those early protocols, a number of protocols were developed, integrating morphogens and molecular cues to direct the differentiation process.

Developmental studies suggested the importance of signaling from the mesoderm. Thus, stromal cell lines were used as substrates for differentiating cultures of Esc in order to increase neurodifferentiation yield. In fact, coculture of hESC or iPSc with a stromal cell line like S2, MS5 or PA6 differentiated with percentages ~50-90% towards the neuronal phenotype. Nevertheless, the efficiency was still too variable and undesired cell types were present in considerable percentages (Mizuseki et al., 2003; Perrier et al., 2004). Another lesson taken from developmental biology was the importance of retinoic acid (RA) in neuronal development. RA was proven to be crucial for neuronal differentiation and regeneration. Concentration differentials of RA in the developing embryo result in neuronal patterning. RA forms a concentration gradient in the antero-posterior axis. In the absence of RA patterning, hindbrain formation does not occur (Maden, 2007). RA has been successfully used in differentiating media in the range of 1-10 μM, depending if the final target are sensory neurons, inter neurons or

motor neurons. In addition to its rule in antero-posterior patterning, RA has been shown to work in coordination with other factors like sonic hedgehog (SHH), fibroblast growth factor (FGF), and bone morphogenic factor (BMP) to determine neuronal fate in the dorso-ventral axis (Baharvand et al., 2007; Dhara & Stice, 2008). BMP is part of the TGFβ (transforming growth factor β) superfamily and is known to have an important and pleiotropic role in the developing nervous system, depending on its temporal and positional expression. It has been associated with early neural induction of neural crest formation. Later in development, it promotes neuronal and astroglial cell formation in detriment of oligodendrocytes. BMP alone seems to specify for forebrain. In association with the SHH (hindbrain specific), BMP seems to induce formation of the ventral forebrain. Thus, early inhibition of the BMP pathway leads to neuro-specific induction. In differentiation protocols, BMP antagonists like noggin have been commonly used both in adherent (laminin/Matrigel) cultures and suspension EB-cultures (Baharvand et al., 2007; Itsykson et al., 2005). Members of the FGF family are known to activate cascades of kinases including Raf (Rapidly Accelerated Fibrosarcoma), MEK (mitogen-activated and extracellular signal-regulated kinase), and MAPK (mitogen activated protein kinase). FGF seems to have a dual activity in neuronal patterning, working as neurogenic in the early stages of differentiation and blocking BMP signaling (Du & Zhang, 2004). Basic FGF (bFGF/FGF2), more specifically stimulates proliferation and cell survival of early forebrain being used and a neuroprogenitor survival and proliferation factor (Mason, 2007; Okabe, Forsberg-Nilsson, Spiro, Segal, & McKay, 1996).

During development, Wnt genes play an essential set of roles. Of the 19 known Wnt genes, several (like Wnt2b, Wnt7a, Wnt7b, and Wnt8b) have been found to be expressed throughout cortical development. They form, along with the receptors Frizzled (Fz) and low-density lipoprotein receptor-related protein (Lrp), a complex spatiotemporal signal matrix that regulates several intracellular pathways, including the activation of the β-catenin pathway. This process, known canonical Wnt pathway, has been reported to promote stem cell self-renewal. An example of that is Wnt1 expression in mouse forebrain which seems to be involved in neuronal expansion by favoring of the neuroprogenitor cell state rather than terminal neurodifferentiation (Hirabayashi et al., 2004). Early gene expression profiling assays also revealed a strong expression of the canonical Wnt pathway components undifferentiated HESCs and stem cell self-renewal (Hirabayashi et al., 2004). Besides signaling for positional information in the anterior-posterior axis, it has been proved to be integral part of the neuronal plate and neural tube specification. Moreover, activation of Wnt signaling promotes neuronal stem cell proliferation and differentiation, inducing dendritic and axon formation and guiding

synapse formation (Mulligan & Cheyette, 2012). When Wnt binds to its receptors Fzd and Lrp, an inhibitory signal is sent through disheveled (Dvl), inhibiting β-catenin phosphorylation by GSK3 and ultimately leading to its degradation. Thus, GSK3's activity is tightly related to β-catenin levels and, consequently, Wnt activity. Hence, it was soon postulated that GSK3 inhibition would allow for stabilization of maintenance of active β-catenin, which would be reflected in increased activity of the Wnt pathway. In fact, chemical inhibition of GSK3 by inhibitors derived from Tyrian Purple Indirubins was able to activate Wnt signaling through β-catenin stabilization and was proved to be able to maintain pluripotency (Meijer et al., 2003; Sato et al., 2005). Nevertheless, the use of inhibitors for human cell differentiation must be as specific and defined as possible. Only in 2004, taking advantage of the KESTREL (kinase substrate tracking and elucidation) a method for identification of kinase substrates, Murray et al, identified Chiron inhibitor CT 99021 (6- nicotinonitrile) (CHIR-99021), so far the most specific GSK3 inhibitor (Cohen & Knebel, 2006; Murray et al., 2004; Xiao, Yuan, & Sharkis, 2006). As research progressed, it became increasingly apparent that *in vitro* differentiation protocols should aim to mimic the temporal sequence of signals occurring during *in vivo* development. However, the first step of differentiation involves destabilization of the pluripotency network, composed of several interconnected pathways. Besides Wnt and FGF, the Nodal/Activin A pathway is involved in pluripotency maintenance (Beattie et al., 2005; James, Levine, Besser, & Hemmati-Brivanlou, 2005; Xiao et al., 2006). Contrary to Wnt/b-catenin activation which is only able to sustain pluripotency of human cells temporarily, Activin A is able to activate Oct4 and Nanog to levels comparable to the ones seen in cell cultured on feeder layer Conditioned Media (CM). Moreover, Activin A activates the Wnt pathway by inducing expression Wnt3 and inhibiting the secreted fizzeled form (SRFP-1); and inducing expression of bFGF and FGF8, thus working as a major regulator of Wnt and FGF signaling pathways. Finally, Activin A acts as a BMP antagonist, reducing Smad1/5 phosphorylation and inhibiting the differentiation signals (Madhu, Dighe, Cui, & Deal, 2016; Xiao et al., 2006).

Since Activin/nodal/TGF-β and BMP-4 compete for Smad4 signal transduction, trophoblast differentiation is thought to be triggered by a stochastic unbalance of these factors, favoring BMP-4 which inhibits the activin/nodal pathway (Wu et al., 2008). Noggin, due to its mammalian origin has been used more frequently in hESC and hiPSc differentiation protocols (Chambers et al., 2009). However, use of recombinant proteins like noggin for clinical applications and routine differentiation protocols is far from ideal: production is considerably more expensive, and the risk of inter-batch variations is higher than in chemical compounds. In 2002, Inman et al (Inman et al., 2002) reported the first

ALK5 selective inhibitor, SB-431542 which albeit being a strong ALK5 inhibitor, also inhibits ALK4 and ALK7 resulting in an undesirable complete inactivation of all activin/TGF-β related Smad-dependent transcriptional activation (Inman et al., 2002; Laping et al., 2002; Patani et al., 2009). Interestingly, while testing dorsomorphin as a BMP antagonist, Chambers et al noticed that a activin/nodal/TGF-b inhibitor (SB431542) and a BMP antagonist promoted a synergistic effect in inducing neuronal differentiation in adherent human ESCs and iPSc, with an efficiency of over 80% despite significant differences in potential within lines (Chambers et al., 2009; Meijer et al., 2003; Surmacz, Fox, Gutteridge, Lubitz, & Whiting, 2012; Zhou et al., 2010). However, dorsomorphin was metabolically unstable and only showed moderate inhibition of Smad1, Smad5 and Smad8. Thus, a derivate compound was synthetized with a higher inhibitory potential for Smad, metabolic stability, and improved pharmacokinetic behavior (e.g. plasma t1/2 = 1.6 h), LDN-193189 which is currently the most used activin/TGF-β inhibitor (Cuny et al., 2008). The last and most recent tool in our differentiation toolbox is N-[N-(3, 5-difluorophenacetyl)-L-alanyl]-S-phenylglycine t-butyl ester (DAPT) which specifically binds to Presenilin-1 and inhibits γ-secretase, blocking the Notch signaling pathway. Besides its newly found effect on promoting nerve regeneration and preventing brain ischemia, Notch inhibition has been proven to direct differentiating cells towards final neuronal commitment in culture conditions (Woo et al., 2009).

The method used in during this thesis follows a state-of-the-art protocol established by Kirkeby et al. in 2013 with minor adaptations. This protocol is based on the accumulated knowledge of several sequential protocols for *in vitro* neuronal induction from pluripotent state (Chambers et al., 2009; Perrier et al., 2004; Zhang, Wernig, Duncan, Brüstle, & Thomson, 2001) . This method is feeder and serum free, substituting traditional fetal bovine serum (FBS) and feeder layer with defined knockout serum replacement (KSR) and Matrigel substrate. Reproducing the stimuli during developmental with small molecules, we were able to mimic the major events which guide cells towards the formation of the neuronal tube and the CNS. through strong dual Smad inhibition, we fine-tuned differentiation by varying SHH and BMP concentrations for dorso-ventral patterning and GSK3 inhibition for rostro-caudal guidance, we managed to generate a reproducible midbrain like neuronal culture. In the present work, fibroblasts from 3 GD type 2 patients harboring different 3 different *GBA1* genotypes were reprogrammed to pluripotency and fully characterized. Two previously reprogrammed and characterized GD type 2 and WT iPSc lines were added to the study. These iPSc clones were then differentiated into the neuronal midbrain phenotype and tested for their GCase levels and activity to confirm the GD type 2 phenotypic hallmarks of low GCase

protein levels and activity. Along with the GCase's protein levels and activity, α-synuclein levels were also measured by WB, in an attempt to test Mazzulli's feedback loop in which GCase's dysfunction leads to α-synuclein which in turn further inactivates GCase. By the 14th day of culture, before starting of the chaperone treatment, all cultures were confluent with no observable morphological difference between GD and WT neurons. These neurons were subjected to a series of 12 chaperones Provided by Dr. J.M Gutierrez, University of Seville from 3 chemical families: iminosugars, such as monocyclic piperidines (MTD131, TMB69, TMB65 and TMB84); bicyclic piperidines (MTD106, MG174, MTD132 and RV21); and nortropanes (MG235, CVI62, DW43 and DW45). some of which have been tested in different genotypes or cell lines but never on human neurons (see Table 5).

Table 5. List and structure of all pharmacological chaperones used during this work.

Monocyclic piperidines	Bicyclic piperidines	Nortropanes (Calisteginas)
MTD131 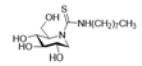 {Mena-Barragán, 2018#507}	**MTD106** 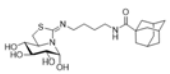 {Aguilar-Moncayo, 2011#245}{Tiscornia, 2013#5}	**MG235** 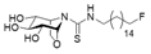 Unpublished
TMB69 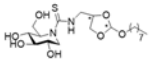 {Mena-Barragán, 2015#133}	**MG174** 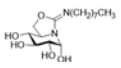 {García-Moreno, 2003#483}{Luan, 2009#244}{Tiscornia, 2013#5}	**CVI62** 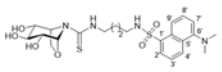 Unpublished
TMB65 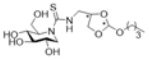 {Mena-Barragán, 2015#133}	**MTD132** 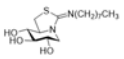 {Mena-Barragán, 2018#507}	**DW43** 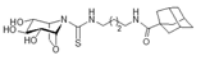 {de la Mata, 2015#243}
TMB84 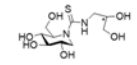 {Mena-Barragán, 2015#133}	**RV21** 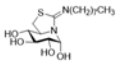 {Aguilar-Moncayo, 2009#505}{Luan, 2009#244}{Tiscornia, 2013#5}	**DW45** 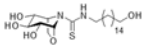 {Alfonso, 2013#242}

In theory, disruption of Mazzulli's serve as both a GD treatment as well as prevention of neuronal loss by α-syn accumulation. Several of our chaperones have been previously tested and proven to enhance GCase activity in different GD models (Table 6). In addition to the screen of these and new chaperones in our model, we aim to compare the effect of the expected increase in GCase activity with the total α-syn levels.

Table 6. Previous results obtained with the chaperones used.

Compound	Treatment duration	Mutations	Best working concentration	Activity variation (fold)	Model	Reference
MTD106	20-60min	none	50μM	3x	Purified enzyme	(Aguilar-Moncayo et al., 2011)
	4 days	L444P/G202R	30μM	3x	iPSc	(Tiscornia et al., 2013)
		L444P/L444P	30μM	no effect	Fibroblasts	(Luan et al., 2009)
		G202R/L444P	30μM	1.5x	Fibroblasts	(Luan et al., 2009)
TMB65	3h	L444P/L444P	50μM	no effect	Fibroblasts	(Mena-Barragán et al., 2015)
MG174	4 days	L444P/L444P	30μM	no effect	Fibroblasts	(Luan et al., 2009)
		G202R/L444P	30μM	3x	iPSc	(Tiscornia et al., 2013)
RV21	4 days	L444P/L444P	30μM	no effect	Fibroblasts	(Luan et al., 2009)
		G202R/L444P	30μM	2x	Fibroblasts	(Luan et al., 2009)
DW45	6 days	L444P/L444P	10μM	3.23x	COS-7 cells	(Alfonso et al., 2013)
DW43	6 days	L444P/L444P	5μM	3.86x	COS-7 cells	(Alfonso et al., 2013)
	96h	L444P/L444P	25μM	1.5X	Fibroblasts	(de la Mata et al., 2015)
TMB65	3h	L444P/L444P	50μM	1,5x	Fibroblasts	(Mena-Barragán et al., 2015)

This page is intentionally left blank

2. Material and Methods

2.1 Cell Culture

Cultures were tested weekly for mycoplasma and discarded if positive. Mechanical passage of pluripotent cells was performed in an *Axioimager* stereoscope (Zeiss) using modified sterile glass pipettes. Incubators in our cell culture facility are kept at a constant temperature of 37ºC, 5% CO_2 and 90% humidity. All cell culture protocols used are described below.

2.2 Patient Derived Wild Type and Gaucher Disease Fibroblasts

Patient cells carrying *GBA1* mutations were gathered from three different sources. Two iPSc lines were provided by CBMR research center, one carrying the L444P/G202R mutation and one Wild type control. Both these lines were reprogrammed via lentiviral vector containing the OSKM factors which were excised through expression of a non-integrative CRE cassette (Tiscornia et al., 2013)

2.3 Fibroblast and PA6 Culture

Human fibroblasts and PA6 mouse bone-derived stromal cells were cultured in complete DMEM media, composed of DMEM (Life Technologies Ref. 21969-035) and supplemented with 10% Fetal bovine serum (Life Technologies Ref. 10270-106), 1x Glutamax® (Life Technologies Ref. 35050-038) and 1x Penicillin/Streptomycin (Life Technologies Ref. 15140-122). Cells were kept at 37°C in a 5% CO2 environment with medium changes every 3 days. When 80-90% confluency was achieved, cells were detached with 0.05% trypsin for 5 minutes at 37ºC, expanded. When required, cells were frozen down for storage in complete DMEM + 10% DMSO (Sigma-Aldrich, Ref. D8418) in a Mr. Frosty™ Freezing Container (Thermo Scientific, Ref. 5100-0001).

2.3 Human Fibroblast Feeder Layer Inactivation

Two fibroblast cell lines were used during the current work to produce feeder layers to reprogram and cultivate iPSc cells: Human dermal fibroblasts (HDF) passage 3, (purchased from Zenbio® (Ref. DF-F)), and Human Foreskin Fibroblasts (HFF) passage

2, (obtained from the Center for Biomedical Research (CBMR)). Frozen vials were thawed in complete DMEM and expanded to subconfluency in 150mm dishes with media changes every 2-3 days. Inactivation was achieved by culturing 90% confluent cultures with DMEM containing Mitomycin-C (Sigma-Aldrich, Ref. M4287) 0.5 mg/mL for 4 hours. Cells were then dissociated in 0.05% trypsin for 5 minutes at 37ºC, counted and frozen down in complete DMEM + 10% DMSO (Sigma-Aldrich, Ref. D8418) in vials of 10^6, $2x10^6$ and $4x10^6$. MitC-HDF/HFF were thawed and plated on gelatin-coated plates at a density of $4x10^6$ on a gelatin (Sigma-Aldrich Ref. G1393) coated 100mm dishes.

2.4 Viral Production

Viral vectors were used to deliver reprogramming factors to cells. Our primary approach was a lentiviral polycistronic vector constitutively expressing Oct4, Sox2, Klf4 and c-Myc (OSKM) and Green Fluorescent Protein (GFP) separated by "2a" self-cleaving peptides. The whole integrative cassette was flanked by LoxP sites (LoxP-OSKM) for future excision upon Cre recombinase expression. Through this system we successfully reprogrammed the genotype A-L444P/L444P. A second vector system was used to reprogram genotypes B-L444P/P415R and C- G325R/C342G. these two genotypes were reprogrammed with the original retroviral system used by Yamanaka. This system consists of 4 independent constitutive retroviral vectors with which one of the OSKM factors. As a production control, PGK-GFP lentivirus and CAG-GFP retrovirus were produced in parallel with the lenti and Retro-OSKM virus, respectively. Viral titer of each harvested supernatant was estimated through counting the number of GFP^+ 293T cells by FACs after transduction of 10^5 cells with 100ul of varying dilutions of viral supernatant (equation 1).It was assumed that these titers represented an acceptable approximation to the titer of the reprogramming vector preparations produced in parallel.

Equation 1. Formula used to estimate viral supernatant titer. Titer (number of viral particles per milliliter) equals the number of 293T cells seeded times the percentage of GFP positive cells (accessed by FACS – between 40-60%), divided by the volume of supernatant used (milliliter) times the dilution used.

$$Titer = \frac{Number\ of\ cells * \%\ GFP\ positive\ cells}{Volume\ supernatant * Dilution}$$

2.4.1 Packaging Plasmids

Reprogramming was achieved with lentiviral and retroviral systems. Third generation polycistronic lentiviral vectors were produced as described by Tiscornia et al, 2006 for lentiviral viral production. Retroviral vector production followed what had been described by Yamanaka et al, 2006 (Takahashi & Yamanaka, 2006; Tiscornia, Singer, & Verma,

2006). Three packaging vectors carrying the essential factors for viral production, pVSV-G, pMDL and pREV (Figure 3) were simultaneously cotransfected into 293T cells. At 48h, 72h and 96h media containing viral particles was harvest and filtered with a 0,22µm strainer.

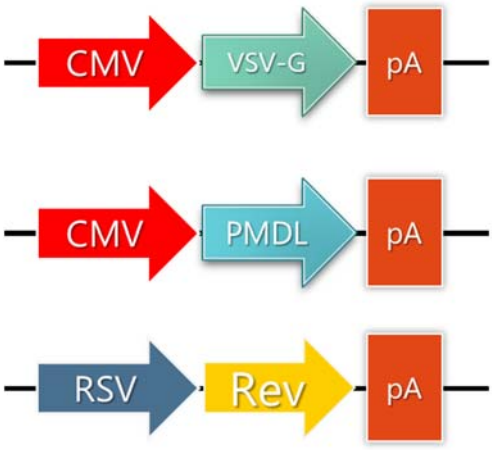

Figure 3. Packaging vector cassette, carrying the necessary factors for viral production VSV-G, PMDL and Rev.

2.4.2 Lentiviral Vector Preparation

Lentiviral supernatant was produced by transfection of HEK 293T cells with the plasmid with the reprogramming factors LoxP-OSKM cassette along with the helper plasmids pVSV-G, pMDL and pREV (Figure 4). In order to achieve this, an overnight culture with $4{,}5x10^6$ HEK 293T per 100mm were transfected with 10 µg of DNA vector plasmid, 6,5 µg of pMDL, 2,5 µg of pREV and 3,5 µg of VSV-G in 970 µl of Sodium Chloride (NaCl) 150 mM with 9 µl of poliethylenimide (PEI) 10 mg/ml after a 5 min incubation, administered dropwise on the cells in complete DMEM. The medium was changed after 16 hours and three consecutive supernatant harvests were done 24, 48 and 72 hs after transfection. Supernatants were filtered through a 0.45µm filter and frozen down at -80ºC in 1 ml aliquots.

Figure 4. Lentiviral reprogramming cassette. Reprogramming factors OSKM and eGFP are separated by 2a self-cleaving peptides and terminates on a PolyA tail (pA). The whole construct is driven by a CAG promoter and flanked by Lox-P sites.

2.4.3 Retroviral Vector Preparation

Individual retroviral vectors carrying the OSKM factors were produced in HEK 293T packaging cell line. These vectors pMXs are derived Moloney murine leukemia virus (MMLV) which contain the viral package signal, transcription and processing elements (Gag-pol fusion proteins). Similar to lentiviral production, retroviral vectors were produced by co-transfection of packaging plasmids pREV and VSV-G in HEK293T cells along with one of the reprogramming factors pMXs-Oct4, Sox2, Klf4, c-Myc. (Figure 5) Three consecutive harvests were performed as with the lentivirus.

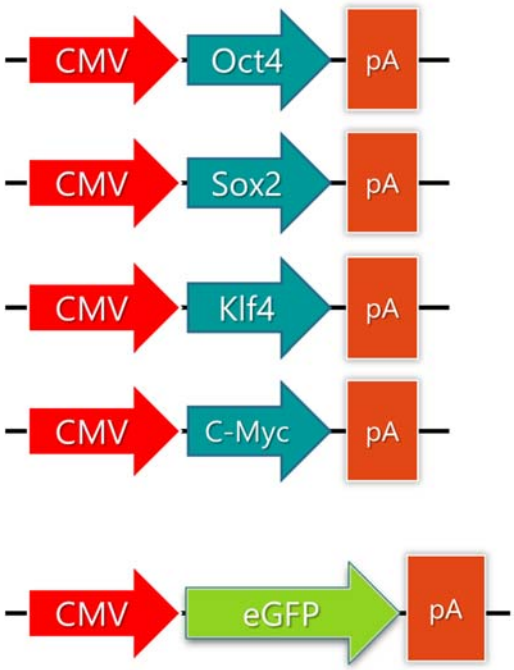

Figure 5. Retrovirus carrying the reprogramming factors and its respective reporter. All retroviral vectors are driven by CMV promoters and end with a poly-A tail (pA).

2.5 Induced Pluripotent Stem cell (iPSc) Derivation

Fibroblasts were thawed and passaged once. When the cultures reached 70% confluence cells were trypsinized and $5x10^4$ cells were seeded per well in 6 well cluster dish) and cultured in complete DMEM. Cells were transduced daily for three consecutive days by adding viral preparation supernatants at a MOI of 10. On the fourth day, the transduced cells were transferred to a previously prepared 6-well cluster dish coated with gelatin and mitcHDF/mitcHFF 0.83 M/well (total of 5M/six-well cluster) and cultured in HES with 10ng/ml bFGF. Medium was changed every 2 days until iPSc colonies appeared and expanded to a fresh feeder when confluent. Fibroblasts with a genotype (L444P/L444P) (called Genotype A) was reprogrammed with a lentiviral LoxP-OSKM

vector with equal stoichiometric expression of the four reprogramming factors which are under the regulation of the same CAG constitutive promoter. Fibroblasts with genotypes (L444P/P415R) (called Genotype B) and (G325R/C342G) (called Genotype C) were reprogrammed by transfection with individual retroviral vectors carrying each the four Yamanka factors. As a transfection control, a well containing the fibroblasts of the same genotype at the same passage was infected either with virus carrying a pSin-CAG-GFP (retro) and Lenti-PGK-GFP, produced in parallel to the reprogramming vectors.

2.6 Induced Pluripotent Stem Cell Culture

After transduction, cells were plated onto mitomycin-c inactivated human fibroblasts and cultivated under pluripotency inducing conditions with daily media changes of Human Embryonic Stem-cell (HES) medium supplemented with basic FGF (bFGF-PreproTech Ref. 100-18B). iPSc colonies were identified by morphology, isolated, mechanically passaged and expanded. If iPSc colonies remained on the same feeder layer for more than 14 days, cells were fed daily with HES media previously conditioned for 48 hs on human fibroblasts, supplemented with 10 ng/ml bFGF. Before differentiation, all iPSc clones were adapted to culture on Matrigel (Becton Dickinson Ref. 356231) substrate. Adaptation to Matrigel consisted in 2 to 3 successive mechanical passages to Matrigel covered dishes containing gradually decreasing density of mitomycin-c inactivated human fibroblasts. Human iPSc were frozen in a 90% HyClone® Fetal Bovine Serum (Thermo Scientific, Ref. SV30143.03), 10% DMSO solution DMSO (Sigma-Aldrich, Ref. D8418).

2.7 *In vitro* and *In vivo* Characterization of iPSc

Newly established iPSc colonies were tested for pluripotency and ability to differentiate into the three germ layers both *in vitro* and *in vivo.* Immunofluorescence analysis was performed in the CMRB (Center of Regenerative Medicine in Barcelona), using the same antibodies and dilutions as described by Watson et al (Watson et al., 2014) (Tiscornia et al., 2013).

2.7.1 Pluripotency Analysis

Sub confluent iPSc cultures of HFF were fixed in 4% PFA for 30 minutes at room temperature and tested by immunofluorescence for expression of the following pluripotency markers: Oct4, SSEA3, Sox2, SSEA4, Nanog, Tra1-60, and Tra1-81 (see Table 7).

Table 7. List of antibodies used in pluripotency analysis. NA – not applied.

Antibody	Host	AB type	Dilution	Fluorochrome	Reference
Anti-Oct4	Mouse	IgG	1:60	NA	Santa Cruz, sc-5279
Anti-SSEA3	Rat	IgM	1:3	NA	Hybridoma Bank, MC-631
Anti-Sox2	Rabbit	IgG	1:100	NA	ABR, PAI-16968
Anti-SSEA4	Mouse	IgG	1:3	NA	Hybridoma Bank, MC-813-70
Anti-Tra-1-60	Mouse	IgM	1:200	NA	Chemicon, MAB4360
Anti-NANOG	Goat	IgG	1:25	NA	R&D, AF1997
Anti-Tra-1-81	Mouse	IgM	1:200	NA	Chemicon, MAB4381
Anti-Mouse IgG	Goat	IgG	1:200	Cy2	Jackson, 115- 225-071
Anti-Rat IgM	goat	IgG	1:200	Cy3	Jackson, 112-165-020
Anti-Rabbit IgG	donkey	IgG	1:200	Cy2	Jackson, 711-225-152
Anti-Mouse IgG	goat	IgG	1:200	Cy3	Jackson, 115-165-071
Anti-Mouse IgM	goat	IgG	1:200	Cy5	Jackson, 115- 175-075
Anti-goat IgG	donkey	IgG	1:200	Cy2	Jackson, 705-225-147
Anti-Mouse IgM	donkey	IgG	1:200	Cy3	Jackson, 715- 165-140

2.7.2 *In vitro* Differentiation

Growing iPSc cultures were mechanically picked and a total of 10-20 fragments were passaged to one ultra-low attachment well and cultured with media formulations designed to induce differentiation to endoderm, mesoderm and ectoderm.

Endoderm

Floating iPSc colony fragments were left in suspension with agitation for 3 days in HES medium, resulting in the formation of embryoid bodies. Twelve medium size EBs were picked and seeded on a slide flask (Thermo Scientific Nunc, Ref. 170920) precoated with gelatin and fed EB media. Medium was changed every 48 to 72 hours for 20 days, after which samples were fixed in PFA 4% (30 min at room temperature) and immunostained with antibodies against the endodermal markers alpha-fetoprotein (AFP -Dako, Ref. A0008) and FoxA2 (R&D, Ref. AF2400).

Mesoderm

Floating iPSc colony fragments were left in suspension with agitation for 3 days in HES medium supplemented with 0.5 mM Ascorbic Acid (Sigma-Aldrich, Ref. A5960), resulting in the formation of embryoid bodies. Twelve medium size EBs were picked and seeded on a precoated slide flask (Thermo Scientific Nunc, Ref. 170920) with gelatin and fed EB media. Medium was changed every 48 to 72 hours for a total of 20 days, after which samples were fixed in PFA 4% for 30 min at room temperature and immunostained with antibodies against the mesodermal markers α-sarcomeric actin (ASA - Sigma Ref. A2172) and α-smooth muscle actin (ASMA - Sigma Ref. A5228).

Ectoderm

Floating iPSc colony fragments were left in suspension with agitation for 4 days N2/B27 medium. Twelve medium-size EBs were picked and seeded on a slide flask precoated with gelatin and 10^6 PA6 cells. N2/B27 media was changed every 48 to 72 hours for a total of 16 days, after which samples were fixed in PFA 4% for 30 min at room temperature and immunostained with antibodies against the ectodermal markers GFAP (Dako #Z0334) and β-III-tubulin (Tuj1) (Covance #MMS-435P).

2.7.3 *In vivo* Pluripotency Analysis

For *in vivo* differentiation potential, frozen vials with mechanically picked iPSc colonies were subjected to teratoma formation and immunostaining analysis. Briefly, these iPSc clones were thawed, picked, treated with *Accutase*® and 1 million iPSc cells were subcutaneously injected into immunocompromised NOD/SCID GAMMA C-/- mice. The animals were sacrificed and the teratomas harvested 8 weeks after injection. After fixation and inclusion, the resulting teratomas were sectioned and stained by immunofluorescence for presence of differentiated cells belonging to the three germ layers with antibodies against the markers for endoderm AFP and Foxa2, ectoderm Tuj and GFAP, and mesoderm ASMA and ASA. Teratoma formation and immunofluorescence analysis was done in the CMRB (Center of Regenerative Medicine in Barcelona), using the same antibodies and dilutions as described by Watson et al (Watson et al., 2014,Tiscornia et al., 2013).

2.8 *In vitro* Differentiation Towards the Neuronal Phenotype

Methods for differentiating iPSc into neurons fall into three distinct categories. The first is a co-culture with an inducer cell line like the bone derived stromal cell line PA6. When

used as a feeder layer, PA6 cells induce neuronal differentiation in iPSc cells. The second method is stepwise differentiation involving embryoid body (EB) formation and expansion or selection of neuronal progenitors. The third and most recent approach is a feeder and serum free two-dimensional monolayer guided through addition and removal of signaling molecules which block and favor different pathways at a specific timepoints. Terminally differentiated neurons can be characterized by their morphology, gene expression, and immunohistochemical stain with neuronal markers. Throughout this project several differentiation protocols were tested for neuronal patterning, focusing in midbrain DA. With the collaboration of our Master students, Ana Rita Martins and Fabio Monteiro, we tested a set of differentiation protocols in H9 ESC line, a WT iPSc line and a GD-iPSc line with genotype D. Several protocols and variations were tested:

(I) iPSc-cell isolation and co-culture with PA6 cells
(II) EB formation and culture in gelatin, laminin and Matrigel
(III) Transduction of lentiviral vector carrying the DA transcription factors ASCL1, NURR1, and LMX1A (Addgene Ref#43918) in a TET-ON fashion
(IV) EB formation followed by co-culture with PA6.

Only IV showed strong differentiation to neurons, with an average of 73% $TUJ1^+$ and 34% TH^+ colonies. Surprisingly, during these tests, the GD-iPSc with genotype D showed the potential for spontaneous neurodifferentiation when dissociated and cultured in Matrigel. Unfortunately, the phenotype was specific to that cell line and a protocol to efficiently differentiate all iPSc clones needed to be developed. With some minor alterations to the protocol published by Kirkeby et al (2013), we were able to consistently generate highly pure neuronal cultures in a chemically defined manner. The different protocols used differentiation are described below:

2.8.1 EB Based Procedure

hESC/iPSc colonies with good pluripotent morphology were selected and mechanically picked under a stereoscope, dissociated to a single cell suspension with collagenase IV and plated in 96-MicroWell™ (VWR Nunc™, Ref. 738-1003) for 72 hours, to induce EB formation. On the third day, the EBs were transferred to a gelatin 0.1% (Sigma-Aldrich, Ref. G1393) coated dish with a confluent PA6 cell substrate. Cultures were cultured in GMEM at 37ºC in a 5% CO2 incubator. Medium was changed every 48 hours for a 21-day period after which the EB-PA6 cultures were fixed and stained for the presence of the neuronal marker TUJ1 and DA marker TH (Martins, 2013).

2.8.2 iPSc Line 21C Spontaneous Differentiation

iPSc cells from genotype D were found to differentiate spontaneously towards the neuronal phenotype when dissociated and seeded under low confluency. Here, well-grown iPSc colonies were incubated for 45 minutes with 10μM iRock Y-27632 (Merck, Ref. MFCD03490488) before manual picking. Suspended colonies were then carefully washed in Dulbecco's Phosphate Buffered Saline (DPBS- Life Technologies, Ref. 14200-067), treated with Accutase (Thermo Fisher Scientific, Ref. A1110501) for 10 minutes and resuspended in mTeSR™1 medium (STEMCELL Technologies, Ref. 05850). This cell suspension was then passed through 70μm Fisherbrand™ cell strainer (Fisher Scientific, Ref. 22-363-548) and counted. Between 20x103 and 200x103 were seeded on a 60mm tissue culture dish previously coated with Matrigel diluted 1:30 (Corning® Matrigel® Basement Membrane Matrix Ref. 356234). A confluent neuronal culture takes 45-60 days, depending on the number of cells seeded. Each dish could be mechanically passaged 1:4 or 1:6. After passage, neurons take on average 14 days to reach confluency (Monteiro, 2016).

2.8.3 Floor Plate Differentiation

Human induced pluripotent stem cells were thawed in mTeSR1™ (Stemcell Technologies) and cultured for 2 passages on Matrigel. The GD genotypes L444P/L444P (genotype A), L444P/P415R (genotype B), G325R/C342G (genotype C) and L444P/G202A (genotype D) were thawed and cultured side-by-side with a hiPSc wild type line. The following protocol was based on a step-by-step differentiation protocol to generate regionalized mesencephalic dopaminergic neurons published by Kirkeby et al in 2013. Before starting, iPSc cultures were carefully observed under the inverted microscope. All colonies which had a differentiated morphology were scraped off the tissue culture dish mechanically with the help of a sterile glass tool. All cultures were then washed with DPBS to remove cellular debris and incubated with EDTA 0,5mM for 5 minutes at 37ºC. The remaining colonies were gently detached by pipetting. The resulting cellular suspension was spun down at low speed for 4 minutes and the EDTA solution aspirated.

Each clone was then resuspended in 2 ml of Neural Induction Media (NIM) + 10 μM Rock inhibitor (Y-27632) + 10 μM TGFβ/ALK5 inhibitor (SB431542) + 50nM BMP4 inhibitor (LDN-1931189) + 200ng/ml SHH + 3 μM CHIR99021 and transferred to an ultra-low attachment 6-well plate (2ml/well). On the second day, EB suspensions were transferred to a 15 ml tube and allowed to settle at the bottom of the tube for 30 seconds. The old media was aspirated and changed for fresh NIM without Rock inhibitor. This

second NIM is supplemented with 10 μM SB431542, 50nM LDN-1931189, 200ng/ml SHH, 0.5 μM Puromorphamine and 3 μM CHIR99021. On the fourth day, medium was changed to Neural Progenitor Media (NPM) supplemented with 10 μM SB431542 + 50nM LDN-1931189 + 200ng/ml SHH + 0.5 μM Puromorphamine + 3μM CHIR99021. EB suspensions were then seeded on 6-well clusters previously coated with Matrigel 1:30 and incubated for 72 hours. On the seventh day, media was changed to NPM with 100nM LDN-1931189 (Stemgent Ref. 04-0074-10), 100ng/ml SHH (Stemgent Ref. 100-45) and 3 μM CHIR99021 (Stemgent Ref. 04-0004-10). On day 11, cells were washed with DPBS and dissociated Accutase (Thermo Fisher Scientific, Ref. A1110501) at 37ºC for 5-10 minutes. Disassociate leftover aggregates were gently pipetted with a P1000. The cellular suspensions were spun down in a 15ml tube at 300× g for 5 minutes and resuspended in 1ml of Neural differentiation media (NDM) supplemented with 20 ng/ml BDNF + 10 ng/ml GDNF + 0.2 mM AA. A total of 250 000 cells/well ~ 132 000 cells/cm^2 were seeded per well of a Matrigel coated 12-well cluster (Sarsted Ref. 83.3921) with 0.5ml of supplemented NDM. Medium was changed every 48h from then on and treated with the respective chaperone molecule from day 14 to day 26, on which cultures were harvested for analysis.

2.9 Chaperone Treatment

Chaperone treatment started 48h after the end of the differentiation protocol, on the 14^{th} day of the experiment. Terminally differentiated neurons were kept in culture and fed NDM. Every 48h the culture was washed with DPBS, the medium changed, and chaperones were added in the concentration present in Table 8, as recommended by the provider (Dr J. M Gutierrez, University of Seville). After 12 days of treatment, media was aspirated, the cells were washed with DPBS and lysed with 75μl of freshly made RIPA buffer, on ice. All protein extracts were aliquoted and frozen at -80ºC.

Table 8. List of the tested chaperones with corresponding solvents, stock and working concentration.

Chaperone	Soluble in	stock (mM)	working concentration (nM)
MTD106	H2O	2	50
MG235	H2O 38% DMSO	2	50
CVI62	H2O 10% DMSO	2	50
MTD132	H2O	2.5	50
MTD131	H2O	2.5	50
TMB69	H2O 10% DMSO	10	50
TMB84	H2O	10	50
MG174	H2O	2	30
RV21	H2O	2	30
DW45	H2O	2	10
DW43	H2O	10	5
TMB65	H2O 10% DMSO	10	5

2.10 Composition of Media Used in Culture

2.11 Somatic Cell Medium

2.11.1 DMEM Complete

DMEM (Gibco #21969-035), 10% FBS (Gibco #10270-106), 1% GlutaMAX (Gibco #35050-038), 1% P/S (Gibco Ref.15140-122).

2.11.2 GMEM Complete

Glasgow's Minimal Essential Medium (Life Technologies, Ref. 21710-025) supplemented with 10% KnockOut™ Serum Replacement (KSR- Life Technologies, Ref. 10828-028), 0.1 mM MEM NEAA (Minimum Essential Medium Non-Essential Amino Acids, Life Technologies, Ref. 11140-035), 0.1 mM β-Mercaptoethanol (Life Technologies, Ref. 31350-010), and 1 mM sodium pyruvate (Life Technologies, Ref. 11360-039).

2.12 Stem Cell Medium

2.12.1 Stem Cell Freezing Media

90% HyClone® Fetal Bovine Serum (Thermo Scientific, Ref. SV30143.03) with 10% DMSO DMSO (Sigma-Aldrich, Ref. D8418).

2.12.2 HES Media

KnockOut™ DMEM (Gibco, Ref. 10829-018), 20%), KnockOut™ Serum Replacement (KSR – Gibco 10828028), 1% MEM Non-Essential Amino Acids Solution (NEAA- Gibco, Ref. 11140035), 1% GlutaMAX™ (Gibco, Ref. 35050038), 0.1% β-Mercaptoethanol (Gibco Ref. 31350010), 0.5% Penicillin-Streptomycin (P/S- Gibco Ref.15140122) and 10ng/ml basic fibroblast growth factor (bFGF- Peprotech Ref. 100-18B).

2.12.3 HES Conditioned Media

Seed 4x10^6 mitC-HFF cells in a 10cm plate. After 24 hours, DMEM complete media was replaced by HES media. Conditioned HES media which had been in contact with the fibroblasts for 24-48 hours was harvested, filtered with a 0.22µm sterile filter and supplemented with 10ng/ml bFGF.

2.12.4 EB media KO

DMEM, 10% FBS, 1% P/S (Gibco Ref.15140122), 1% GlutaMAX (Gibco, Ref. 35050038), 1% MEM NEAA (Gibco, Ref. 11140035), 0.1% β-Mercaptoethanol (Gibco Ref. 31350010).

2.13 Culture Dish Substrate Preparation

2.13.1 Gelatin Coating of Culture Dishes

Culture dishes were coated with gelatin by covering its surface area with a sterile 0,1% gelatin solution for over 1-2 hours at 37ºC. Excess gelatin solution was removed, and the culture dish was used immediately.

2.13.2 Matrigel Coating of Culture Dishes

Matrigel Matrix solution (BD Biosciences, Ref. 356234) was thawed at 4°C overnight and diluted (1:30) in cold Knockout DMEM (Gibco, Ref. 10829-018), laid over the vessel's surface and incubated at 4˚C overnight. Excess solution was removed, and the culture dish was used immediately.

2.13.3 Neuronal Cell Maintenance

<u>N2/B27 media</u>

50% DMEM/F12 (Gibco, Ref. 21331046), 50% Neurobasal™ Medium (Gibco Ref. 21103049), 1% P/S (Gibco Ref.15140122),1% GlutaMAX (Gibco, Ref. 35050038), 0.5% N-2 Supplement (Gibco Ref. A1370701), 1% B-27 Supplement (Gibco, Ref. A3582801).

2.14 Neurodifferentiation

2.14.1 EB method

Glasgow media

Glasgow's Minimal Essential Medium (Life Technologies, Ref. 21710-025) with 10% KnockOut™ Serum Replacement (Life Technologies, Ref. 10828-028), 1 mM sodium pyruvate (Life Technologies, Ref. 11360-039), 0.1 mM MEM NEAA (Minimum Essential Medium Non-Essential Amino Acids, Life Technologies, Ref. 11140-035), and 0.1 mM β-Mercaptoethanol (Life Technologies, Ref. 31350-010).

2.15 Floor Plate Differentiation

To induce stepwise neuronal differentiation, several supplements and small molecules were added and removed from the media at different time points (see Table 9). Media composition and timepoints are listed below.

Table 9. List of reagents used during the differentiation protocols

Supplement	Supplier	Reference
Recombinant Human GDNF	PeproTech	450-10
Recombinant Human BDNF	PeproTech	450-02
Recombinant Human Sonic Hedgehog (SHH)	PeproTech	100-45
Recombinant Human FGF-8 (FGF-8b)	PeproTech	100-25
Recombinant Human TGF-b3	PeproTech	100-36E
DAPT (Inhibitor of g-secretase)	Tocris Biosciences	2634
SB 431542	Tocris Biosciences	1614
LDN-193183	Stemgent	04-0074-10
Purmorphamine	Stemgent	04-0009
CHIR99021	Stemgent	04-0004-10
Rock inhibitor (Y-27632 dihydrochloride)	Merck	MFCD03490488
cAMP (N6,2"-O-Dibutyryladenosine 3":5"Cyclic)	Sigma-Aldrich	D0627
N-2 Supplement	Gibco	17502-048
B-27 Supplement	Gibco	17504-044

2.15.1 Neural Induction Medium (NIM)

DMEM/F-12: Neurobasal (1:1), 1× N2 (life technologies, Ref.17502-048), 1× B27 (GIBCO, Ref. 17504-044), 2 mM L-Glutamine (1:100).

NIM supplementation

Day 0 to day 2: Rock inhibitor (Y-27632 (10 μM)) + TGFβ/ALK5 inhibitor (SB431542 (10 μM)) + BMP4 inhibitor (LDN-1931189 (50nM) + SHH (200ng/ml) + Puromorphamine (0.5 μM) + CHIR99021 (3 μM)

Day 2 to day 4: SB431542 (10 μM) + LDN-1931189 (50nM) + SHH (200ng/ml) + Puromorphamine (0.5 μM) + CHIR99021 (3 μM).

2.15.2 Neural Proliferation Medium (NPM)

DMEM/F-12: Neurobasal (1:1) + 0.5× N2 (1:200) + 0.5× B27 (1:100) + 2 mM L-Glutamine (1:100)

NPM supplementation

Day 4 to day 7: SB431542 (10 μM) + LDN-1931189 (50nM) + SHH (200ng/ml) + Puromorphamine (0.5 μM) + CHIR99021 (3 μM).

Day 7 to day 9: LDN-1931189 (100nM- Stemgent Ref. 04-0074-10) + SHH (100ng/ml - PeproTech 100-45) + CHIR99021 (3 μM- Stemgent Ref. 04-0004-10).

Day 9 to day 11: LDN-1931189 (100nM) + SHH (100ng/ml) + CHIR99021 (3 μM – Stemgent Ref. 04-0004-10).

2.15.3 Neural Differentiation Medium (NDM)

Neurobasal, 1× B27 (1:50) + 2 mM L-Glutamine (1:100)

NDM supplementation

Day 11 to day 23: BDNF (20 ng/ml– PeproTech Ref. 450-02) + GDNF (10 ng/ml – PeproTech Ref. 450-10) + Ascorbic acid (0.2 mM - Sigma-Aldrich Ref. A5960) + db-cAMP (500 μM - Sigma-Aldrich Ref. D0627) + DAPT (1μM – Tocris Biosciences Ref. 2634).

2.16 Imaging

2.16.1 Pluripotency and Differentiation Potential

Neuronal culture characterization

Differentiation efficiency and degree of commitment of the neuronal cultures was accessed through immunocytochemical stain for the neuronal marker TUJ1, the neuroprogenitor marker *Nestin*, TH for DA neurons and GFAP for the presence of glial cells. Terminally differentiated neuronal cell cultures were fixed with 4% paraformaldehyde (Sigma-Aldrich, Ref. P6148) for 20 minutes at room temperature (RT), washed with 1x DPBS, permeabilized for 5 minutes in 1% Triton X-100, washed in DPBS and blocked in Blocking solution (6% Donkey Serum with 0.2% Tween-20 in DPBS) for 90 minutes. Primary antibodies were diluted in blocking solution at the appropriate dilution and incubated overnight at 4ºC. After washing the cultures with DPBS, the cells were incubated with compatible *AlexaFluor*® fluorescent antibodies for 60 minutes at RT, washed and marked with DAPI (4',6-diamidino-2-phenylindole, dilution 1/1000, Sigma-Aldrich, Ref. D9542) (1:1000). Each AB stain contained a control sample in which the primary antibody was removed. Fluorescence detection and visualization was done in an *Axioimager Z2* microscope (Carl Zeiss) with *AxioVision* software. A list of all antibodies used for neuronal characterization are described in Table 10.

Table 10. Antibodies used to characterize the neuronal cultures.

Antibody	Supplier	Reference	Host	Dilution
Anti-β-III-Tubulin (TUJ1)	Covance	MMS-435P	Mouse	1:1000
Anti-Tyrosine hydroxylase (TH)	Sigma	T8700	Rabbit	1:200
Anti-Nestin	Abcam	ab6142	Mouse	1:200
Anti-Alexa Fluor Donkey anti-mouse 594 nm	Invitrogen	A21203	Donkey	1:200
Anti-Alexa Fluor Goat anti-rabbit 488 nm	Invitrogen	A11008	Goat	1:200

2.17 Biochemical analysis

2.17.1 Western Blot

Protein quantification

Protein samples were diluted 1:5 to 30ul, and 10ul of each standard or unknown sample were transferred into a microplate well (working range 125-2000ug/ml). Two hundred microliters of BCA working reagent (Pierce™ BCA Protein Assay Kit, Ref. 23225) were added to the well. The plate was covered, thoroughly mixed on a plate shaker for 30 seconds and incubated for 30 minutes at 37ºC. After reaching RT and absorbance was measured at 562nm.

Western blot analysis

Terminally differentiated neurons from genotypes A, B, C, D and WT were incubated with chaperones for 10 days, after which the cells were harvested in RIPA buffer, aliquoted so that each sample would only thaw once and frozen down at -80ºC. Protein concentration was determined with the Pierce™ BCA Protein Assay Kit (Thermo Fisher, Ref. 23225) and 30µg whole protein extract were denatured (90ºC 10 min with loading Buffer), run on a 12% SDS-polyacrylamide gel electrophoresis and transferred to an activated PVDF membrane (Amersham™ , Ref. GE10600021) in a wet transfer system (Bio-Rad). Protein carrying membranes were fixed in 0.4% paraformaldehyde for 30 minutes, washed and blocked with a 5% PBST solution (blocking solution) for 1 hour at RT. Blocked membranes were cut at the 35KDa protein marker level, resulting in two blots (above and below 35KDa) and incubated overnight at 4ºC with blocking solution containing the respective primary antibody in the optimized concentration (see Table 11). On the following day the membranes were washed and incubated with blocking solution containing the secondary anti mouse-HRP (horseradish peroxidase) IgG antibody for 1

hour at RT. Protein was detected by chemiluminescent reaction to ECL HRP Substrate (Nzytech, Ref. MB19301).

Table 11. Antibodies used in Western Blot analysis.

Antibody	Host	Dilution	Mono/Pol	Brand	Brand Ref
Anti-GCase	Mouse	1:1000	Monoclonal	Sigma	WH0002629M1-100ug
Anti-α-syn (42/α-syn)	Mouse	1:1000	monoclonal	BD	610786
Anti-β-Actin	Mouse	1:100000	monoclonal	Sigma	A5441
Anti-Mouse IgG Peroxidase conjugated	Goat	1:10 000	Monoclonal	Jackson ImmunoResearch	115-035-003

2.17.2 GCase activity

Acid-β-glucosidase enzymatic activity assay

Whole protein samples were thawed on ice and diluted 1:2 with a pre-chilled phosphate citrate solution to a total volume of 35ul. GCase enzyme activity was determined in triplicate. Each well was loaded with 10ul of sample (phosphate-citrate buffer in the negative control), 20ul of fresh substrate solution (4-MU-b-d-glucopyranoside) and left to incubate for 1 hour in a 96 well plate (Lumox® multiwell, 96 - Sarstedt Ref. 94.6120.096). Enzymatic activity was stopped with 200ul of Glycine buffer, kept on ice protected from light and read. A calibration curve with 8 sequential dilutions of the fluorescent component 4-MU [4-methylumbelliferone] was added to the plate and measured in an Infinite M200 (Tecan) microplate reader (excitation at 365nm emission at 448nm).

Substrate solution

A freshly made 4-Methylumbelliferyl β-D-glucopyranoside (4-MU-β-D-Glucopiyranoside) solution was consistently used, kept at 4ºC or in ice and protected from light. In order to prepare 100ml of substrate solution, 0.169g of 4-MU-β-D-Glucopiyranoside (Sigma-Aldrich, Ref. M3633) and 0.3g Sodium taurocholate hydrate (Sigma-Aldrich, Ref. 86339) were weighed and dissolved in Phosphate-Citrate buffer PH 5,8 with 100µl of Triton-X (Sigma-Aldrich, Ref. 93443).

Phosphate-Citrate solution

Phosphate-Citrate solution is composed of 0.2M Phosphate (sodium phosphate, Sigma S-0876) and 0.1M Citrate (Sodium Citrate Tribasic Dihydrate, Sigma-Aldrich, Ref. S4641) solution adjusted to PH 5,8 and autoclaved.

Glycine buffer

To prepare 100ml solution, 20mM Glycine Sigma-Aldrich, Ref. G8898), 12.5mM Sodium Carbonate (Sigma-Aldrich, Ref. 451614), 16mM of NaOH (Merck, Ref. 1.06498.1000) were dissolved in miliQ H20 and the PH adjusted to 10.8.

Standard curve

A calibration curve was achieved using 4-MU (4-Methylumbelliferone - Sigma-Aldrich, Ref. M1381). 4-MU was resuspended in DMSO to a final concentration stock concentration of 10mM. Serial dilutions (see Table 12) were made in ethanol absolute.

Table 12. Serial dilution of standard reagent 4-MU used in GCase activity calibration curve.

Tube	**Stock**	**A**	**B**	**C**	**D**	**E**	**F**	**G**
µM	10000	100	25	12.5	6.25	3.13	1.6	0
Vol ethanol (µl)	0	990	75	50	50	50	50	50
Vol previous solution (µl)	-	10	25	50	50	50	50	0
Dilution factor	-	100	4	2	2	2	2	-
Total vol (µl)	-	1000	100	100	100	100	100	50

3. Results

3.1 iPSc Derivation and Characterization

Since its early development by Yamanaka et al, several reprogramming protocols have been reported, varying in type and number, as well as delivery method. Choice of the most adequate method depends on factors such as the abundance and phenotype of the initial cell type, as well as the final use foreseen for the resulting reprogrammed cells. While therapeutic applications tend to require genomically intact iPSc lines, applications such as disease modelling and drug screening platforms are more forgiving in this regard. When reprogramming vector integration into the host genome is not a major concern, integrative lentiviral and retroviral vectors offer the most practical reprogramming method. Starting with low passage fibroblasts from type II GD patients, three genotypes (A, B and C – see Table 13) were reprogrammed through exogenous expression of the OSKM factors delivered by viral transduction of lentiviral (genotype A) and retroviral (B and C) vectors. Lenti- and retro-GFP virus produced in parallel with reprograming vectors were used as transduction efficiency reporters. Reprogramming factors were delivered in a multiplicity of infection (MOI) of 10.

Table 13. Details and genotype of cells used during the current work.

Clone	Genotype	Origin	Reprogramming	Cell type at arrival
WT	Wild type	(Tiscornia et al., 2013)	Non-integrative lentivirus (OSKM)	iPSc
A	L444P/L444P	(Luan et al., 2013)	Lentivirus (LoxP-OSKM)	Fibroblast
B	L444P/P415R	Coriell - GM01260	Retrovirus (O, S, K, M)	Fibroblast
C	G325R/C342G	Coriell - GM02627	Retrovirus (O, S, K, M)	Fibroblast
D	L444P/G202R	(Tiscornia et al., 2013)	Non-integrative lentivirus (OSKM)	iPSc

Morphological changes were evident between the 5th and the 10th day after transduction (Figure 6). Colonies were allowed to grow for a month or until the iPSc morphology of clearly defined colonies appeared. The best-looking colonies were selected under an inverted microscope and individual clones were mechanically passaged to a fresh feeder layer. Genotypes D and WT were previously established and characterized by Prof. Gustavo Tiscornia (Tiscornia et al., 2013). These clones were thawed, expanded and cultured to re-establish iPSc lines for this work.

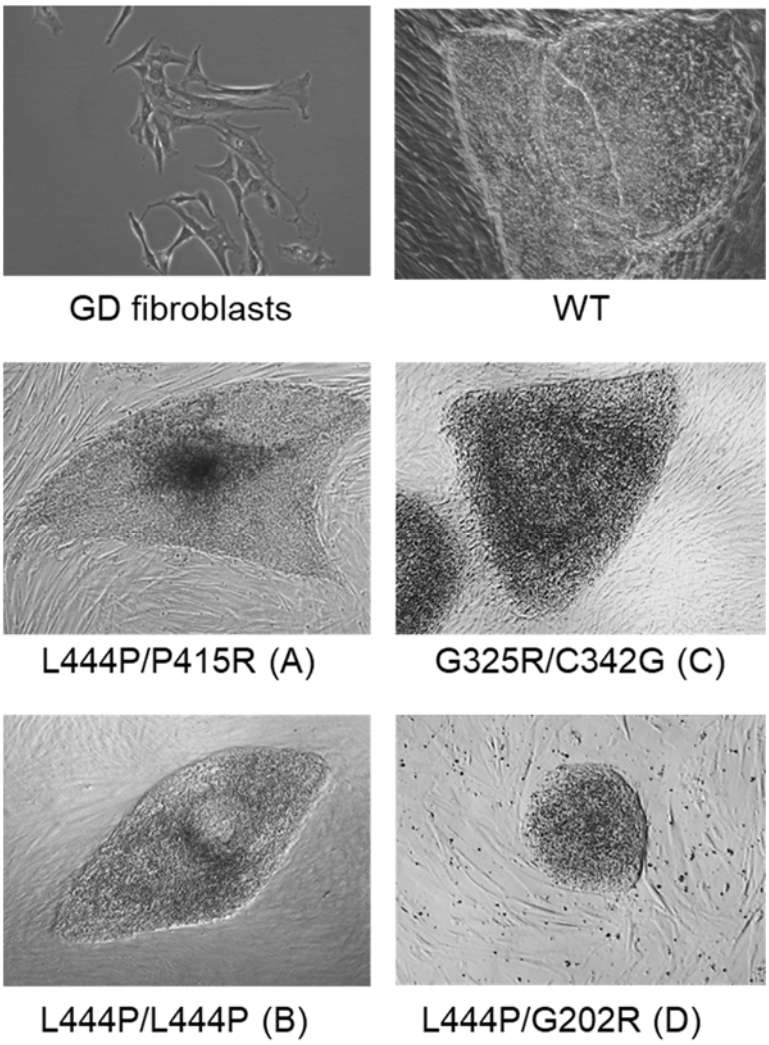

Figure 6. Contrast phase pictures of GD cells. GD type 2 primary fibroblasts were transduced with viral vectors containing the reprogramming factors Oct4, Sox2, Klf4 and c-Myc. Approximately one week after transduction, iPSc colonies developed. These cultures were expanded and individual colonies , re-expanded and frozen. Representative pictures of the growing GD fibroblasts and resulting iPSc colonies (A, B and C) grown on mitomycin-C inactivated HFF feeder layer at passage 2. Wild type (WT) and genotype D iPSc were thawed and cultured in the same condditions as the new clones. Photos taken in phase contrast 40x magnification.

Established iPSc cell lines were demonstrated to be pluripotent by ascertaining the presence of pluripotency markers. Slide flasks with growing pluripotent iPSc colonies were fixed tested by immunohistochemical analysis for the presence of the pluripotency markers Oct4, SSEA3, Sox2, SSEA4, Nanog and Tra1-60 (Figure 7).

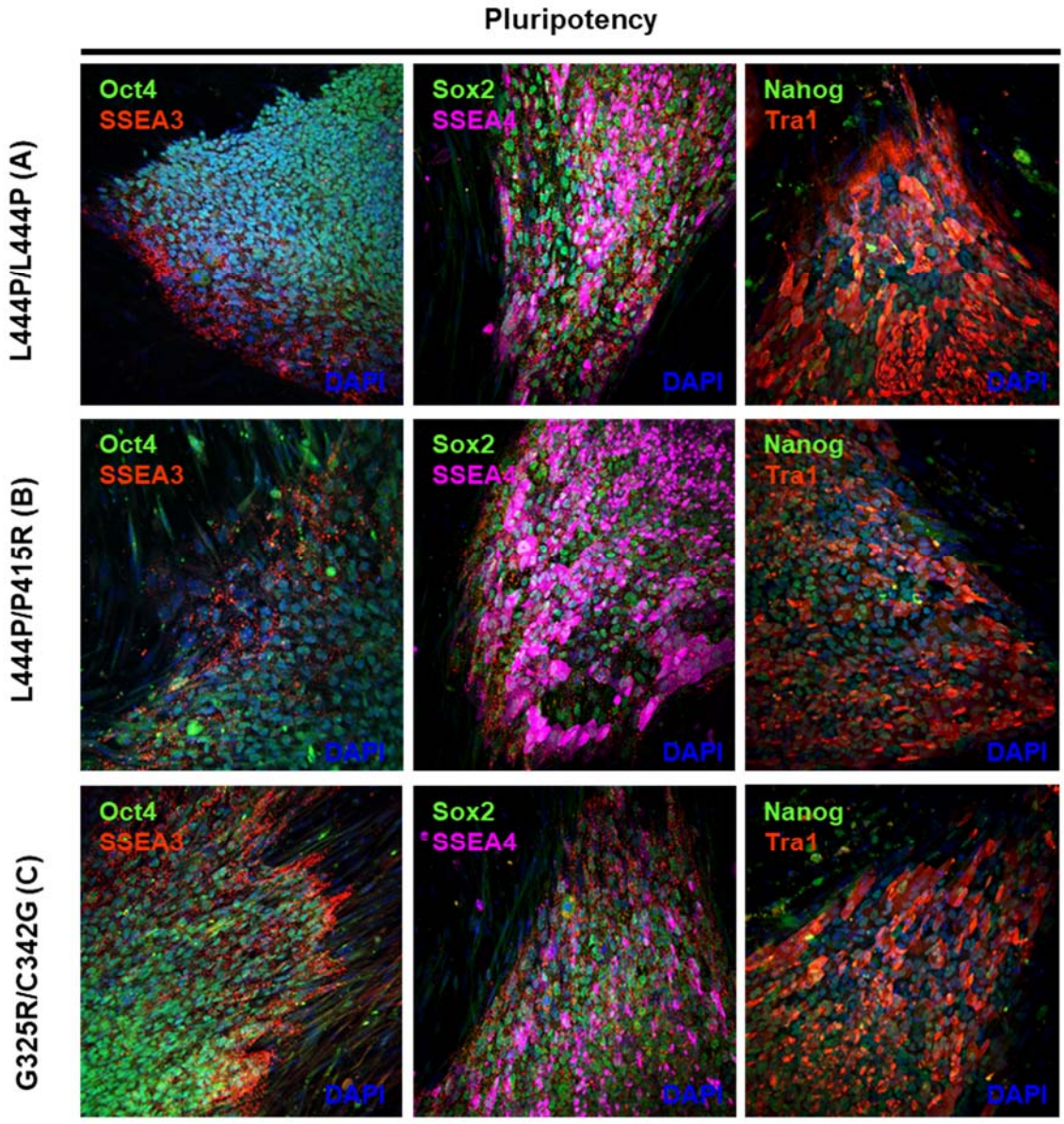

Figure 7. *In vitro* pluripotency characterization of GD iPSc clones. In order to confirm the pluripotent nature of the generated clones, they were expanded, fixed and stained for the presence of the pluripotency markers Oct4, SSEA3, Sox2, SSEA4, Nanog and Tra-1. Magnification 40x.

In vitro differentiation followed standard EB-based differentiation protocols. All clones showed both the pluripotency markers and ability to differentiate towards the 3 germ layers *in vitro*. As seen in Figure 8, all clones tested positive for the presence of endoderm markers, alpha fetoprotein (AFP) and FoxA2; mesoderm, α-smooth muscle actin (ASMA) and α-skeletal actin (ASA); ectoderm markers, β-III-Tubulin (Tuj1) and glial fibrillary acidic protein (GFAP).

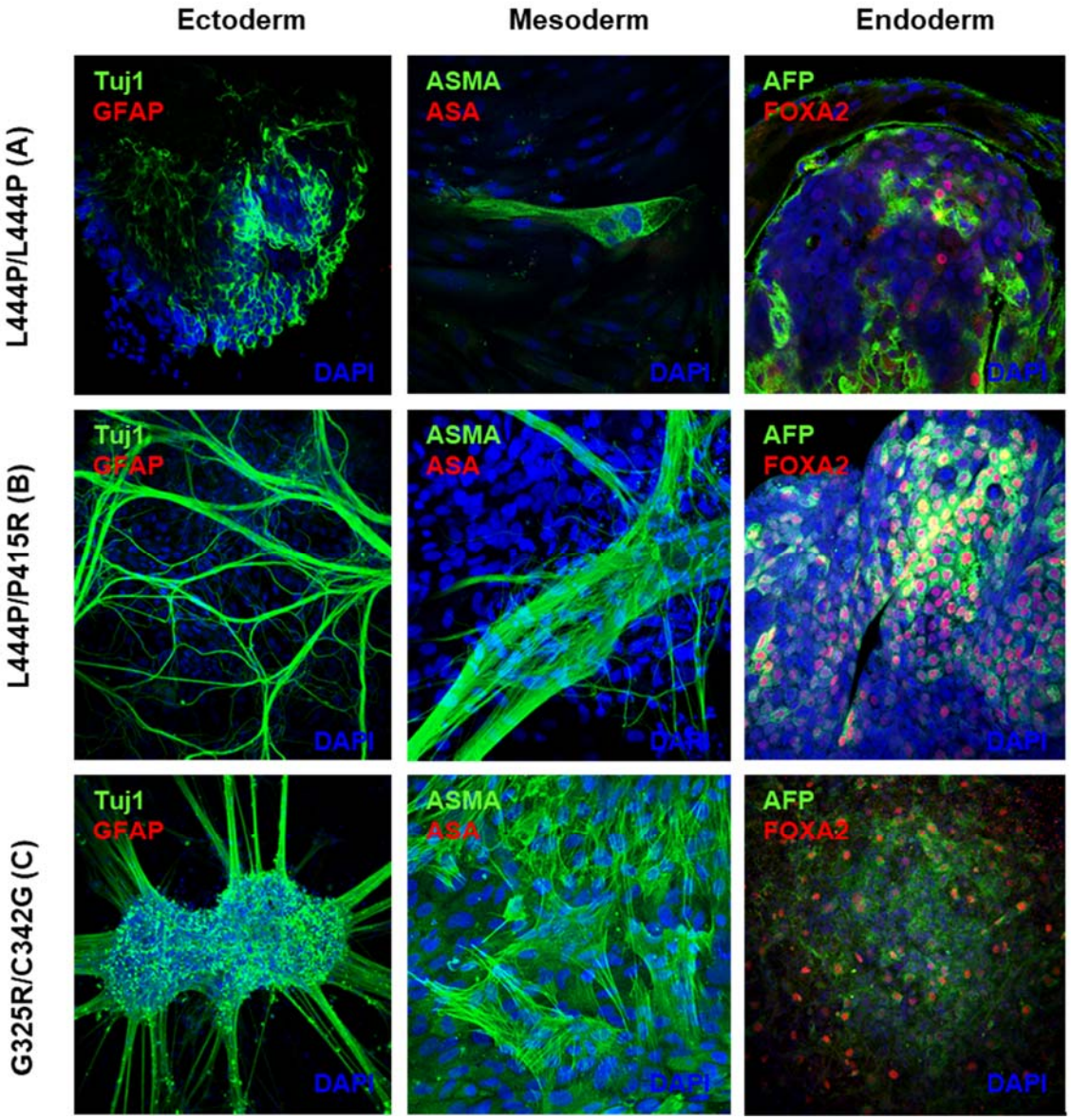

Figure 8. *In vitro* differentiation of GD iPSc clones. In order to confirm the differentiation potential of our clones, they were subjected to standard EB-based differentiation protocols towards endoderm, mesoderm and ectoderm. Slides were then stained for the presence of Tuj1-GFAP, as ectoderm, neuronal markers; AFP-FOXA2 for mesoderm and alpha smooth muscle actin as an endoderm marker. All clones showed both the pluripotency markers and ability to differentiate towards the 3 germ layers. Magnification 40x.

To test for *in vivo* differentiation capability 10^6 iPSc cells were subcutaneously injected into immunocompromised SCID mice as indicated in Materials and Methods. These animals were sacrificed 8 weeks after injection and the resulting teratomas were harvested, fixed, sectioned and analysed by immunofluorescence with the same antibodies used for the *in vitro* differentiation. Similar to what has been seen *in vitro*, all tissue samples contained cells belonging to the three germ layers (Figure 9), being positive for differentiated cells in mesoderm (ASMA and ASA), endoderm (AFP and FoxA2) and ectoderm (Tuj1 and GFAP). Therefore, the iPSc developed in this work met standard criteria for pluripotency.

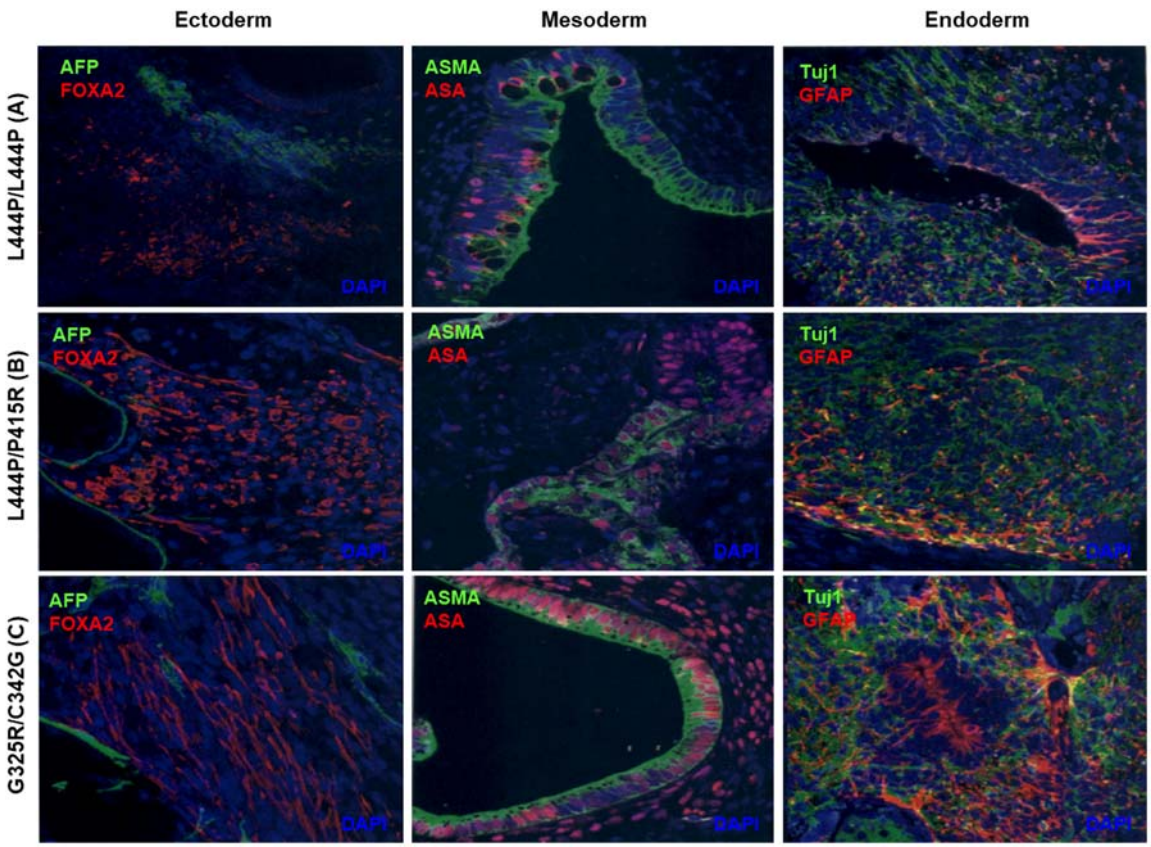

Figure 9. IHC characterization of GD iPSc clones for *in vivo* differentiation. Immunocompromised mice were injected with one million cells and the resulting teratoma was stained for presence of cells belonging to mesoderm (ASMA; ASA), endoderm (AFP; FoxA2) and ectoderm (TUJ; GFAP). All clones successfully differentiated towards the three germ layers.

3.2 iPSc Differentiation and Characterization

Initially we attempted differentiation of neural progenitors from pluripotent stem cells by either co-culture with stromal cell line PA6, or through a multistep EB based method guided by molecular signalling molecules like Sonic hedgehog (SHH) or fibroblast growth factor (FGF8). As described below, these protocols yield heterogenous and variable populations that lack the purity necessary for drug testing. Here we tested several differentiation protocols on our iPSc clones. Surprisingly, one of our clones (genotype D), was capable of spontaneous differentiation to the neuronal fate. For the other genotypes (A, B and C), we started with a combination of EB-based differentiation with PA6 co-culture and progressed to an adaptation of Kirkeby's feeder and serum free multi-step regionalized neuronal differentiation. Due to our interest in the mechanistic connections between GD and PD, we sought to direct differentiation towards the midbrain phenotype, with a predominance of DA neurons, the neuronal type most severely affected in PD. Terminally differentiated cultures were stained by

immunofluorescence for the presence of the neuronal markers β-III-tubulin (a neuron-specific marker) and Tyrosine hydroxylase (TH) (a marker of dopaminergic neurons). DA neurons should stain for both β-III-tubulin and TH. The results from each of the protocols tested are described below.

3.1.1 EB Based Differentiation

Based on what had been described in literature, an EB based differentiation protocol was used to produce neuronal cultures from GD iPSc clones. Using an initial protocol previously established in our lab (Master thesis of Ana Martins, 2013), we obtained differentiated cultures with abundant cells staining positive for β-III-tubulin. Overall, 50% of neuronal rosettes were β-III-tubulin $^{+}$. β-III-tubulin - TH double positive cells were also detected (Figure 10), albeit with less frequency and noticeable variability between experiments. Additionally, since the differentiation protocol involves culturing embryoid bodies which are subsequently induced to attach to a substrate, the procedure results in a 3D mass of cells which are, for the purpose of drug testing, less convenient than a monolayer of cells, as the treatment may affect cells differently depending on their position in the cellular mass. Therefore, this differentiation protocol was not used further (Martins, 2013).

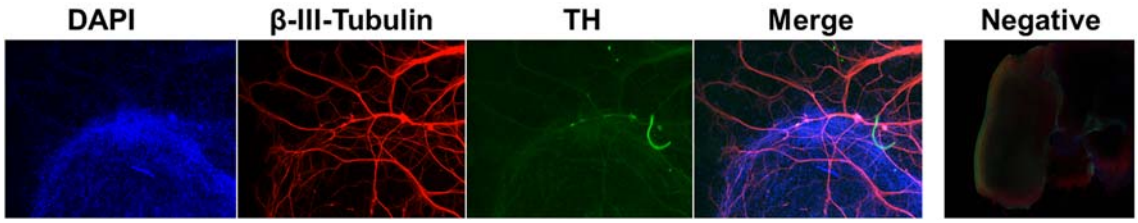

Figure 10. Immunofluorescence analysis of EB on PA6 based neurodifferentiation. Terminally differentiated cells were marked with antibodies against β-III-tubulin (TUJ1) and TH. Negative control was performed without using primary antibodies during the IHC protocol. Representative picture showing strong β-III-tubulin (Tuj1) signal with sparced TH-positive cells. Magnification 40x.

3.1.2 Spontaneous Differentiation

Every iPSc cell line behaves in a singular way in culture, depending on their background genotype and epigenetic status, as well as past culture conditions, iPSc cell lines tend to have idiosyncratic behaviours during differentiation protocols. Genotype D reached our lab as an established iPSc cell line and was thus used in preliminary optimization of differentiation protocols, involving culture on both mitC-HFF feederlayers and Matrigel-coated cell culture plastic. In collaboration with a lab colleague (Fabio Monteiro) we found that this iPSc line (genotype A) has an intrinsic tendency to differentiate towards the neuronal fate when cultured at very low density on Matrigel coated surfaces, even when

cultured in pluripotent media. Whole iPSc colonies were picked mechanically, disassociated with *Accutase*® into a single-cell suspension, strained, seeded at a density of $9x10^3$ cells/cm^2 on Matrigel and fed with mTesR1 media. Neuronal-like cells, distinguishable by elongated axons and characteristic networks after the second day, grew to a fully confluent culture within a month. Well-grown dishes could be split into new Matrigel covered dishes by a mechanical passage (Figure 11). Under these culture conditions, cultures generated a monolayer of neurons enriched in dopaminergic neurons. Unexpectedly, maintenance of pluripotency conditions was crucial for culture growth and neuronal differentiation. We attempted to improve neuronal growth by increasing seeding density, using gelatine and poly-ornithine as substrates culturing cells in presence of N2/B27 rich media; however none of these variations increased growth or differentiation rate, and in the case of N2/B27, resulted in high cell death during the first passage and complete culture arrest (data not shown).

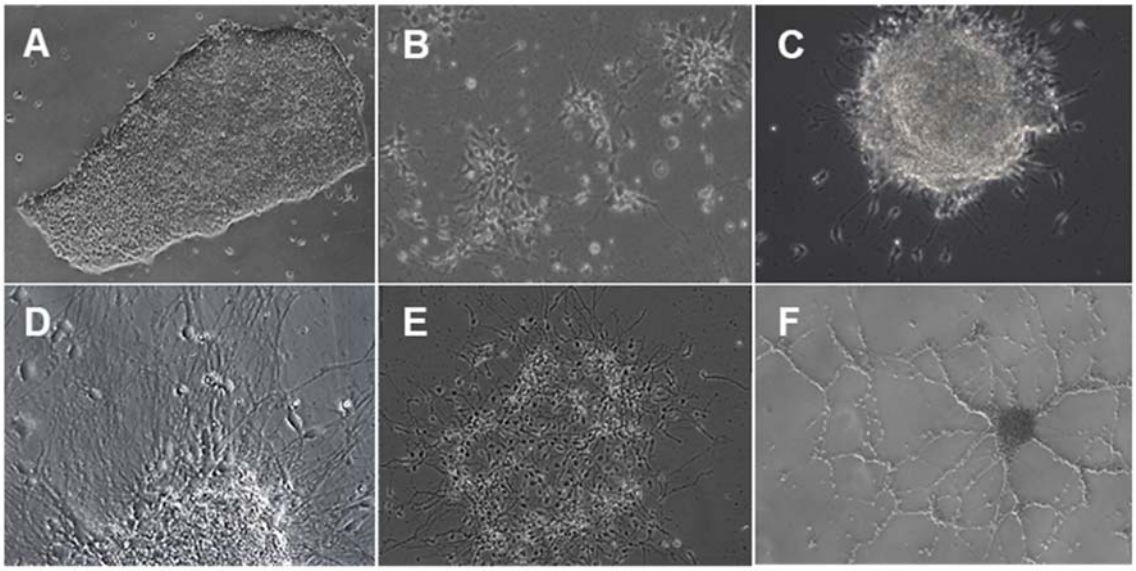

Figure 11. Pictures of clone L444P/G202A during culture. Pluripotent iPSc cells cultured in MG (A-40x) were dissociated with accutase and seeded on MG.48h after seeding, neuronal rosettes appear (B-100x) and grew into neuroprogenitor-like colonies (C-40x) which extend along the dish(D-40x). Mechanically split colonies rapidly grow from small rosettes (E-100x) to a higly plure neuronal network (F-40x).

As seen in Figure 12, immunohistochemistry analysis conducted with antibodies against β-III-tubulin (TUJ1) for neurons, and TH a DA marker showed that, relative to EB on PA6 based differentiation, this method generated a highly pure neuronal culture with a higher percentage of DA neurons.

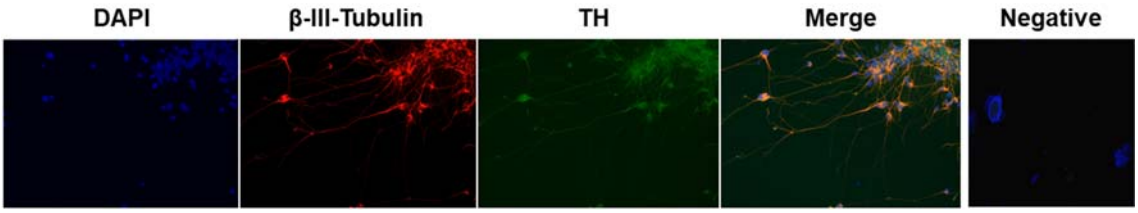

Figure 12. Immunofluorescence analysis of L444P/G202A spontaneous neuronal differentiation. Single cell iPSc cells were seeded on MG in mTesR1 and left to grow for 3 weeks. Sub confluent cultures were stained with antibodies against β-III-tubulin (Tuj1) and TH. Negative control was performed in absence of primary antibodies during the IHC protocol. 40x magnification.

The fact that this iPSc line could be cultured and expanded, retaining its pluripotent morphology, and generating neurons when plated at low density, even in pluripotent media, indicates that the line has extremely high propensity of differentiation towards the neurogenic fate. This differentiation protocol was robust and reproducible but failed to work for the other genotypes in this study. Therefore, a differentiation protocol effective for all iPSc lines was sought.

3.1.3 Regionalized Floor Plate Differentiation

Based on the protocol described by Kirkeby et al. in 2013, we developed a step-by-step differentiation protocol to midbrain DA neurons that worked on all four of our GD iPSc lines. This differentiation protocol reproduces mammal neuronal patterning with consecutive dual SMAD and glycogen synthase kinase 3 (GSK3) inhibition combined with SHH and bone morphogenetic protein (BMP) activation. Through sequential activation of signalling pathways with chemically defined molecular signals, it was possible to induce a robust dose dependent patterning which is both rostro-caudal and dorso-ventral (Figure 13). Using this protocol, all genotypes WT, A, B, C and D differentiated efficiently towards the neuronal phenotype. Before starting the protocol, all clones were adapted to a feeder free Matrigel® substrate and mTesR1® media. Rock inhibitor is added during the first 48h to avoid stress induced apoptosis. On the 4th day, the resulting EBs were resuspended in NPM and transferred to a previously Matrigel coated 60mm dish. By day 11, neuron-like extensions were apparent. Cells were then dissociated with *Accutase*® and seeded at a confluency of 15,000 cells/µl, on polyornithine (PO), in supplemented NDM.

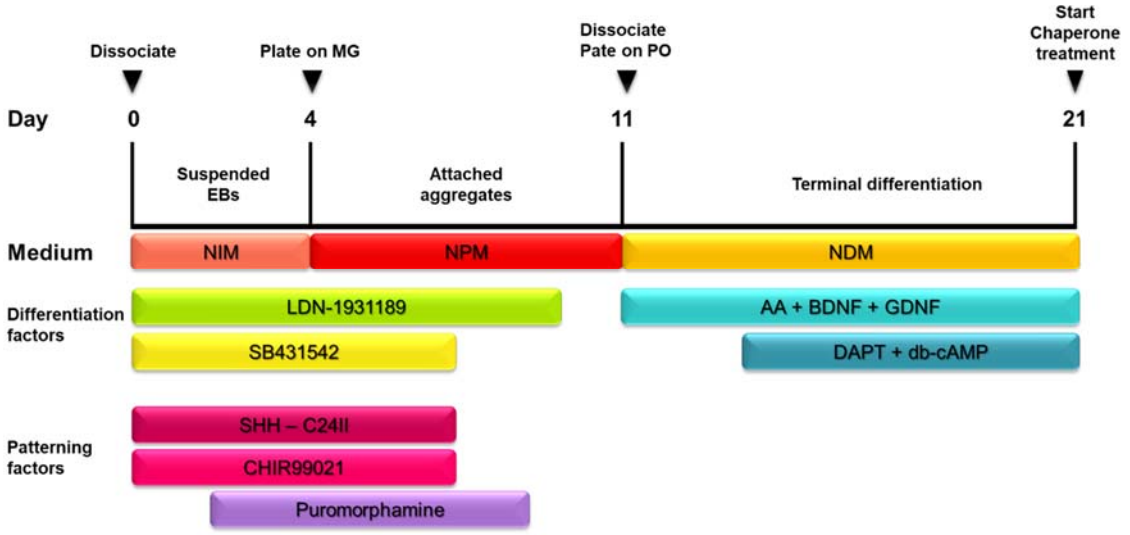

Figure 13. schematic representation of the differentiation protocol.

The cultures went through several morphological changes during the phases of patterning, from day 1 to 11 and terminal differentiation from day 11 onwards. Patterning included the floating and adhered EB phases characterized by large cell aggregates which delaminated neuronal-like cells and project long axons outwards. After the final dissociation, a uniform monolayer was seeded and left to grow for the following ten days. The cells appeared as small cellular nuclei and sprouted axons which contacted with nearby cells. By the end of the differentiation process, despite some inter-clonal differences, especially in growth rate and size of the cellular aggregates, we obtained fully confluent neuronal cultures (Figure 14).

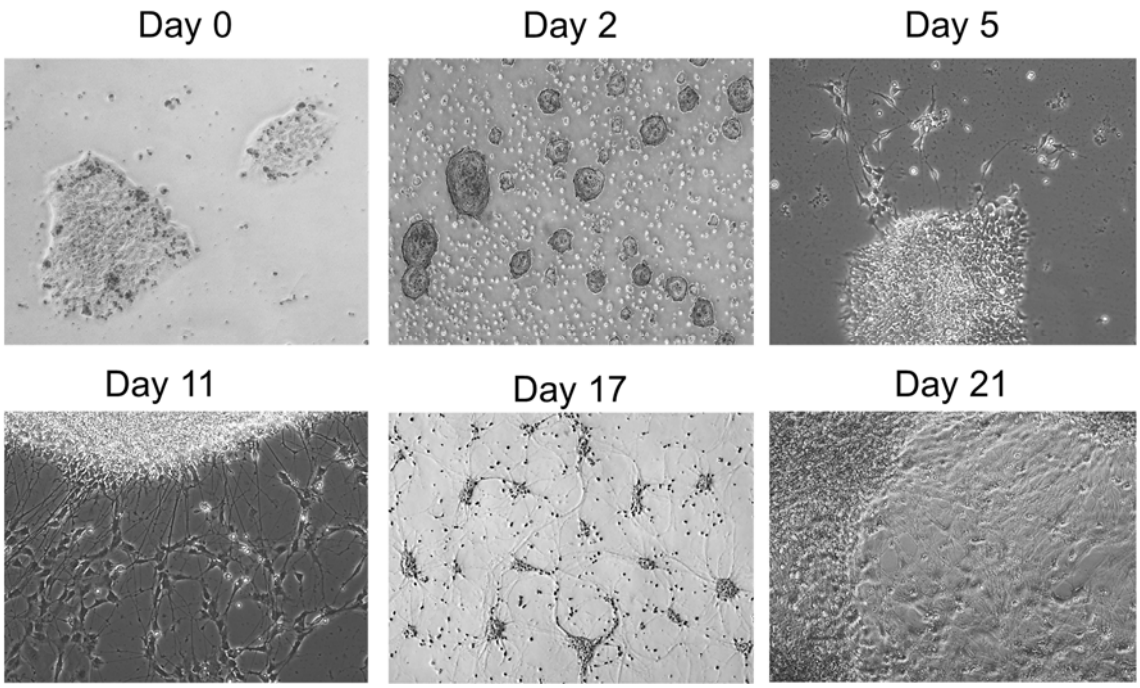

Figure 14. Representative pictures of iPSc clones during the regionalized floor plate differentiation protocol. iPSc clones growing on MG (day 0) were lifted and moved to a ULA dish. EBs were formed 2 days in low attachment conditions. One day after sitting down on MG, neuro-like cells delaminate from the adhered EB. A culture composed of large cell aggregates surrounded by a growing neuronal network is dissociated and re-seeded homogeneoulsy on PO and let grow to a confluent dish by the 21st day. Magnification 40x.

To further characterize our neuronal cultures, we performed a series of IHC to determine the degree of purity, maturity and percentage of DA neurons. Most stochastic or EB based differentiation methods suffer to a certain degree from contamination with undesired cell types. In neuronal differentiation protocols, the most common contaminant are glial cells which while very useful *in vivo*, can mask or change neuronal assessment. IHC with antibodies against GFAP and β-III-tubulin showed a highly pure neuronal culture, with little or no GFAP signal (Figure 15).

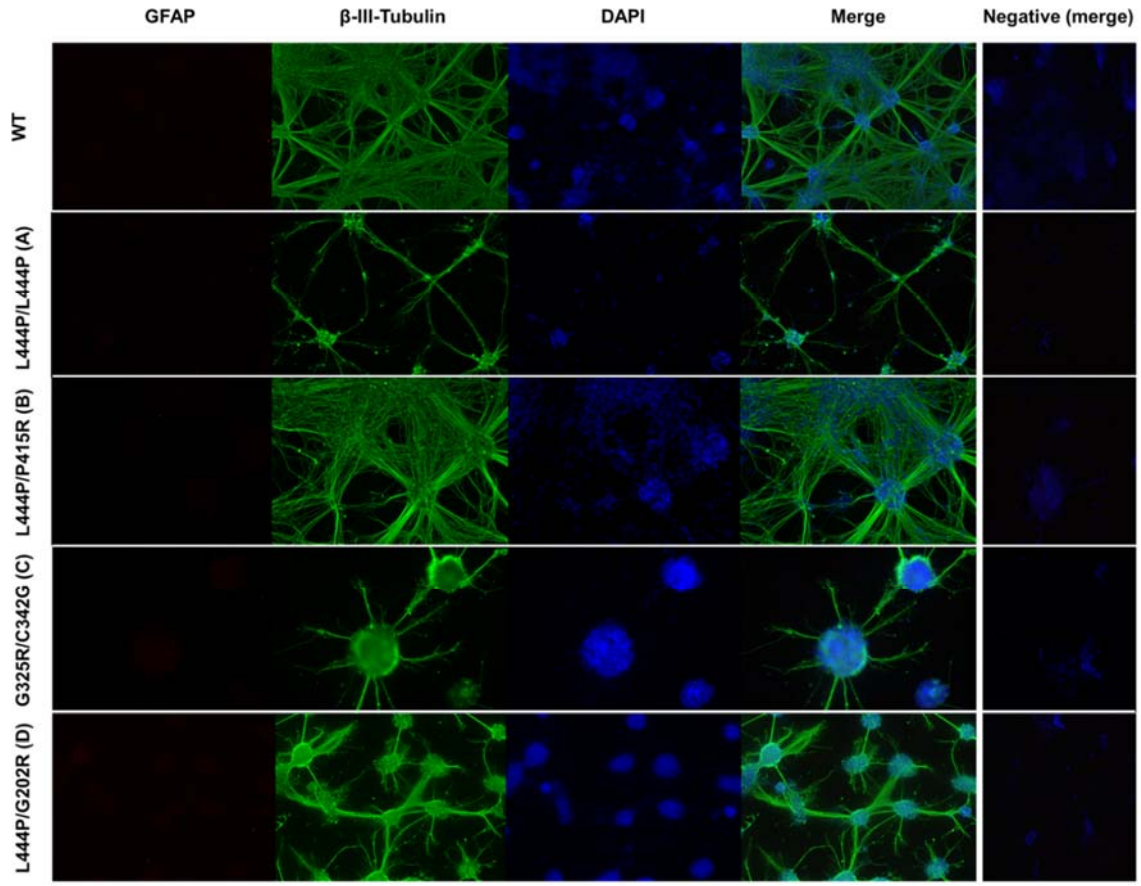

Figure 15. Terminally differentiated neurons from WT and GD iPSc. Clones are aligned by rows, top to bottom: WT, genotype A, B, C and D. Pictures are representative for all lines (40x) All clones were negative for GFAP and positive for β-III-tubulin. DAPI was used to mark cellular nuclei.

Presence of immature neurons or neuronal progenitors is another of the most common problems in neurodifferentiation. While useful in some points of the culture, enabling growth and expansion, testing phenotypic traits on an immature culture can lead to non-representative or unreliable data. Using antibodies against the neuroprogenitor marker Nestin, we tested our cultures for the presence of immature cells (Figure 16). Nestin positive cells were present on average one per culture, which in a total of $500x10^3$ cells, we considered to be negligible.

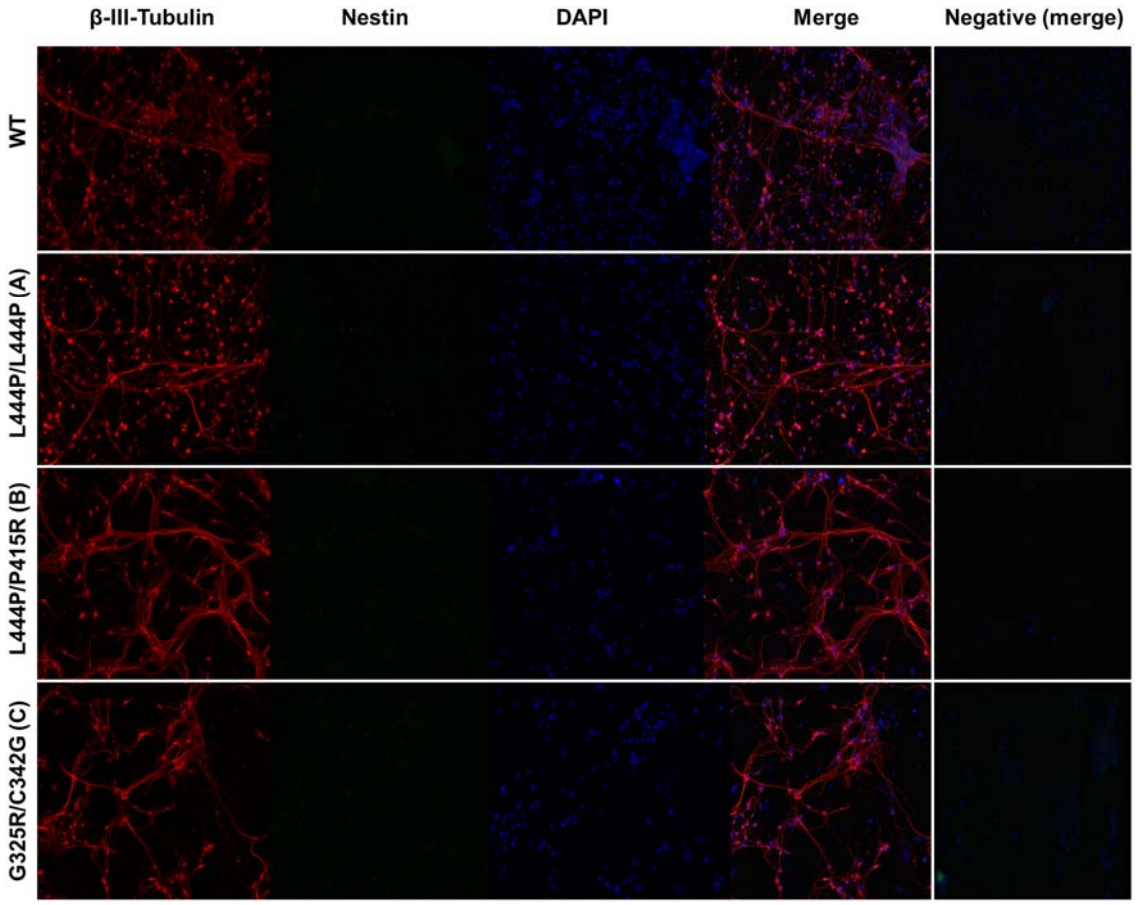

Figure 16. IHC analysis of terminally differentiated neurons from WT and GD iPSc. Clones are aligned by rows, top to bottom: WT, genotype A, B, C and D. Pictures are representative for all lines (40x) All clones were stained for Nestin β-III-tubulin. DAPI was used to mark cellular nuclei.

Finally, we assessed the efficiency of differentiation towards the DA phenotype through a double marking β-III-tubulin (Tuj1) and the DA specific marker TH (Figure 17). Basal plate ventralization of the neuronal population was induced through supplementation with higher concentrations of SHH and addition of purmorphamine from day 2 to 9. On average 10-20% of the neurons in terminally differentiated cultures were dopaminergic (TH^+). Although PD's symptoms are typically associated with DA neuronal death in *Substantia nigra*, both the autophagic impairment and α-syn accumulation is thought to be transversal to all neuronal types (García-Sanz, Orgaz, Fuentes, Vicario, & Moratalla, 2018; Zeng, Geng, Jia, Chen, & Zhang, 2018) thus, a basal plate neuronal culture like the one we achieved works in theory as the best *in vitro* model for GD-PD modelling.

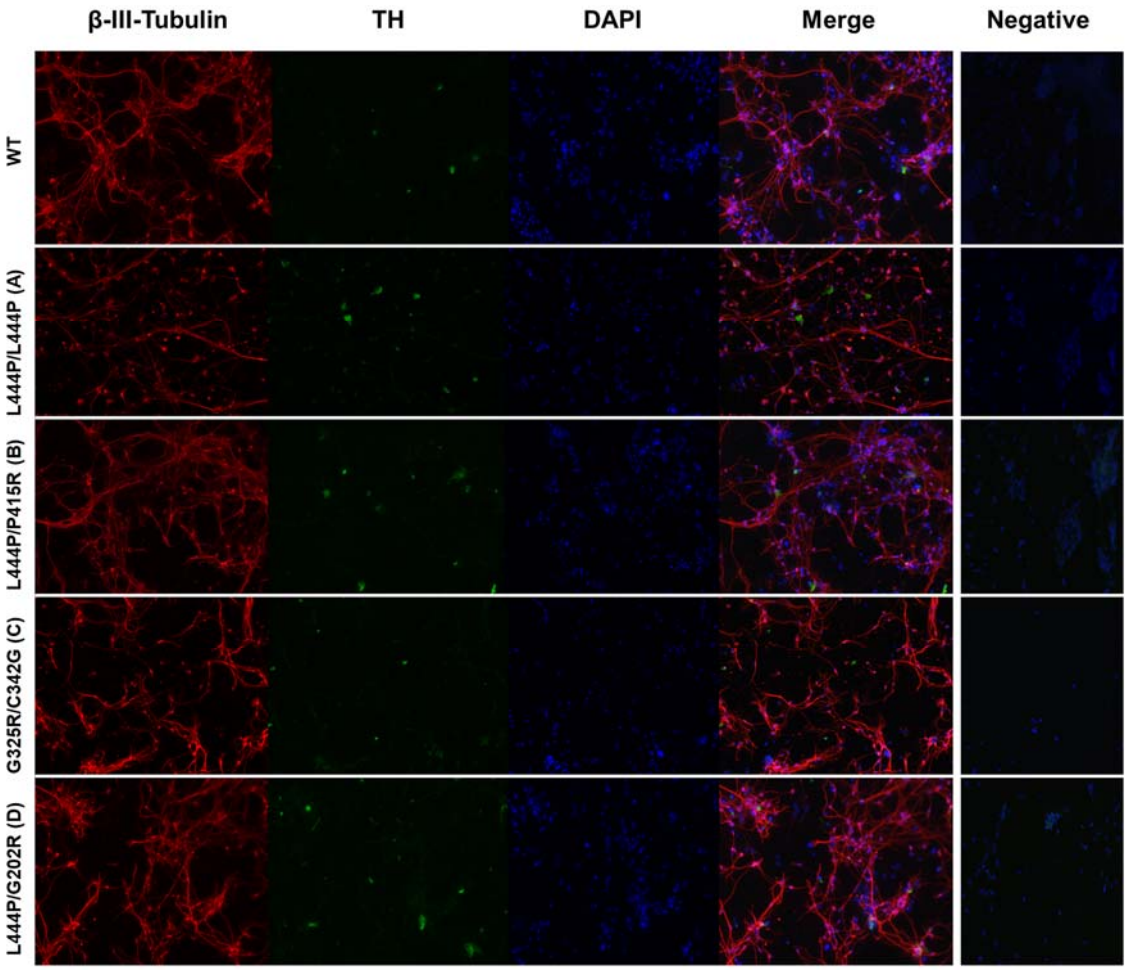

Figure 17. IHC analysis of terminally differentiated neurons from WT and GD iPSc. Clones are aligned by rows, top to bottom: WT, genotype A, B, C and D. Pictures are representative for all lines (40x) All clones were stained for β-III-tubulin and TH. DAPI was used to mark cellular nuclei.

Throughout our experiments, a persistent low level of cell death of about 5-10% was observed in the GD neurons, but not in the WT. These higher death levels in GD neurons, more prevalent between days 4 and 11, have recently been described by Awad et al as being due to an intrinsic Wnt/β-Catenin downregulation in GCase deficient neurons (Awad et al., 2017).

3.2 Biochemical Analysis

3.2.1 Model validation

As previously discussed, the present work was performed in four independent GD lines, carrying different GD type 2 genotypes and a WT line. GD fibroblasts were acquired through different sources. Our first collaborating group, (Katsumi Higaki, Tottori University, Japan), kindly sent clone A (L444P/L444P), passage 2 (Luan et al., 2013). Two other Gaucher Type 2 fibroblast lines (clone B - L444P/P415R and clone C - G325R/C342G) were acquired from the *Coriell* Repository. WT and clone D - L444P/G202R iPSc were previously described by Prof. Gustavo Tiscornia and used for chaperone testing (Tiscornia et al., 2013). All GD mutations have been previously sequenced and had their *GBA1* mutation confirmed by the providers.

GCase levels and activity are highly cell type specific and to our knowledge have not been systematically tested in differentiated neurons. Thus, before evaluating the effect of the chaperones on iPSc derived neurons, we set up to validate the models regarding their GCase protein levels and activity. Here, all iPSc clones including a WT were differentiated side-by-side towards the neuronal phenotype using the floor plate differentiation protocol described in materials and methods (Figure 18). Cultures were maintained in confluency for 10 days and whole protein extracts were harvested with the RIPA buffer protocol described in Materials and Methods. The resulting lysates were used for GCase and α-syn protein quantification and GCase activity determination.

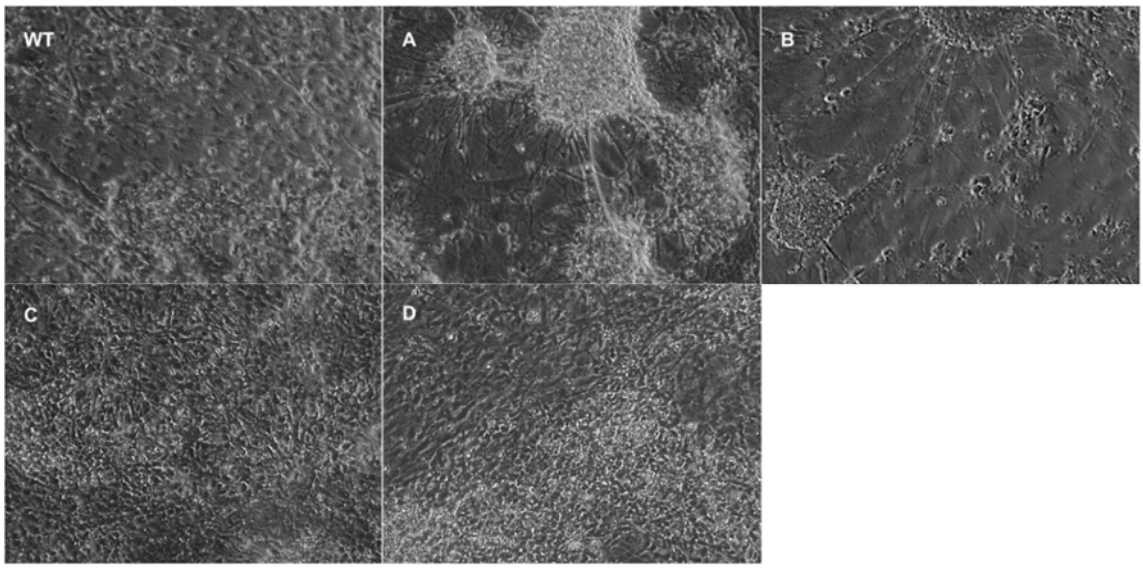

Figure 18. Representative pictures of neuronal cultures from all genotypes. Phase contrast photos taken on day 21 of differentiation (40x magnification). Panels: WT: (wild type); A: (L444P/L444P); B:L444P/P415R (Coriell - GM01260); C: G325R/C342G (Coriell - GM02627); D: L444P/G202R.

The L444P mutation is considered severe and neuronopathic, but little is known regarding the behaviour of specific effects of the other mutated GCase alleles in our iPSc lines (P415R, G325R, C342G, G202R). Obtaining high purity neuronal cultures of GD genotypes can be time consuming and technically challenging. Thus, GCase activity measurements is usually performed in non-neuronal cell types. However, due to epigenetic and functional variations between cell-types variations in the enzyme's activity may be cell-type specific. Previously published measurements of GCase activity have been mainly performed in fibroblasts (clones A and B) and fibroblast derived induced pluripotent cells (clone D - L444P/G202R), but not in neurons, the main cell type involved in GD type 1. A recent study has estimated GCase activity in fibroblast derived cells to be significantly lower than the original cell type, with iPSc, neural progenitors and neurons having 20%, 27% and 19% lower reproducing activity levels found in patient tissues, respectively.(Sun et al., 2015). This natural tendency persists in the presence of *GBA1* mutations, and is ever more evident in severe mutations like the ones in Clone C (G325R/C342G), where fibroblasts' activity has been estimated to be as low as 8% that of WT (Fog et al., 2018). Therefore, the intrinsic GCase activity in neuronal populations were measured and differentiated from each of our iPSc lines (Figure 19).

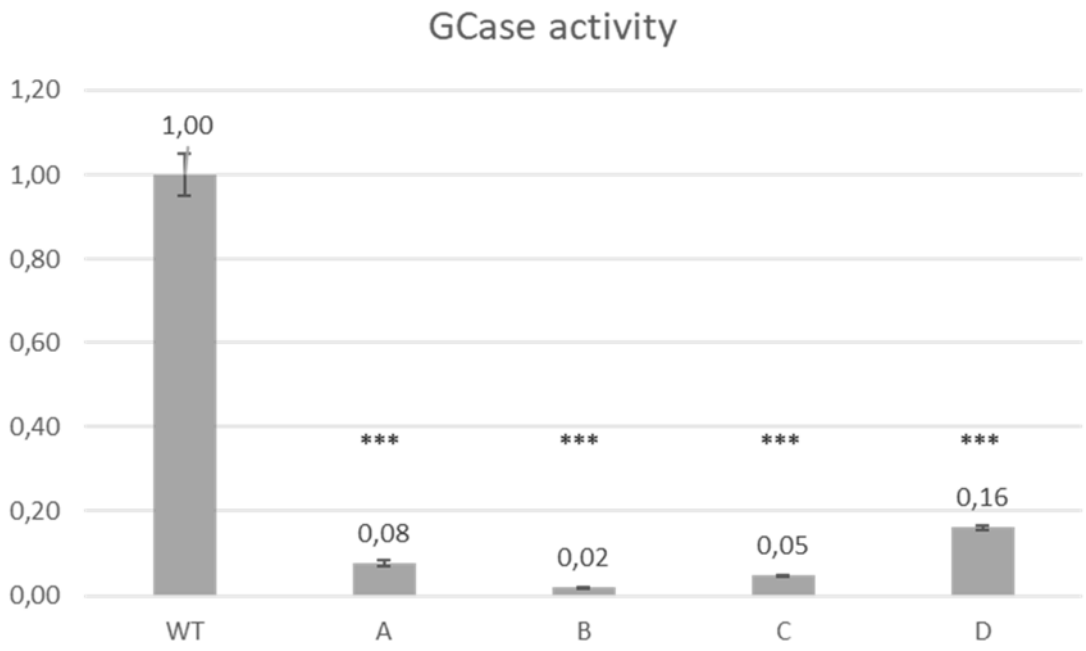

Figure 19: GCase activity in neuronal populations differentiated from iPSc lines with genotype A (L444P/L444P); genotype B (L444P/P415R); genotype C (G325R/C342G) and genotype D (L444P/G202R), as compared to WT. *** p<0,0001.

Although the correlation between GD's phenotype, severity and molecular markers is still not completely clear, GCase activity is still the best outcome predictor. Studies show that visceral only symptoms start appearing when activity drops just below 50% of WT.

Neuropathological manifestations start to emerge when activity is lower than 30%. The acute severe neuropathological phenotype is thought to only manifest if the total GCase activity is below 18% of WT (Lu et al., 2010; Parenti, Andria, & Valenzano, 2015; Sun et al., 2015). As expected, GCase enzymatic activity significantly decreased in all samples, showing levels ranging between 2% and 16%, depending on the genotype. Neurons derived from Clone A (L444P/L444P) showed 8% of WT's activity levels which, although lower than the 10% reported in fibroblasts, correlates with the overall cell-type differences (Parenti et al., 2015). Clone B (L444P/P415R) has one of the most common *GBA1* mutations which makes it one of the most well described phenotypes. Despite genetic background and inter experiment variations, our results for Clone C(G325R/C342G) reflect what's been reported for its genotype, with activity levels ranging from with 2.7% (Sun et al., 2015) to 12% (Parenti et al., 2015) in fibroblasts, 4.8% (Sun et al., 2015) in neuronal cultures and 6.7% in brain samples (Choi et al., 2011). Notably, Clone C (G325R/C342G) had only 5% of WT's activity, contrasting with other studies which show higher activity levels (Sun et al., 2015). Nevertheless, it corroborates other estimations and agrees with the expected activity levels for type II GD (Fog et al., 2018; Sun et al., 2015). Clone D (L444P/G202R) showed the highest activity levels in our model, albeit lacking fibroblast activity, and our results follow what has been described in overexpression *in vitro* models and iPSc (Tiscornia et al., 2013; Torralba et al., 2016).

Following what had been described by Sun et al, our terminally differentiated neurons are in line with what had been reported (Table 14) (Sun et al., 2015).

Table 14. Summary of GCase residual activity in GD genotypes A, B, C and D relative to WT and previous reports. Residual activity was accessed from protein extracts obtained from terminally differentiated neurons. NA-not accessed.

Clone	Mutation	Measured activity in neurons	Reported Activity in fibroblasts	Reported Activity hiPSc cells	Reference
A	L444P/L444P	8%	10%	NA	(Parenti et al., 2015)
B	L444P/P415R	2%	3-5.2%	NA	Coriell biobank Ref. GM01260(Sun et al., 2015)
C	G325R/C342G	5%	8%-28%	NA	Coriell biobank Ref. GM02627 (Fog et al., 2018; Sun et al., 2015)
D	L444P/G202R	16%	NA	19%	(Tiscornia et al., 2013)

Depending on the mutation and its location within the protein, *GBA1* mutations can show a wide variation of GCase protein levels and activity, with both parameters behaving interdependently. However, with GCase protein, the level and activity are far from the classical binomial pattern of presence-activity vs. absence-inactivity. For example, large amounts of protein trapped in the ER would lead to detection of relatively high levels of protein correlating with low levels of GCase activity due to the absence in the lysosomal compartment. A direct comparison by WB of GCase protein levels between all *GBA1* mutants and WT corroborates a decrease in protein levels of the same magnitude of the overall decrease in activity (Figure 20). Levels of GCase protein were almost undetectable, indicating that these mutations result in severe degradation of GCase.

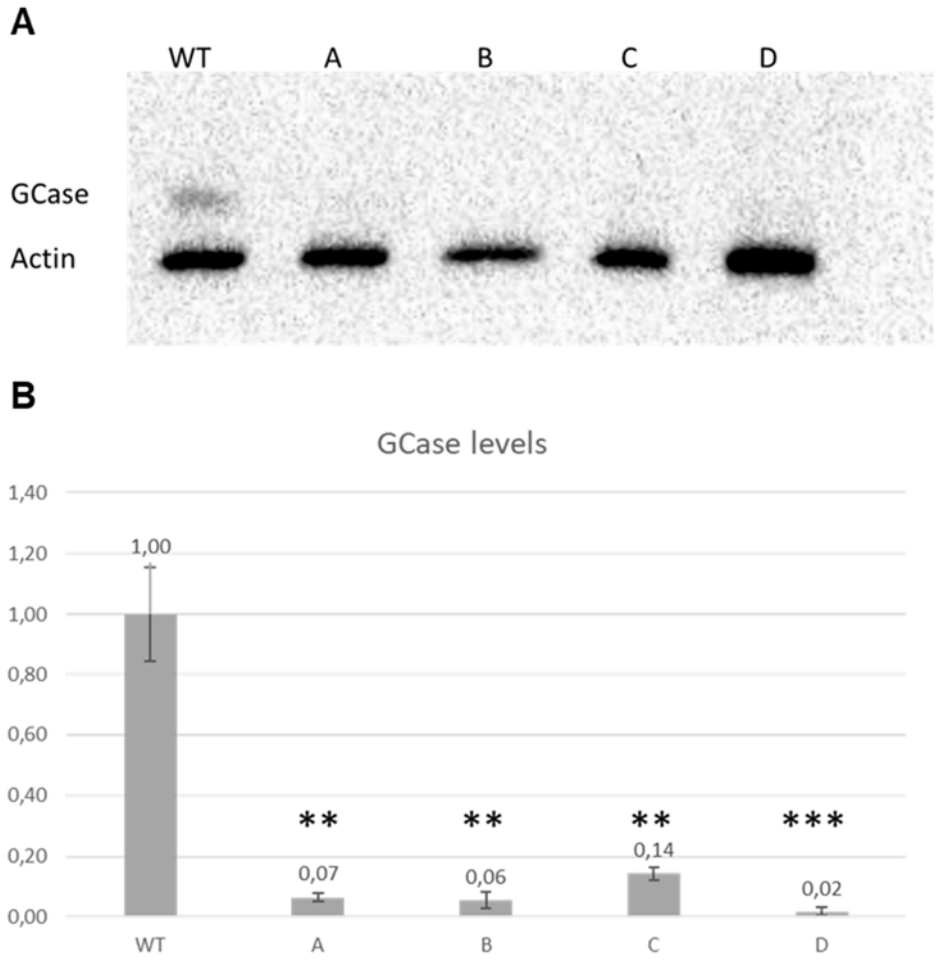

Figure 20: Western blot analysis of GCase levels in neurons derived from iPSc cell lines. Quantitation was based on three technical replicates for each of 3 biological replicates. A representative image of the WB is showed in A. Quantification was performed using the providers recommendations and each value was normalized, converted into a data point and statistically analyzed performed to determine significance (B). * p<0,05; ** p<0,001, *** p<0,0001.

The protein levels observed and measured are on the lower levels of detection on the WB. The enzyme assay had greater sensitivity and indicate that some GCase protein was indeed present. Lastly, we measured the levels of α-synuclein protein levels in 1-month old neuronal cultures. After one month of culture, all GD neuronal cultures showed increased levels of α-synuclein, supporting Mazzulli's observation of increased α-synuclein protein levels in GD neurons (Figure 21). As postulated by Mazzulli et al, GCase protein levels and α-syn protein levels seem to be inversely proportional. Observation in our 4 GD lines, taken as a group, decreased GCase protein levels and activity result in higher α-syn levels. When comparing the clones individually, we can observe that measurement of only one GCase parameter, either protein levels or enzymatic activity, are weak predictors of the α-syn levels.

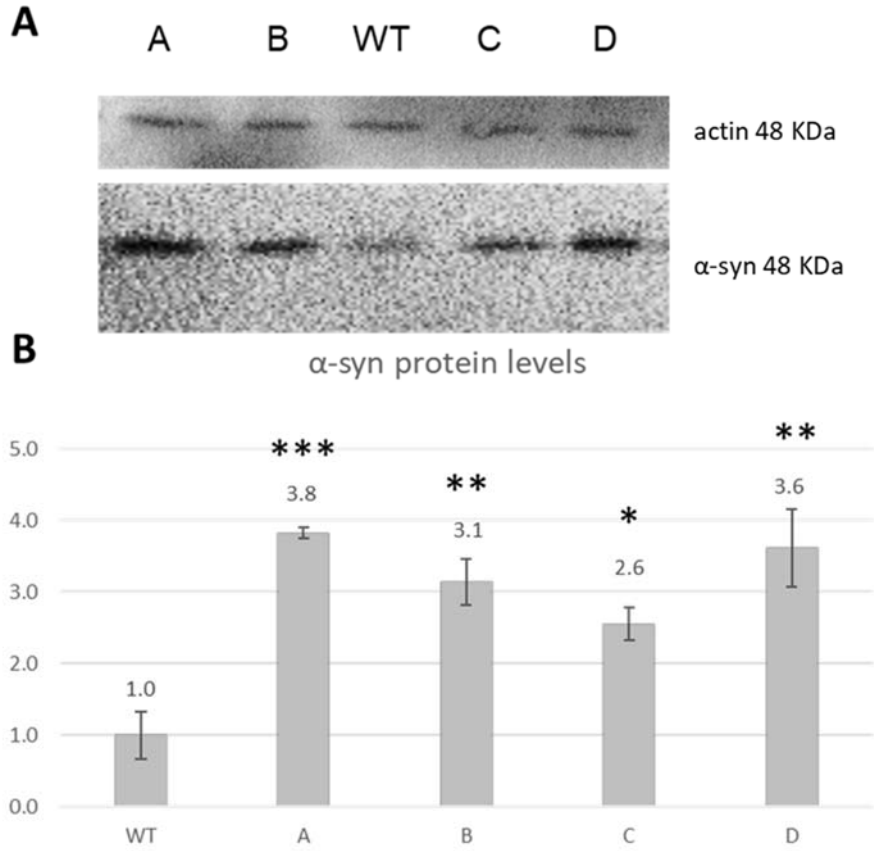

Figure 21 α-synuclein protein levels by WB in GD derived untreated neurons cultured for 30 days. Western blots were performed for each of the biological triplicates. A representative image of the final WB is showed in A. Quantification was performed using the providers recommendations and each value was normalized, converted in a data point and statistical analysis was performed to determine significance (B). * p<0,05; ** p<0,001, *** p<0,0001.

3.3 Effect of Chaperones on Differentiated Neurons

The panel of neurons derived from GD iPSc with the genotypes A - L444P/L444P, B - L444P/P415R and C - G325R/C342G (reprogrammed in-house) along with a WT and genotype D - L444P/G202R, (obtained from the CMRB in Barcelona) were used to test the effect of 12 chaperones on GCase protein and activity levels and α-syn protein levels in neuronal populations derived from each of the lines. The assay was set up to test the effect of each chaperone regarding a) GCase protein levels, b) GCase activity level, and c) α-syn protein levels, with the aim to test correlation between the 3 parameters for each of the genotypes. Each clone was subjected to three simultaneous, independent differentiation protocols for each condition and each neuronal culture was subjected to either a chaperone or “mock” treatment for 10 days. Chaperones were divided in three families, based on their molecular composition: monocyclic piperidines, bicyclic piperidines and nortropanes. The effect of each chaperone was compared with its untreated counterpart. After treatment, cells were harvested for protein extracts. Each

protein extract was used to test for GCase protein levels, GCase activity and α-syn protein levels. Protein levels were determined by WB with biological triplicates, normalized to actin and compared to cultures not treated with chaperone. Statistical analysis was used to identify significative differences.

3.4 WT

Initially, we tested the effect of the chaperones in the WT genotype, i.e. an unaffected individual. Due to their ability to bind to GCase ’s active center, pharmacological chaperones act as selective reversible inhibitors which, depending on the a.a. sequence and three-dimensional conformation of the protein may present different binding affinities and differential effects on the 3D structure of the enzyme. Although the intended primary use of these chaperones is for mutated forms of GCase, it is important to understand their effect on the WT enzyme.

3.4.1 WT GCase Protein Levels

The effect of chaperones on the WT enzyme may greatly affect its biosafety profile and, thus, limit or expand its clinical application. In order to understand the effect of our chaperones in WT neurons we started by evaluating their effect on total WT GCase levels (Figure 22).

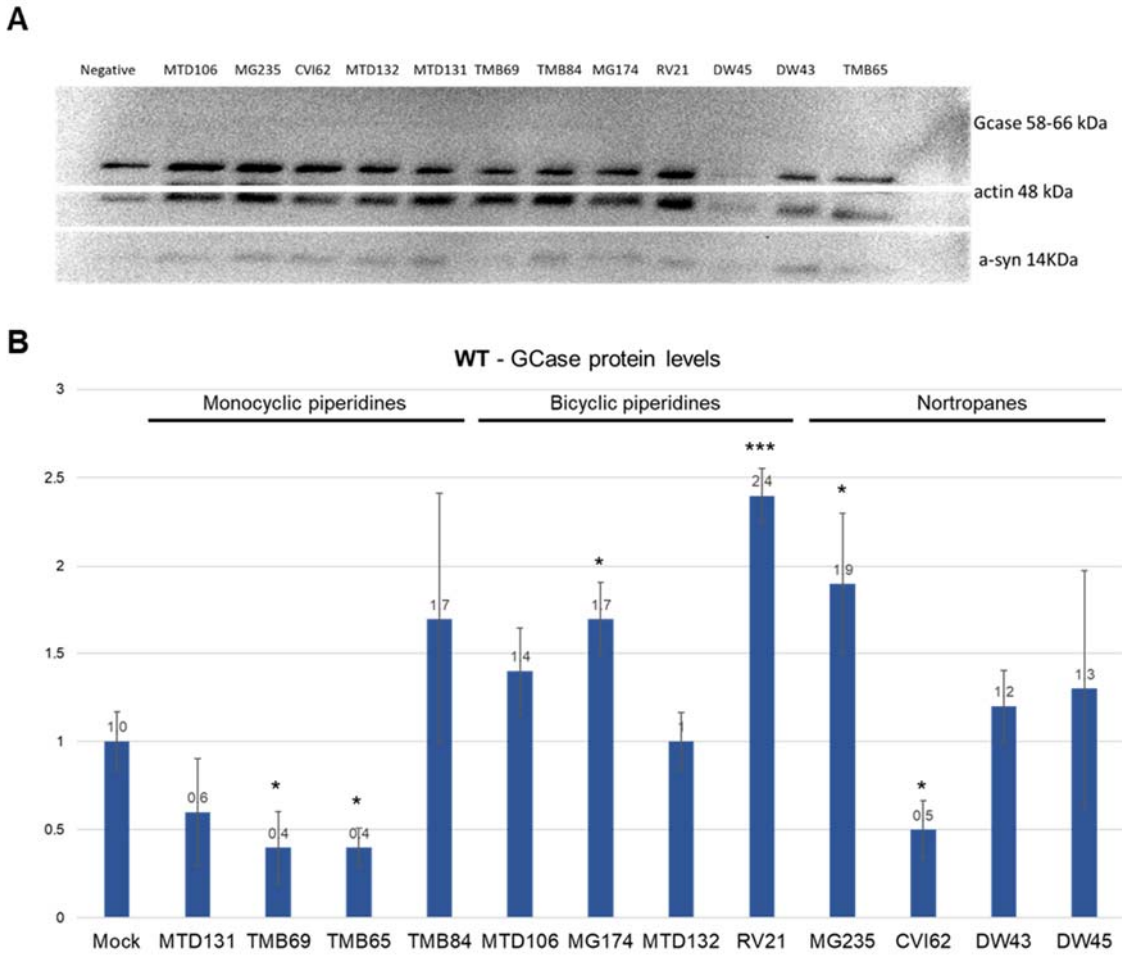

Figure 22. WT - WB protein quantification. Western blots were performed for each of the biological triplicates. A representative image of the final WB is showed in A. Quantification was performed using the provider's recommendations and each value was normalized, converted in a data point and statistical analysis was performed to determine significance (B). * p<0,05; ** p<0,001, *** p<0,0001.

Half of the tested chaperones did not produce any effect on the protein levels (Figure 23). Two members of the monocyclic piperidine family, TMB 69 and TMB65, decrease GCase protein levels by 60%. The only other chaperone with deleterious effects on the amount of protein was CVI62, a member of the nortropane family, which decreased the available GCase by half. Nevertheless, nortropanes showed no consistent effect. Another member of this family, MG235, increased the GCase protein levels by 90%.

Bicyclic piperidines are the most consistent in this regard, showing an overall tendency to increase GCase protein levels. Nevertheless, only RV21 and MG174 show a statistically significant increase in the enzyme levels. Regarding GCase protein levels, we can say, in general, monocyclic piperidines tend to have no effect or decrease GCase levels, bicyclic piperidines tend to have no effect or increase GCase protein levels, and nortropanes, had a higher variation, showing both an increase and decrease of protein levels (Figure 22).

3.4.2 WT GCase Activity Levels

Somewhat counterintuitively, GCase activity does not follow the same pattern as protein levels. Only 3 chaperones had any effect on the enzyme's activity**.** None of the tested chaperones were able to increase protein activity (Figure 23). Overall, the effect of the activity was very limited. Those which did influence enzyme function, MTD131, MTD132 and RV21, decreased it severely, with reductions of 90%, 100% and 40%, respectively.

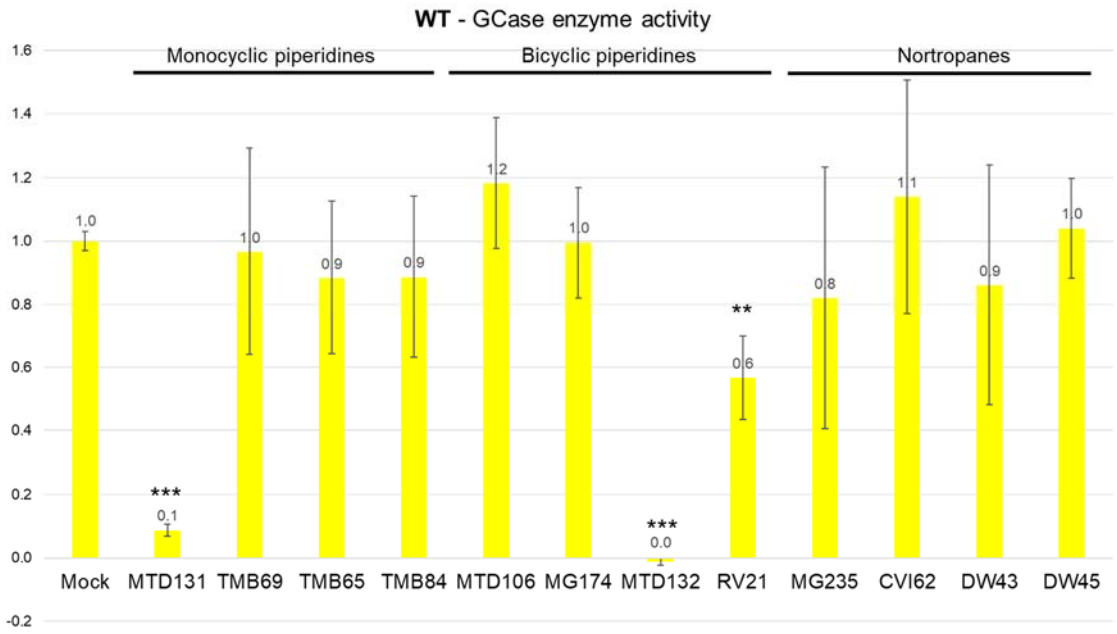

Figure 23. GCase activity in WT. GCase activity was accessed for each of the biological triplicates. Statistical analysis was performed for each of the conditions and p-values are represented as * p<0,05; ** p<0,001, *** p<0,0001.

3.4.3 WT α-syn Protein Levels

Six of the chaperones had an effect on α-syn levels. Five of the six significant variations showed an increase in α-syn levels, and one chaperone showed a decrease. All other chaperones led to higher variability in α-syn levels but were not statistically significant.

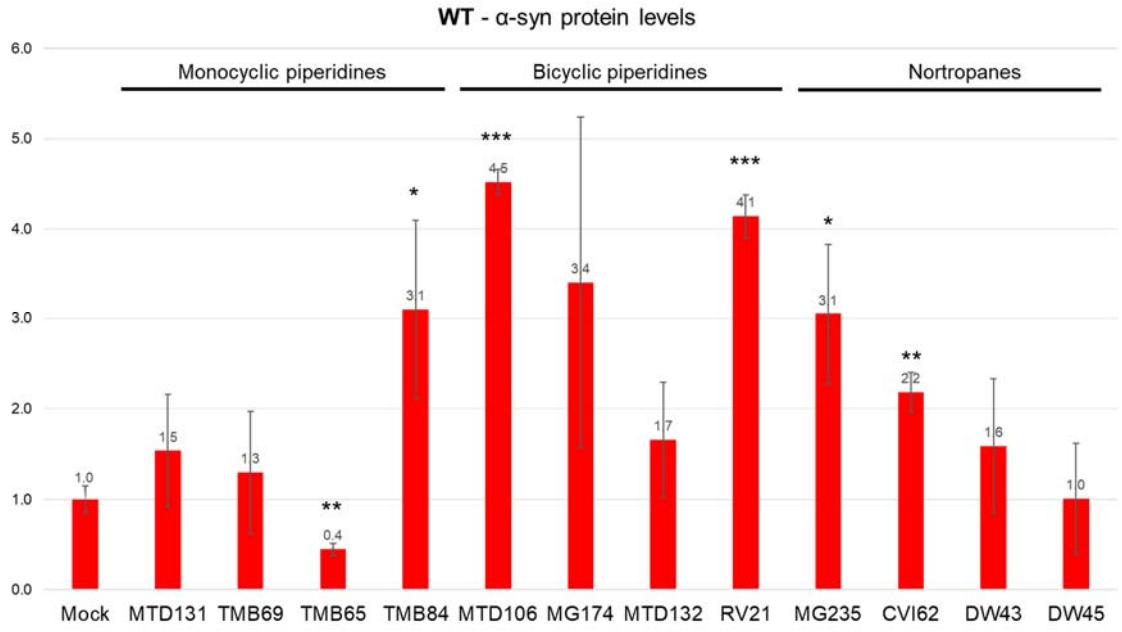

Figure 24. α-synuclein levels in WT. Western blots were performed for each of the biological triplicates. A representative image of the final WB is showed in 23-A. Quantification was performed using the providers recommendations and each value was normalized, converted in a data point and statistical analysis was performed to determine significance. * p<0,05; ** p<0,001, *** p<0,0001.

The effects on α-syn accumulation were major and observed in all three chaperone families, most strongly with the bicyclic piperidines. Only TMB65 managed to decrease the amount of intracellular α-syn. The addition of TMB84, MTD106, RV21, MG235 and CVI 62 to WT neurons resulted in more than a 2-fold increase of the total α-syn levels, with a surprising 4,6- and 4.1-fold increase in MTD106 and RV21 (Figure 24).

3.5 Genotype A - L444P/L444P

L444P is one of the most frequent mutations in GD. It's associated with aggressive neuronopathic forms of the disease. It is known to severely decrease GCase protein levels due to misfolding and subsequent degradation in the ER. Modulation of the final 3D structure would theoretically allow a higher percentage of mutated GCase to escape ER degradation and greatly increase its protein levels and activity in the lysosome, preventing GlcCer and α-syn accumulation.

3.5.1 GCase Protein Levels in Clone A (L444P/L444P)

In clone A (L444P/L444P), the chaperones tended to increase GCase protein levels. Three of the monocyclic piperidines, MTD131, TMB69 and TMB84, doubled the amount of GCase protein levels. TMB65 only raised by GCase protein levels by 40%. Two of the four bicyclic piperidines MG174 and RV21 had no effect at the protein level. Nevertheless, MTD106 increased the protein levels 3.7 times and MTD132 doubled the amount. Nortropanes increased protein levels by 40% (DM43), 90% (DW45) and, notably, 6.7 times by MG235 (Figure 25).

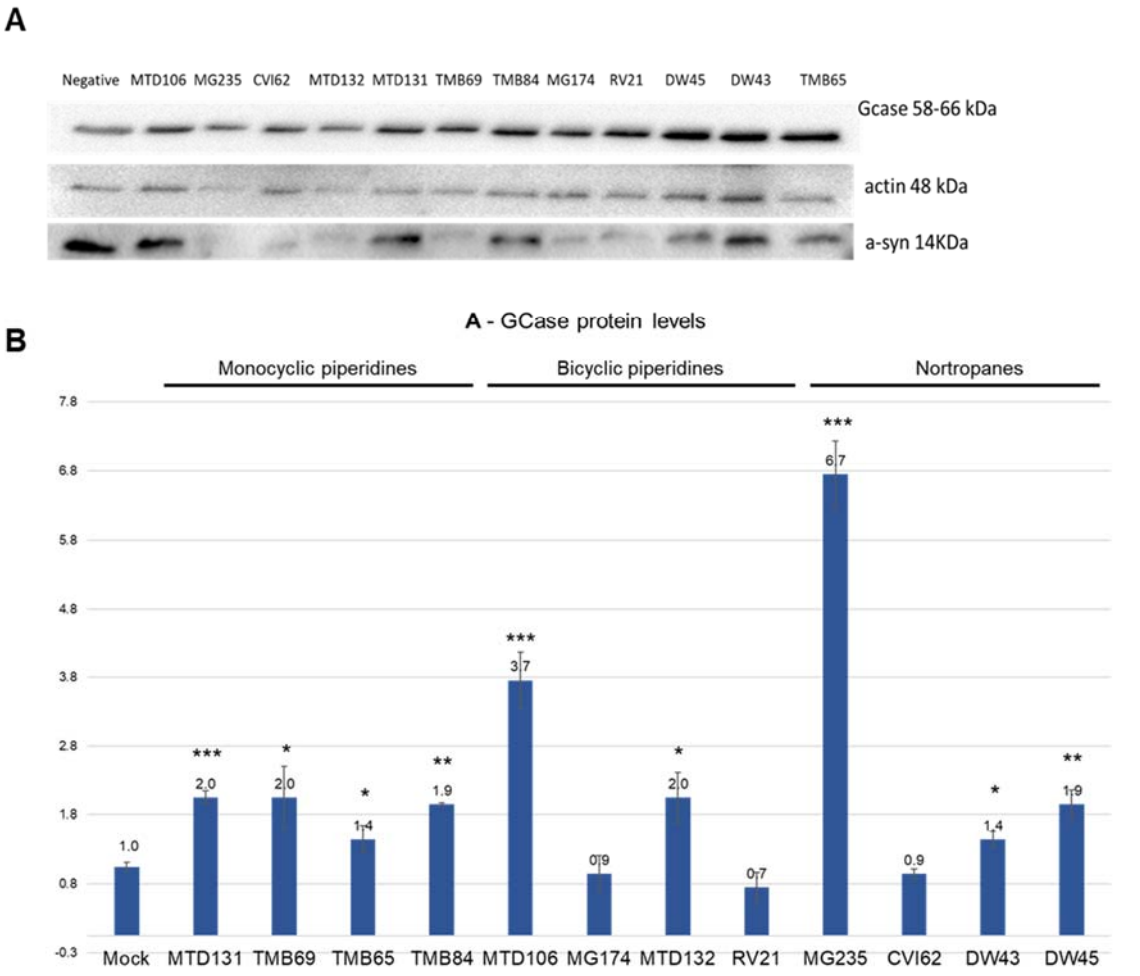

Figure 25. Clone A - WB protein quantification. Western blots were performed for each of the biological triplicates. A representative image of the final WB is showed in A. Quantification was performed using the providers recommendations and each value was normalized, converted in a data point and statistical analysis was performed to determine significance (B). * p<0,05; ** p<0,001, *** p<0,0001.

3.5.2 GCase Enzymatic Activity Levels in Clone A (L444P/L444P)

All chaperones had a deleterious effect on GCase activity (Figure 26). With 60% inhibition, MTD132 showed the strongest inhibition. MTD131, TBM 69, RV21 and MG235 inhibited the enzyme between 40 and 50%. All other compounds resulted in a small inhibition which did not surpass 10-20%.

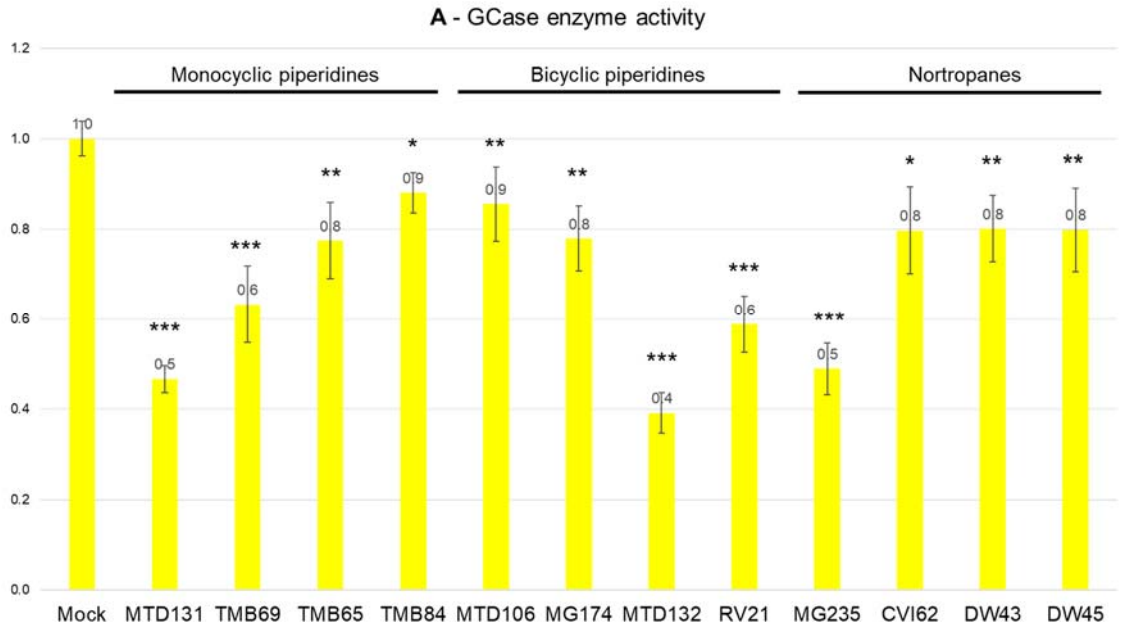

Figure 26. GCase activity in genotype A. GCase activity was accessed for each of the biological triplicates. Statistical analysis was performed for each of the conditions and p-values are represented as * p<0,05; ** p<0,001, *** p<0,0001.

3.5.3 α-syn Protein Levels in Clone A (L444P/L444P)

Most chaperones tested showed a tendency to decrease α-syn levels in this genotype. Seven of the twelve tested chaperones significantly decreased α-syn, while only one increased α-syn levels (Figure 27).

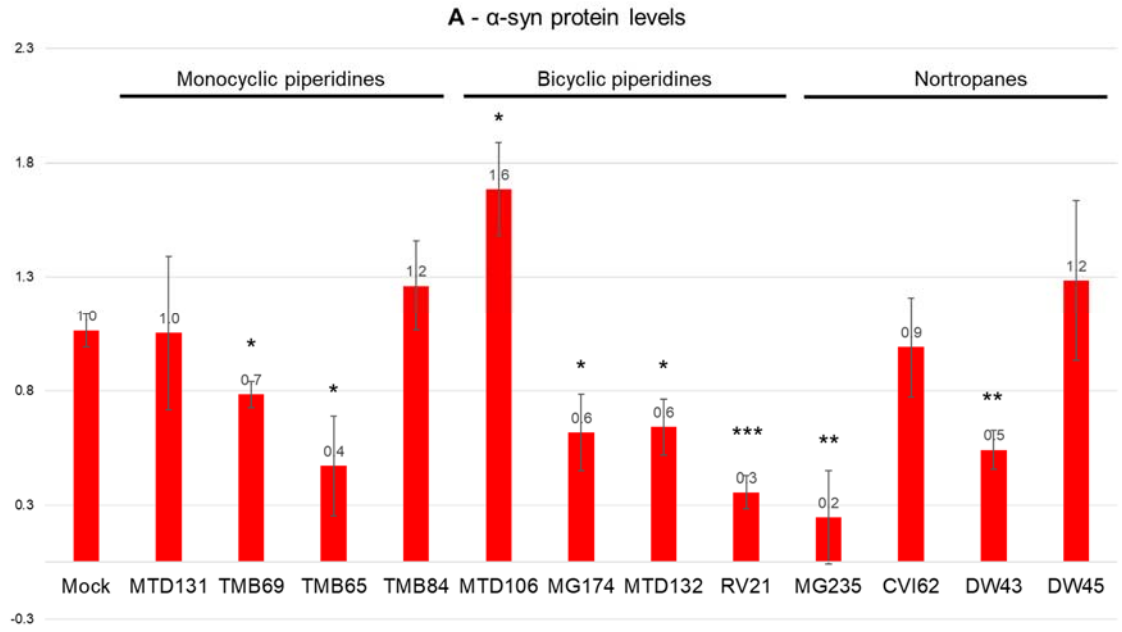

Figure 27. α-synuclein levels in the genotype A. Western blots were performed for each of the biological triplicates. A representative image of the final WB is showed in figure 26-A. Quantification was performed using the providers recommendations and each value was normalized, converted in a data point and statistical analysis was performed to determine significance. * p<0,05; ** p<0,001, *** p<0,0001.

None of the chaperone families had a consistent effect on α-syn levels when applied to genotype A. Nevertheless, within each group there was a tendency to decrease α-syn levels. MTD106 was the only chaperone which increase in α-syn protein levels. This increase of around 60% contrasted with the general tendency to decease α-syn levels. MTD131, TBM69 CVI62 and DW45 had no effect on α-syn levels. Decreases of 40% (MG174 and TD132), 50% (DW43), 60% (TMB65), 70% (RVI21) and 80% (MG235).

3.6 Genotype B - L444P/P415R

Genotype B has a strong phenotype, consistent with the fact that it involves two neuropathic alleles, L444P and P415R. Contrary to L444P, the effect of the P415R's mutation is thought to affect GCase's ability to bind LIMP-2, resulting in mistrafficking towards the extracellular medium, without triggering degradation via the ERAD pathway. Thus, leading to low GCase intracellular levels, without a severe effect on degradation pathways (Reczek et al., 2007).

3.6.1 GCase Protein Levels In Clone B (L444P/P415R)

Half the compounds had an effect on GCase levels. Overall, the number of chaperones able to increase GCase levels in this genotype is much smaller than that of the L444P homozygous clone A (L444P/L444P). Although Clone B (L444P/P415R) shares the L444P mutation with Clone A (L444P/L444P), the overall pattern of response to the tested compounds is significantly different (Figure 28).

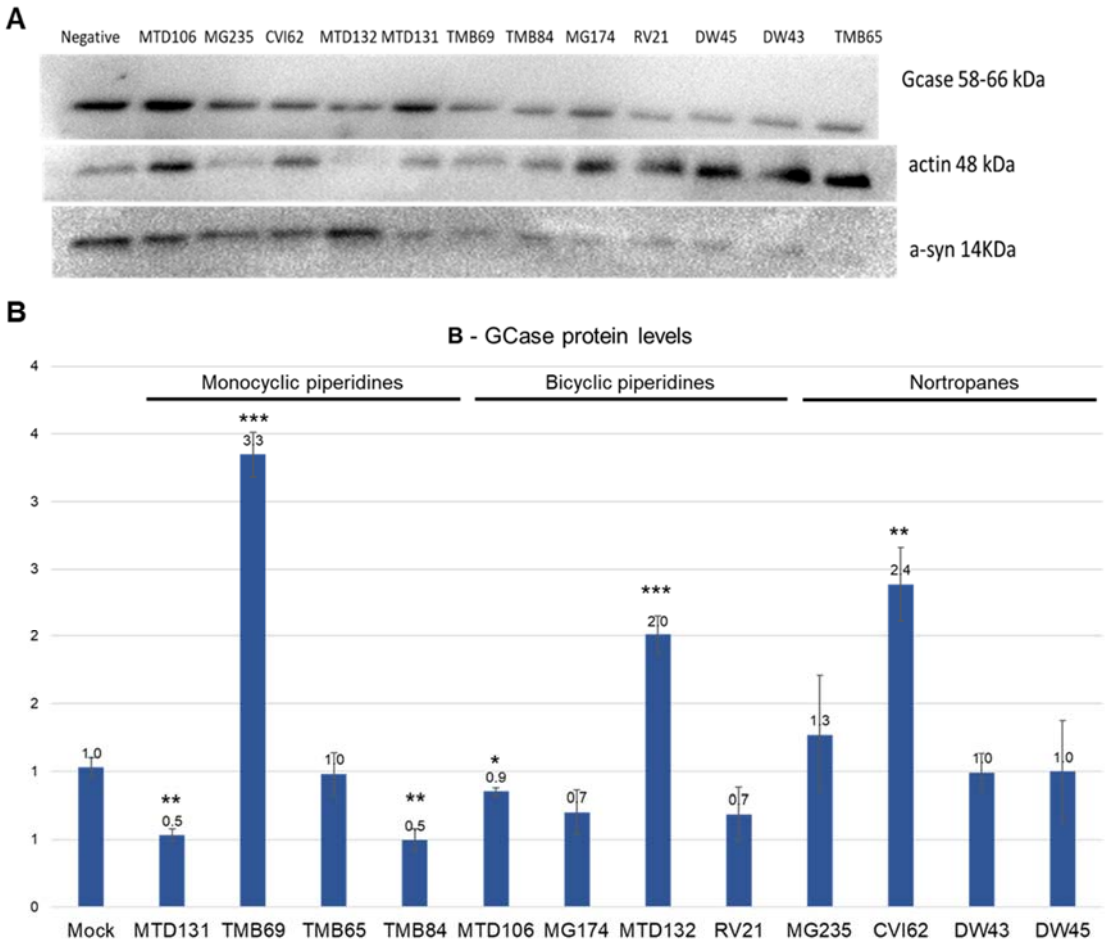

Figure 28. Clone B - WB protein quantification. Western blots were performed for each of the biological triplicates. A representative image of the final WB is showed in A. Quantification was performed using the providers recommendations and each value was normalized, converted in a data point and statistical analysis was performed to determine significance (B). * p<0,05; ** p<0,001, *** p<0,0001.

There was no observable consistent family effect, with both monocyclic and bicyclic piperidines showing a strong compound variation. Only one of the nortropanes showed an effect on GCase, increasing it. On a compound level, GCase protein levels dropped by half with MTD131, TBM84, and to 10% with MTD106. Alternatively, three chaperones were able to sharply increase the protein levels. While CVI62 and MTD132, reached double the levels of the untreated line, TBM69 managed to increase the protein levels by 3.3 times (Figure 28).

3.6.2 GCase Activity Levels in Clone B (L444P/P415R)

No positive effect on GCase activity was achieved by any of the compounds tested. Similar to what was observed in GCase protein levels, there is no observable family-wide effect on the enzyme's activity, with seven of the twelve compounds showing a inhibitory effect (Figure 29).

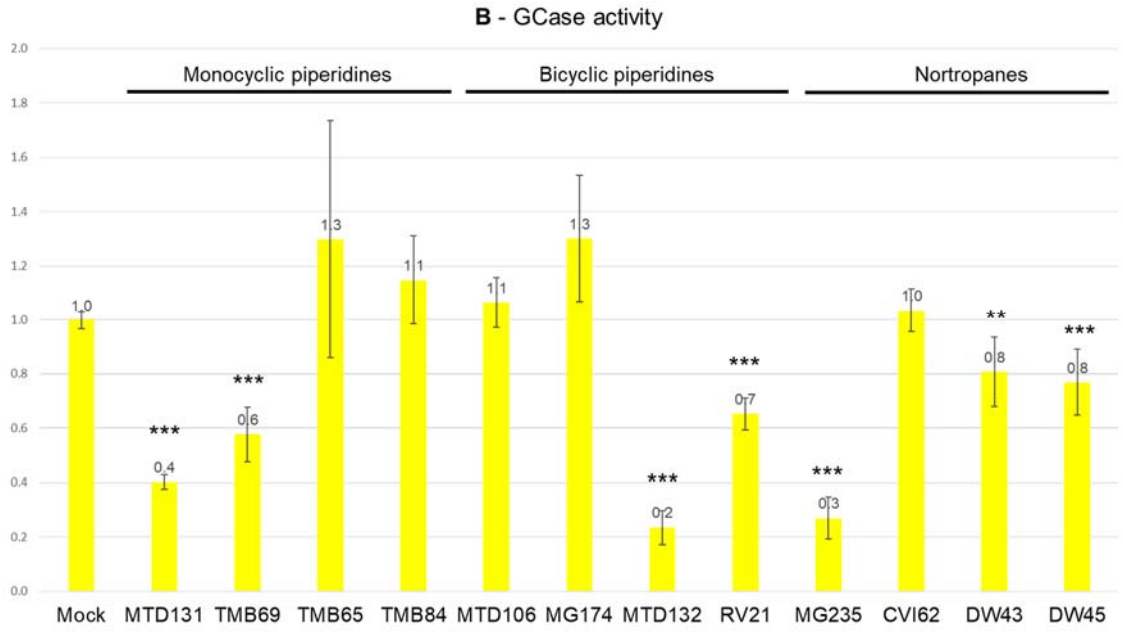

Figure 29. GCase activity in the genotype B. GCase activity was accessed for each of the biological triplicates. Statistical analysis was performed for each of the conditions and p-values are represented as * p<0,05; ** p<0,001, *** p<0,0001.

Individually, inhibition ranged from 80% (MTD132), 70% (MG235), 60 (MTD131) 40% (TMB69), 30% (RV21), 20% (DW43 and DW45).

3.6.3 α-syn Protein Levels in Clone B (L444P/P415R)

Globally, chaperone compounds show a tendency to decrease α-syn levels which was transversal to all chaperone families. Of the 12 tested compounds, 7 significantly decreased α-syn levels and 2 increased its levels (Figure 30).

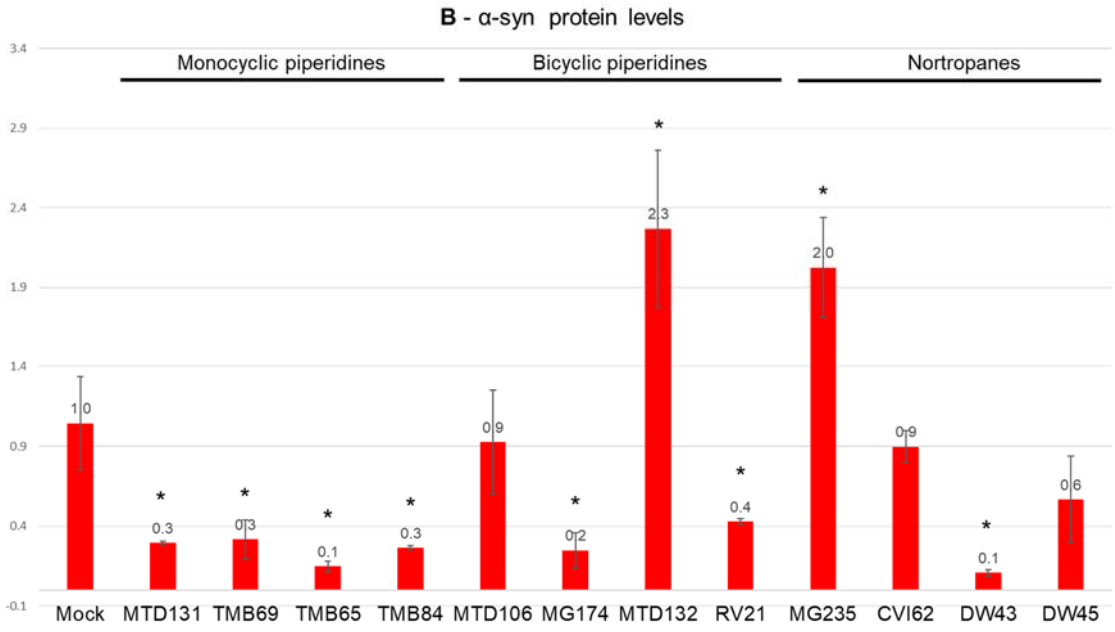

Figure 30. α-synuclein levels in the genotype B. Western blots were performed for each of the biological triplicates. A representative image of the final WB is showed in figure 29-A. Quantification was performed using the providers recommendations and each value was normalized, converted in a data point and statistical analysis was performed to determine significance. * p<0,05; ** p<0,001, *** p<0,0001.

Monocyclic piperidine chaperones seem have a more consistent effect on α-syn levels, decreasing them on average by 70% (MTD131, TMB69 and TMB84) and reaching 90% decrease with TMB65. Bicyclic piperidines MG174 and RV21 decrease the α-syn by 80% and 40%, respectively. One of which, MTD132, led to a 2.3X increase in the amount of synuclein. MTD106 has no effect on α-syn levels. Nortropanes also show a level of variation, with MG235 doubling the amount of synuclein, while DW43 decreased the amount of synuclein by 90%. CVI62 and DW45 did not have any effect on the levels of synuclein.

3.7 Genotype C - G325R/C342G

Both these alleles are highly associated with neuronopathic forms of the disease (Sun et al., 2015). Contrary to the effect of most *GBA1* mutations, where structural changes lead to ER degradation, mutations G325R and C342G directly affect the active site, resulting in milder conformational changes but an intrinsic decrease in hydrolytic activity (Smith, Mullin, & Schapira, 2017).

3.7.1 GCase Protein Levels in Clone C (G325R/C342G)

Alterations in GCase cause by mutations in genotype C are highly responsive to chaperone compounds. GCase protein levels increased in 6 (MTD131, TMB69, TMB84, MTD132, RV21 and DW45) out of 12 compounds. Only compound TMB65 led to a significant decrease of GCase protein levels (Figure 31).

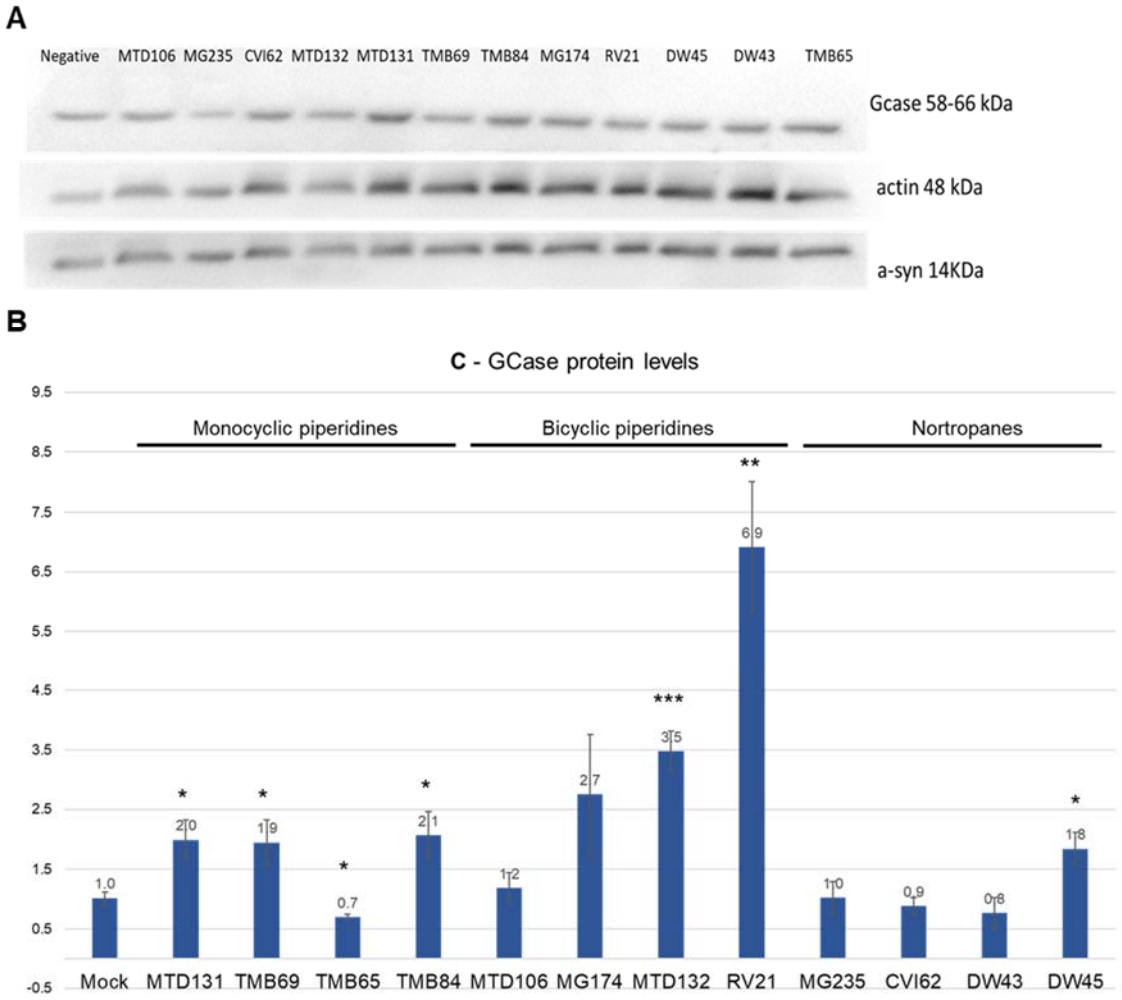

Figure 31. Clone C - WB protein quantification. Western blots were performed for each of the biological triplicates. A representative image of the final WB is showed in A. Quantification was performed using the providers recommendations and each value was normalized, converted in a data point and statistical analysis was performed to determine significance (B). * p<0,05; ** p<0,001, *** p<0,0001.

Monocyclic piperidines, with the exception of TMB65, which does not have any effect, increase the GCase protein levels by two-fold. Bicyclic piperidines do not work uniformly. MTD132 and RV21 increase GCase protein levels by 3.5 and 6.9-fold, respectively while MTD106 and MG174 have no effect on the protein levels (Figure 31).

3.7.2 GCase Activity Levels in Clone C (G325R/C342G)

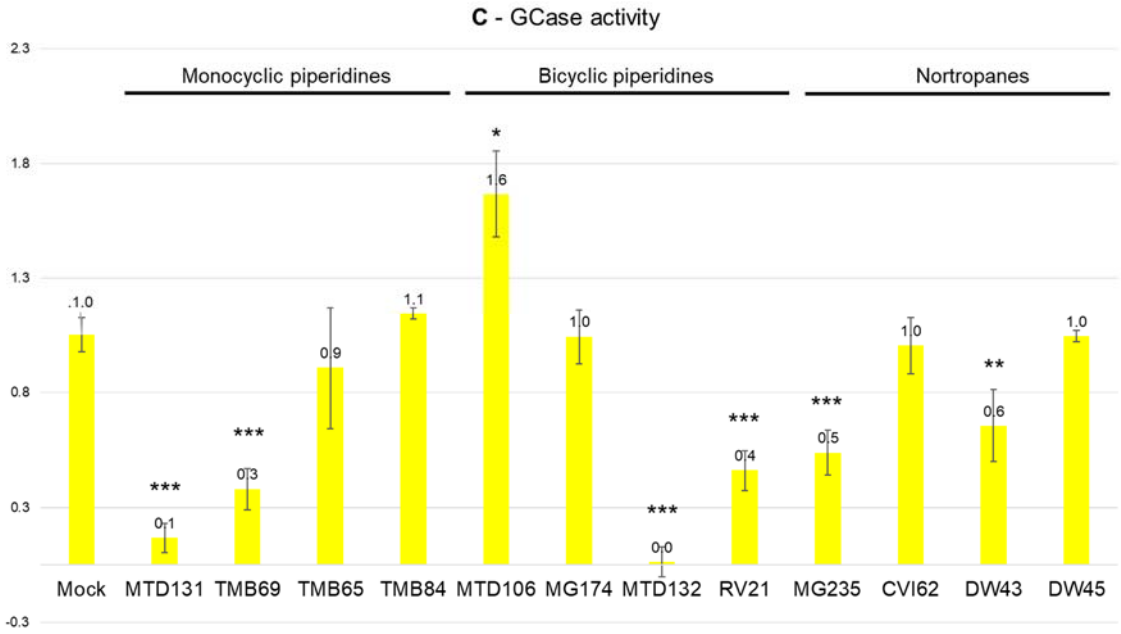

Figure 32. GCase activity in the genotype C. GCase activity was accessed for each of the biological triplicates. Statistical analysis was performed for each of the conditions and p-values are represented as * p<0,05; ** p<0,001, *** p<0,0001.

Similar to what has been seen in the previous clones, GCase activity is highly chaperone-specific, with chaperones having a predominantly repressive effect over GCase, in this genotype. Only MTD106 was able to increase GCase activity with a total increase of 60%. Several degrees of inhibition were seen, since the severe inactivation of GCase activity by MTD132 (100%), MTD131 (90%) and TMB69 (70%), to milder effects in RV21 (60%), MG235 (50%) and DW43 (40%). All the other chaperones showed no effect on the enzyme's activity (Figure 32).

3.7.3 α-syn Protein Levels in Clone C (G325R/C342G)

Although all chaperones tended to decrease α-syn levels, only six resulted in a significative decrease in total α-syn (Figure 33). The effect seems to be compound-specific, since no chaperone family showed a distinct and coherent effect.

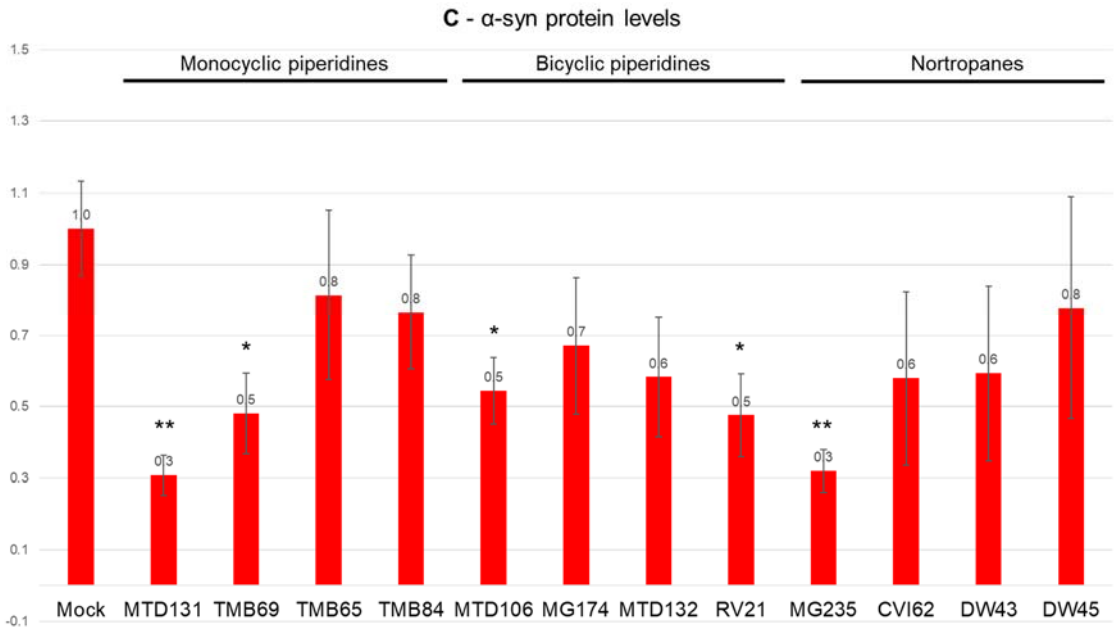

Figure 33. α-synuclein levels in the genotype C. Western blots were performed for each of the biological triplicates. A representative image of the final WB is showed in figure 32A. Quantification was performed using the providers recommendations and each value was normalized, converted in a data point and statistical analysis was performed to determine significance (B). * p<0,05; ** p<0,001, *** p<0,0001.

Individually, chaperones MTD131 and MG235 decreased the amount of synuclein by 70%; TMB69, MTD106 and RV21 decreased α-syn protein levels by half. None of the other chaperones were able to significantly alter α-syn levels.

3.8 Genotype D - L444P/G202R

Similar to L444P, G202R is a severe mutation in *GBA1* which causes conformational changes and is strongly associated with the neuronopathic forms of GD (Bendikov-Bar & Horowitz, 2012; Koprivica et al., 2000).

3.8.1 GCase Protein Levels in Clone D (L444P/G202R)

Genotype D responds to most chaperones, with significant changes in GCase protein levels in 10 of the 12 tested chaperones. Six chaperones decreased GCase protein levels, while 4 were able to increase GCase concentration (Figure 34).

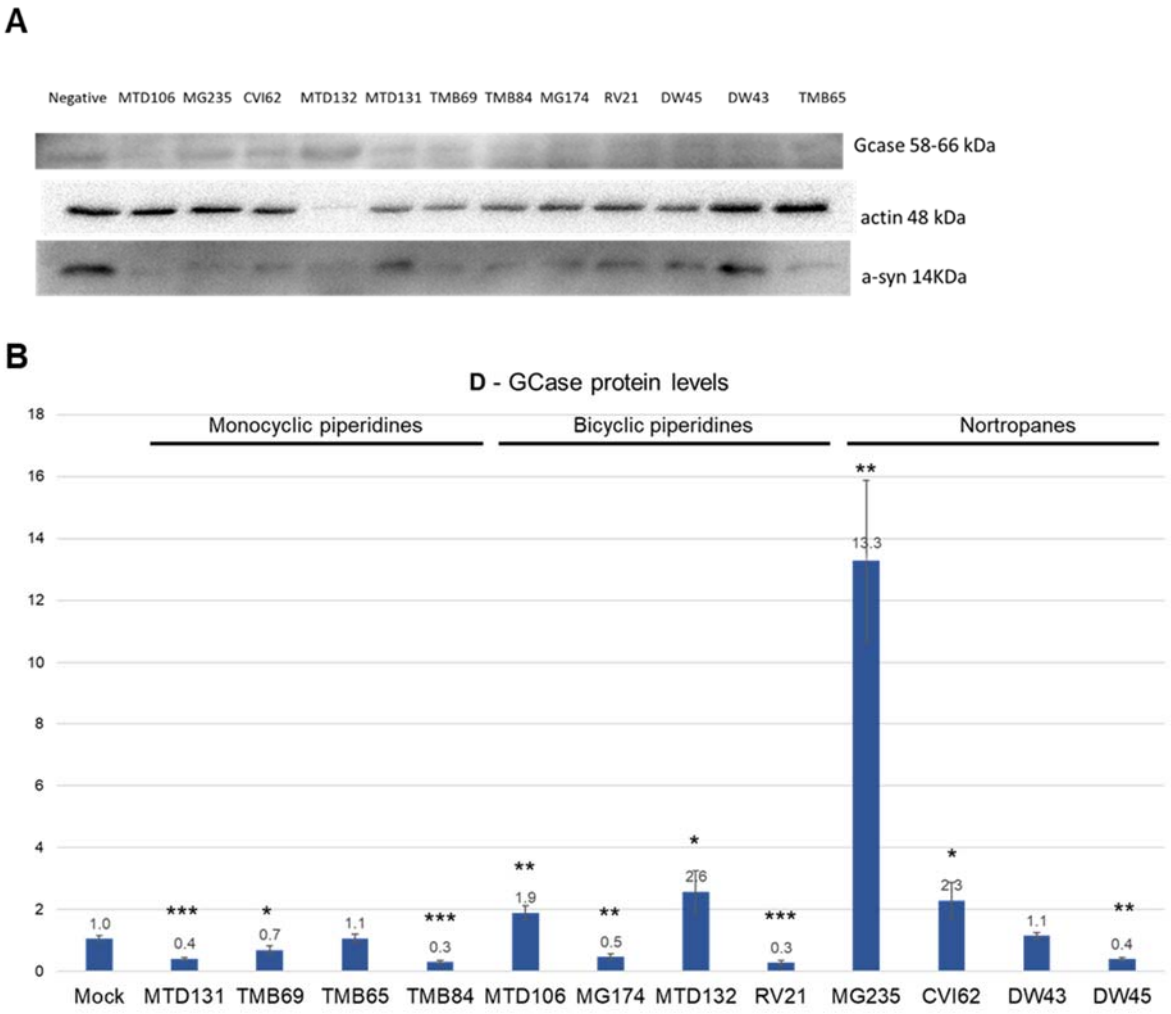

Figure 34. Clone D - WB protein quantification. Western blots were performed for each of the biological triplicates. A representative image of the final WB is showed in A. Quantification was performed using the providers recommendations and each value was normalized, converted in a data point and statistical analysis was performed to determine significance (B). * p<0,05; ** p<0,001, *** p<0,0001.

In general, these chaperones seem less effective at increasing GCase protein levels in this genotype. Monocyclic piperidines were unable to increase the enzyme's levels. Bicyclic piperidines MTD106 and MTD132 and Nortropane CVI62 double the GCase

protein levels. The biggest increase was induced by MG235 which was able to increase GCase protein levels 13-fold. With the exception of TMB65, which had no effect, every other chaperone decreased GCase levels (Figure 34).

3.8.2 GCase Activity Levels in Clone D (L444P/G202R)

Similar to the results in GCase protein levels, GCase activity in genotype D is very responsive to chaperoning, with only one chaperone had no effect. All other compounds affected GCase 's hydrolytic ability in a family-independent manner (Figure 35).

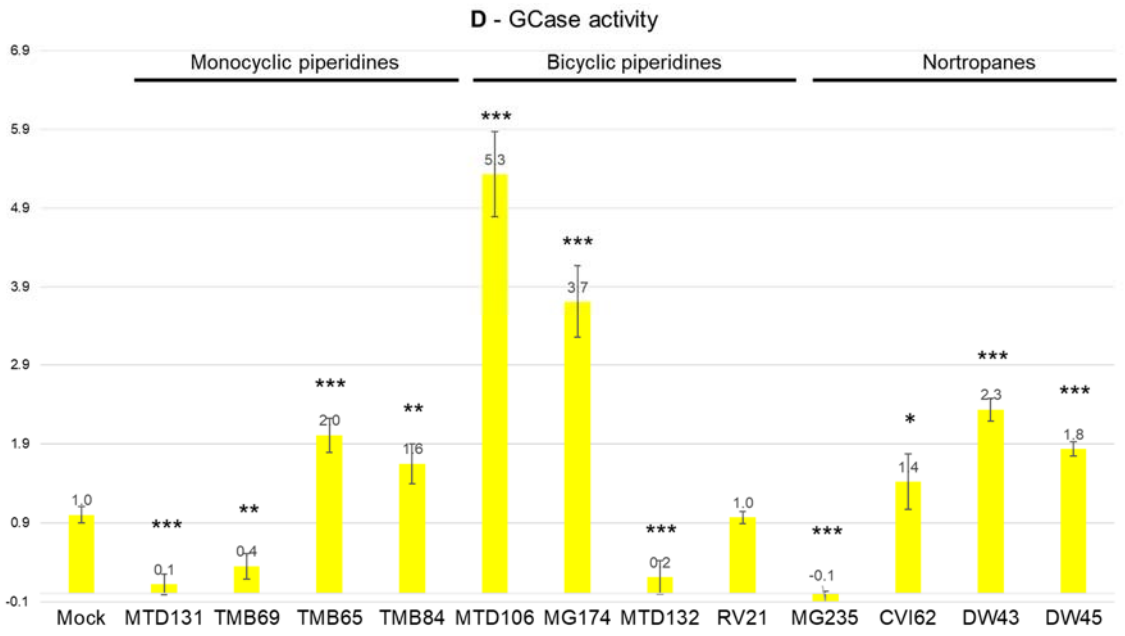

Figure 35. GCase activity genotype D. GCase activity was accessed for each of the biological triplicates. Statistical analysis was performed for each of the conditions and p-values are represented as * p<0,05; ** p<0,001, *** p<0,0001.

Half the chaperones managed to increase GCase activity to some degree (Figure 36). TMB65, TMB84, DW43 and DW45 increased the activity roughly by two-fold. The best were undoubtedly the bicyclic piperidines, with MTD106 increasing activity 5.3x and MG174 to 3.7x the value of the untreated cells. Two of the chaperones, RV21 and CVI62, had no effect on activity. The remaining chaperones heavily inhibited GCase 's activity, to 40% (TMB69), 20% (MTD132), 10% (MTD131) the control activity. MG235 completely ablated GCase 's activity in this genotype.

3.8.3 α-syn Protein Levels n Clone D (L444P/G202R)

Contrary to what happened with the other genotypes, none of the tested chaperones was able to decrease α-syn levels in this line (Figure 36). In fact, all nortropanes increased

synuclein levels. Only TMB69, MTD106, MG174 and RV21 had no effect on synuclein levels

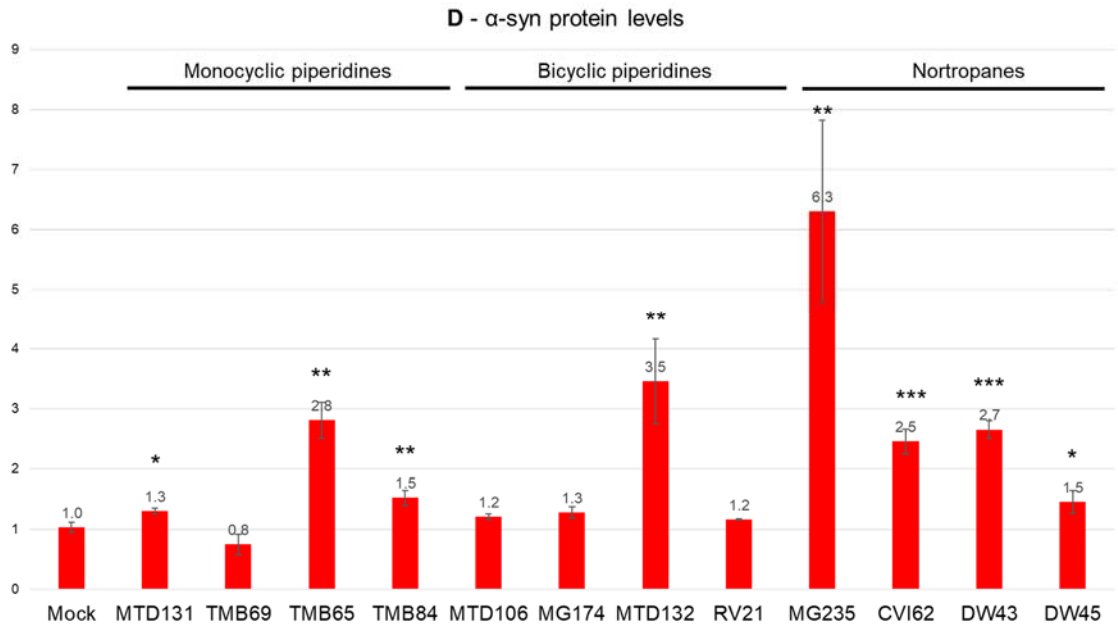

Figure 36. α-synuclein levels genotype D. Western blots were performed for each of the biological triplicates. A representative image of the final WB is showed in figure 35A. Quantification was performed using the providers recommendations and each value was normalized, converted in a data point and statistical analysis was performed to determine significance (B). * p<0,05; ** p<0,001, *** p<0,0001.

.

4. Discussion

Development of new pharmacological therapies implies an integrated view of the intracellular environment. In order to understand the link between GCase efficiency and α-syn accumulation, we designed a system with three variables which have been described above: GCase protein levels, GCase activity and α-syn protein levels. However, in order to fully understand the effect of GCase on α-syn, and the effect of each individual chaperone on the system, the following data must be addressed simultaneously.

4.1 Chaperone Effects on WT iPSc Derived Neurons

GCase protein levels depend mostly on the transcription/degradation ratio and half-life of the enzyme; increases in protein levels can result from chaperones promoting higher stability of the enzyme, increasing its half-life; decreases in protein levels are thought to be the result of either chaperone mediated misfolding in the ER or enhanced post-translational signaling for destruction. GCase activity is affected by not only the enzyme levels but also the availability of the active center and the ability for the chaperones to bind to and be released from the GCase hydrolytic center upon reaching the lysosome. An often-offered explanation of GD pathogenesis is that mutations in GCase (present in the active site of the enzyme or other regions of the protein) alter the 3D structure of the enzyme. As a consequence, the protein may be degraded, accumulated in the ER, mis-trafficked or affected in its catalytic activity (Awad et al., 2015). The explanation for beneficial effect of chaperones for GD is thought to derive from the ability of the chaperone to interact with the mutated GCase in such a way that the 3D structure of the enzyme is stabilized. As a consequence, the mutated enzyme would resemble more a WT GCase structure and the effects of the mutation (degradation, accumulation, mis-trafficking and decreased activity) would be alleviated or avoided. Nevertheless, factors like intracellular net charge, activity and enhancement of autophagic pathways, as well as previous presence of protein, can result in GCase aggregation known to affect α-syn levels.

Figure 37 (and Figures 38, 39, 40 and 41) below show relative GCase protein levels, GCase activity and α-syn protein levels in response to chaperone treatment. In order to analyze these results, we a) looked at the relative levels of GCase protein levels

and activity to determine the effect of a given chaperone on GCase itself, b) looked at the levels of α-syn in response to chaperone treatment and c) determined whether there was a correlation between GCase behavior and α-syn levels. We also looked at whether any effects observed were specific to individual chaperones or also found in other chaperones of the same chemical family.

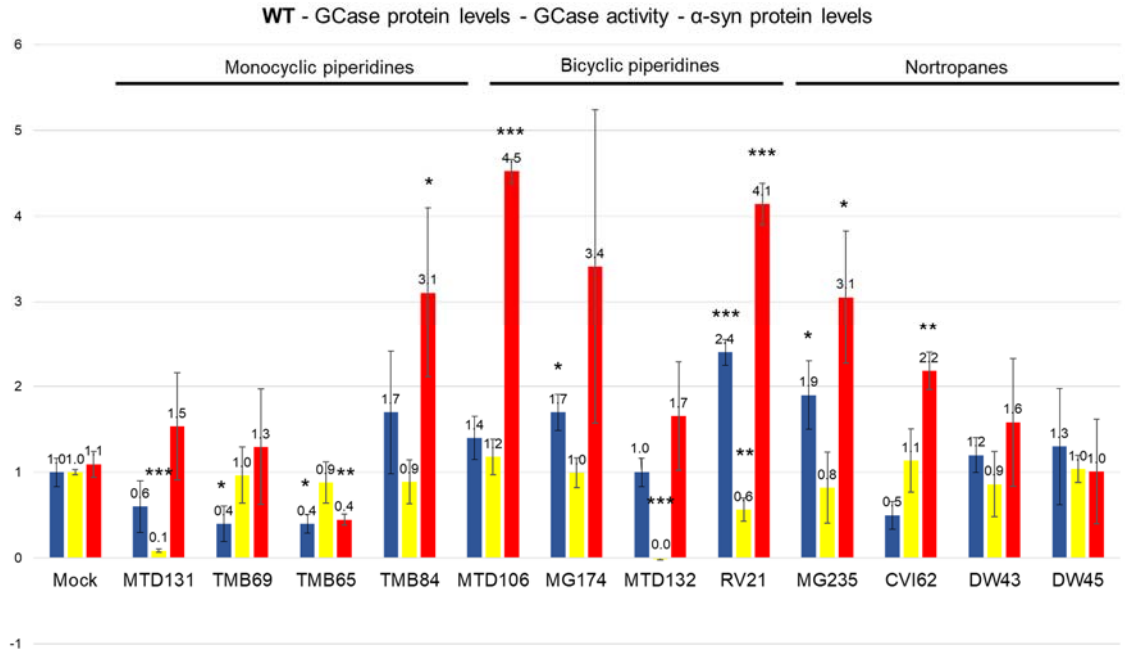

Figure 37. Chaperone effect on WT- resume. GCase protein levels (blue bars), GCase activity (yellow bars) and α-syn protein levels (red bars) in terminally differentiated neurons. Protein levels and activity are normalized to the mock (no chaperone treatment) and statistically significant differences are marked as * p<0,05; ** p<0,001, *** p<0,0001.

In general, chaperone treatment resulted in fold changes between 0.4 and 2.4 for GCase protein levels, between 0 (undetectable) and 1.2 for GCase activity and between 0.4 and 4.5 for α-syn. Overall, well to well variability in each measurement (done in triplicates) was within reasonable levels. Considering that the assay involved differentiating iPSc lines to neurons for 4 weeks, we conclude that stochastic variability in differentiation conditions is not a major factor in these assays. For 5/12 chaperones (TMB84, MTD106, CVI62, DW43, DW45), there was no effect on GCase protein or activity levels. Notably, chaperones MTD131 and MTD132 almost completely inhibited GCase activity without affecting GCase protein levels, suggesting these chaperones are strong and irreversible inhibitors of GCase activity. In the '3D structure rescue by chaperones' scenario, chaperones would not be expected to have any effect on the WT GCase. However, our results suggest that WT GCase may also be affected in a way that depends on the chemical structure of the chaperone in question and how it interacts with the protein. This has been observed previously (Tiscornia et al, 2013). In general, enzyme activity should

mirror protein content; however, we do not observe this. Chaperone RV21 increases GCase protein levels 2.4-fold and decreases GCase activity by 40%. As for the case of the behavior of MTD131 and MTD132 it is possible that this chaperone, while stabilizing (and therefore increasing) GCase protein levels, has high affinity for the GCase binding site and therefore continues to act as a competitive inhibitor of GCase activity once the protein is in the lysosome. Chaperones TMB84 and MG235 increase GCase protein levels but show no effect on enzyme activity levels, which could be interpreted as a milder form of the same behavior. In contrast, chaperones TMB65 and TMB69 decreased GCase protein levels by 60%, but showed no effect on GCase activity levels, a behavior that is hard to explain. One possible explanation is that the GCase activity assay was performed with limiting amount of substate; however, this does not explain the result, as identical assays in other experiments have measured activities 5.3-fold higher than the control. Further experiments will be required to validate these results.

Regarding α-syn levels, the chaperones tested resulted in statistically increased expression for TMB84, MTD106, RV21, MG235 and CVI62, no change for MTD131, TBM69, MG174, MTD132, DW43 and DW45, and decreased expression for TMB65. While MG174 had an average increase of 3.4-fold compared to the control, the variability of this measurement was high enough to render the difference non-significant. It is possible that further testing may show that MG174 actually does increase α-syn expression. However, we observed that the all the chaperones which did not result in α-syn protein level changes (except for DW45) all had average levels higher than the control but did not reach significance due to high variability. Therefore, 10/12 chaperones increased or tended to increase α-syn protein levels. This does not support the Marzulli model, but rather suggests that each chaperone has clear effects on α-syn protein levels (and very probably other aspects of cell physiology) that are independent of the effect of the chaperone on GCase protein levels and activity. According to Mazzulli et al, the α-syn levels are intimately related with the GCase levels and activity. The Mazzulli model predicts an inverse correlation between GCase levels and activity and α-syn (Mazzulli et al., 2011). Indeed, we measured an increase between 2.6 and 3.8 in α-syn levels in neurons derived from our 4 different GD iPSc cell lines compared to WT (see Fig. 20). If this correlation were generally true and no other factor were in play, several predictions can be made. First, any manipulation (genetic or pharmacological) capable of increasing GCase protein levels and activity would be predicted to result in a decrease in α-syn levels. Second, no change in GCase protein levels or activity should be accompanied by no variation in α-syn protein levels. Third, a decrease in GCase protein levels and activity should result in an increase in α-syn protein levels. We do not generally see this

behavior. For example, chaperones DW43 and DW45 do not affect any of the outputs. It could be argued that the fact that MTD131 and MTD132 show no change in GCase protein levels but a drastic reduction in GCase activity while showing no significant increase in α-syn, does not support the Mazzulli model. However, in both these cases the average levels of α-syn show a tendency to increase, when compared to the control (1.5-fold and 1.7-fold for MTD131 and MTD132 respectively). Nonetheless, due to high variability in these particular measurements, these differences are not statistically significant. If the measurement were repeated and this tendency were confirmed, it would suggest that the Mazzulli hypothesis is correct, but is mediated by activity of GCase and not its protein level, which does not change significantly compared to the control.

The single exception to the tendency of chaperone induced increases α-syn protein levels is TMB65. This compound reduces GCase protein levels significantly (to 0.4-fold relative to control), does not affect GCase activity levels and yet decreases α-syn protein levels significantly (to 0.4-fold relative to the control). In sum, the results of our assays with neurons derived from WT iPSc do not support the Mazzulli model, but taken as a screen for compounds that could be used to decrease α-syn protein levels in PD patients, suggest TMB65 could be a potential candidate for follow up studies. When considering the effect of families of compounds, in broad terms, the chaperone effect is more dependent on its individual structure than on the general structure of the family it belongs to.

4.2 Chaperone Effects on GD Genotype A (L444P/L444P) iPSc Derived Neurons

Substitution of a Leucine for a proline at the position 444 (L444P) is one of the most frequent mutations associated with GD and is usually associated with the neuronopathic forms of the disease. The severity of this genotype is due to a cumulative set of alterations imposed by the mutation to the normal enzyme 3D structure. In addition to folding impairment, L444P has been associated with altered glycosylation at the Leu-Asn glycosylation site at postion 462. Furthermore, it disturbs GCase -Saposin C's interaction residue (a.a. 443-445). GCase forms with conformational and post-translations changes are recognized and marked for Endoplasmic-reticulum-associated protein degradation (ERAD). ERAD overload leads to lysosomal dysfunction, further disrupting the normal autophagic flow responsible for mitochondrial and α-syn degradation. Finally, aberrant folding can also affect a.a. residues between domain II and III which are postioned on the surface of the enzyme and have been found to interact with α-syn C-terminal in acidic conditions. Ultimately, these alterations lead to high

intracellular levels of α-syn which, when in excess, is thought to create GCase membrane-bound complexes that further inhibit GCase activity (Smith et al., 2017). According to these characteristics, L444P should respond to chaperone treatment. Our measurements, shown in Figure 38, show sharp increcreases in GCase protein levels with chaperone treatment. Surprisingly, these increments did not result in increased GCase activity.

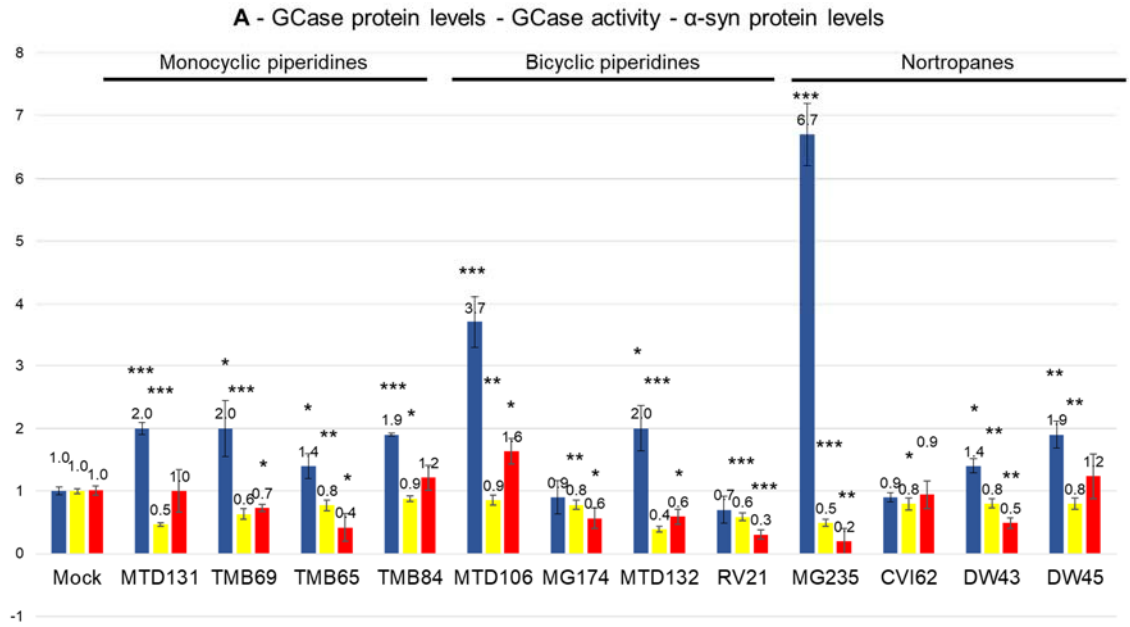

Figure 38. Chaperone effect on genotype A (L444P/L444P) – resume. GCase protein levels (blue bars), GCase activity (yellow bars) and α-syn protein levels (red bars) in terminally differentiated neurons. Protein levels and activity are normalized to the mock (no chaperone treatment) and statistically significant differences are marked as * p<0,05; ** p<0,001, *** p<0,0001.

Regarding GCase protein levels, we observed that 9 out of 12 chaperones resulted in statistically significant increases in protein levels (MTD131, TMB69, TBM65, TMB84, MTD106, MTD132, MG235, DW43 and DW45). Of these, most were modest increases (MTD131, TMB69, TBM65, MTD132, DW43 and DW45). Two chaperones, however, showed higher fold increases: 3.7 and 6.7-fold for MTD106 and MG235, respectively. MG174, RV21 and CVI62 showed no change in their GCase protein levels. The results regarding GCase activity show a tendency of a modest but statistically significant decrease in enzyme activity for all 12 chaperones. Variation among replicates was particularly low for this experiment, and therefore most reductions in activity, though statistically significant, biologically meaningless. All chaperones except 4 (MTD131, TMB69, RV21 and MG235) had reductions of 0.8 or 0.9. The level of reduction observed for the remaining chaperones was 0.5-fold for MTD131 and MG235, and 0.6 for TMB69 and CV21, respectively. Compounds DW45 and DW43 which had been reported to increase GCase activity in L444P fibroblasts, leading to increases of around 4 and 5 fold,

respectively, did not have the have the same effect on our model (Alfonso et al., 2013). This genotype A shows general increase in GCase protein levels correlating with a general decrease in GCase activity, which is difficult to rationalize. As mentioned above, GCase enzyme levels would be expected to approximately mirror GCase protein levels. Increases in GCase protein levels correlating with decreased activity can be explained by positing that a given chaperone has excessively high affinity for the enzyme, resulting in strong binding that cannot be easily reversed in the lysosome. However, in this genotype, this behaviour appears in 9 out of 12 compounds, which is very unlikely. A second possibility is to propose that there is something about the L444P GCase active site that explains the behaviour. One could hypothesize that the 3D structure of the active site resulting from the L444P mutation has acquired a 'switch-like' behaviour, such that chaperones can access the site and this interaction between the chaperone and the protein results in a 'conformational switch' of the active site so that the chaperone becomes 'trapped' in it, resulting in decreased hydrolytic activity. Testing this hypothesis would likely require a structural biology or biophysical approach.

When comparing the 3 parameters, we see no direct relation between them. On the one hand, the increase in GCase is associated with a decrease in GCase levels (MTD 131, TMB 69, TBM 65, MTD 106, MTD132, MG235, DW43 and DW45). On the other hand, these two tendencies do not predict behaviour of the α-syn levels. Within the chaperones with this same behavior (increase in GCase protein levels and decrease in activity), α-syn levels may remain unchanged (MTD131, TMB69 and DW45), decrease (TMB65, MG174, MTD132, MG235 and DW43) or increase (TMB84 and MTD106).

4.3 Chaperone Effects on GD Genotype B (L444P/P415R) iPSc Derived Neurons

Heterozygote of L444P/P415R also generates a strong neuropathic phenotype. Although rare, P415R leads to a severe neuronopathic phenotype strongly associated with type 2 GD (Ron & Horowitz, 2005). While L444P can still be transported to the lysosome, P415R mutants are unable to bind to lysosomal integral membrane protein-2 (LIMP-2), and thus, their lysosomal transport is impaired (Reczek et al., 2007). L444P/P415R has a different pattern of response to chaperones than L444P homozygous, unveiling the need for the development of a mutation or mutation group-specific chaperone treatment. Contrary to what would be expected, heterozygotes seem to have a completely different response to individual chaperone compounds at all the observed levels, being it GCase protein levels, activity or α-syn levels. Thus, generating a complex set of interactions, in which levels of expression, degradation and trafficking of each GCase molecule and

individual affinity to the chaperone affect the outcome. In this particular case, as seen in Figure 39, although the number of compounds able to increase GCase protein levels is lower than for the L444P homozygous genotype (9 to 3, respectively), these increases are over 2-fold. None of the tested compounds was able to increase GCase activity albeit α-syn levels decreased with 7 out of 12 tested chaperones.

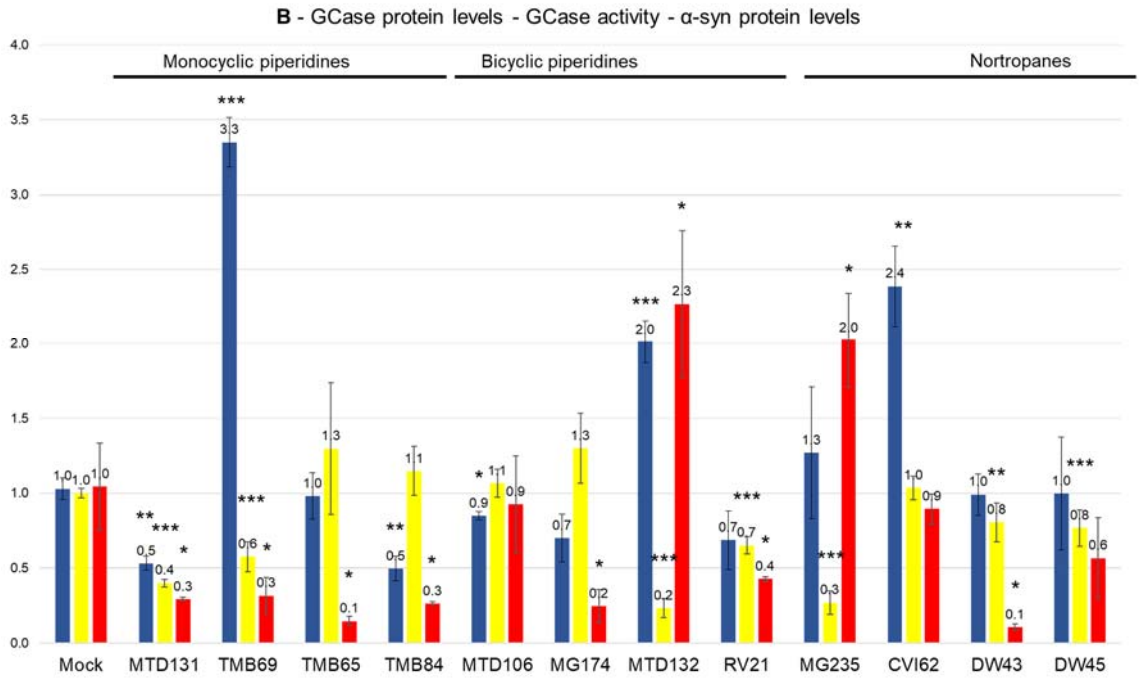

Figure 39. Chaperone effect on genotype B (L444P/P415R) – resume. GCase protein levels (blue bars), GCase activity (yellow bars) and α-syn protein levels (red bars) in terminally differentiated neurons. Protein levels and activity are normalized to the mock (no chaperone treatment) and statistically significant differences are marked as * p<0,05; ** p<0,001, *** p<0,0001.

Regarding GCase protein levels, we observed that 3 out of 12 chaperones resulted in over 2-fold statistically significant increases in protein levels (MTD69, MTD132 and CVI62). Three chaperones, however, showed a decrease in GCase: MTD131 and TMB84 showed a 50% decrease on GCase, while MTD106 had a decrease of 10% compared to untreated. TBM65, MG174, RV21, MG235, DW43 and DW45 showed no change in their GCase protein levels. The results regarding GCase activity show a tendency of modest but statistically significant decrease in enzyme activity for 3 chaperones, with a decrease of 20% for DW43 and DW45; and 30% for RV21. Stronger inhibitions were observed in MTD131, TMB69, MTD132 and MG235 with residual activities of 0.4, 0.6, 0.2 and 0.3, respectively. Again, the low variation between replicates resulted in reductions that although statistically significant, might not imply biological significance.

While the pattern of increase of GCase protein levels and decrease in GCase activity is clear for TMB69 and MTD132, their effects on synuclein levels are opposite; while treatment withTMB69 leads to a decrease synuclein level, suggesting a protective effect, treatment with MTD132 results in an over two-fold increase in synuclein levels. Within the monocyclic piperidines, despite the decreased levels of GCase protein in TBM84, and protein and activity MTD131, α-syn levels were reduced by 90% and 70%, respectively. With the exception of MTD132, the bicyclic piperidines have little (10% MTD106 reduction) or no effect on GCase protein levels. Although not statistically significant, a tendential increase in GCase activity in TMB65, TMB84 and MG174, would explain the decrease in α-syn. Nortropanes have a less consistent behaviour. DW45 decreases activity but has no significant effect on any of the other parameters. DW43, despite decreasing the activity by 20%, also reduces the synuclein levels by 90%. CVI 62 increases the GCase levels but has no direct effect on activity or synuclein.

4.3 Chaperone Effects on GD Genotype C (G325R/C342G) iPSc Derived Neurons

Both the mutations in genotype C directly affect the GCase's active site. Cysteine 342 is located at the active site, in the vicinity of the catalytic dyad and is considered to be important to the catalytic activity. Mutations (such as C342G) in this free cysteine greatly decrease GCase activity. The glutamic acid residue at the position 325 is involved in active site protection and pH-induced conformational changes. At pH 7, G325 is bound to tyrosine 313 via hydrogen bonds, keeping the active site closed. Upon contact with GlcCer at acid pH (<6), tyrosine 313 changes and binds glutamic acid at position 340, inducing conformational changes in aspartate 315 which changes the nearby loop 3 to a helical conformation and consequently opening the active site (Dvir et al., 2003; Smith et al., 2017).

Piperidines seem to have a stronger effect on Genotype C, when compared to nortropanes (Figure 40). The predicted increase in GCase activity dependent on GCase protein levels is absent in all chaperones albeit α-syn levels show a clear tendency to decrease when GCase protein levels increase.

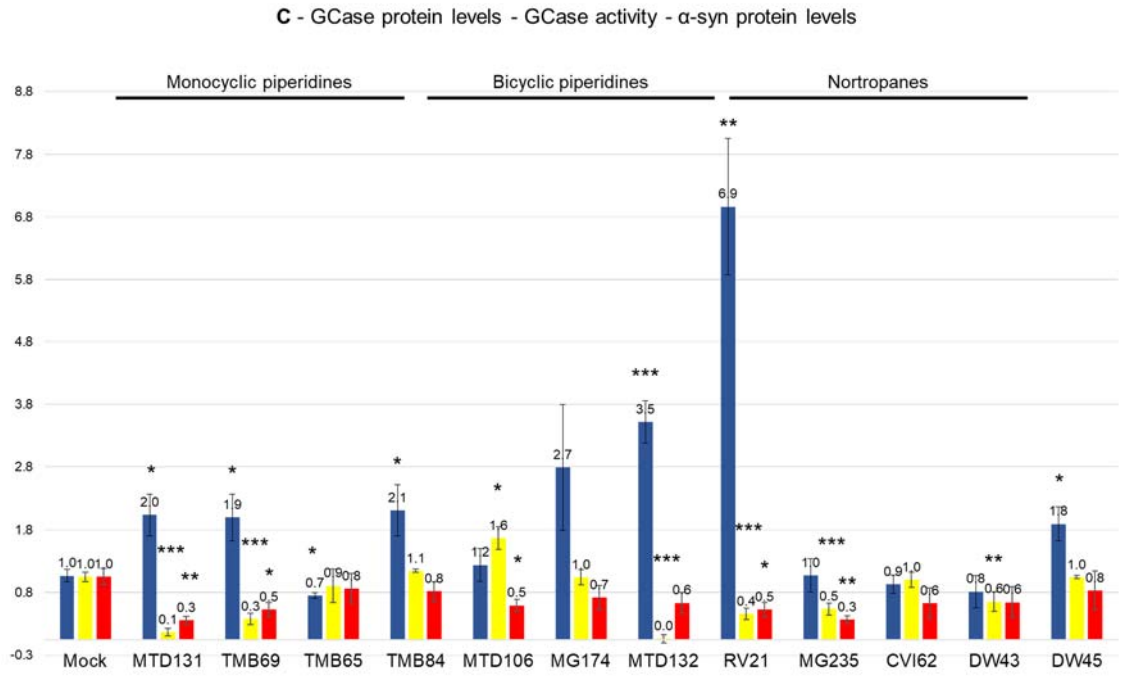

Figure 40. Chaperone effect on genotype C (G325R/C342G) – resume. GCase protein levels (blue bars), GCase activity (yellow bars) and α-syn protein levels (red bars) in terminally differentiated neurons. Protein levels and activity are normalized to the mock (no chaperone treatment) and statistically significant differences are marked as * p<0,05; ** p<0,001, *** p<0,0001.

Looking at the chaperones individually, we observed that 6 out of 12 chaperones resulted in significant increase in GCase protein levels (MTD131, TBM69, TBM84, MTD132, RV21 and DW45). Of these, most were 2-fold increases (MTD131, TBM69, TBM84 and DW45). Two chaperones (MTD132 and RV21) however, showed higher fold increases: 3.5 and 6.9-fold, respectively. MG106, MG174, MG235, CVI62 and DW43 showed no change in their GCase protein levels. The results regarding GCase activity show a tendency of statistically significant decrease in enzyme activity when GCase protein levels increase (MTD131, TMB69, MTD132, RV21). However, two chaperones with statistically significant increases in GCase protein levels (TMB84 and DW45) showed no effect on GCase activity. Surprisingly, two chaperones affected GCase activity without any measurable effect on the enzyme protein levels: MTD106 was able to increase GCase activity 1.6x; and DW43 decreased GCase activity to 0.6 of the control, without changing its protein levels.

The final graph shows a tendency for α-syn levels to decrease if either GCase protein levels (MTD131, TMB65 and RV21) or GCase activity (MTD106) are increased. In some cases (TMB84), even a two-fold increase in the GCase protein level does not significantly change enzyme activity nor or α-syn protein levels. A small decrease of enzyme activity with normal protein levels does not change α-syn levels (DW43). Neither TMB65, MG174 or CVI 62 had any effect on the evaluated parameters.

4.4 Chaperone Effects on GD Genotype D (L444P/G202R) iPSc Derived Neurons

G202R is one of the few specific alleles of neuronopathic forms of GD. The genotype L444P/G202R in particular seems to be specific of the acute neuronopathic form of the disease (GD type 2). G202R leads to a conformational change so extensive that almost all of the peptides are subjected to ERAD and thus never reach the lysosome (Bendikov-Bar & Horowitz, 2012; Ron & Horowitz, 2005). Following the same pattern as the other genotypes, genotype D escapes the present paradigm established by Mazzulli. Our results for this genotype, presented in Figure 41 show an apparent independence between GCase protein levels, activity and α-syn levels. Surprisingly, despite sharing the L444P allele which responded with α-syn decrease to some of the compounds in the other genotypes, none of the tested compounds was able to decrease α-syn levels in genotype C.

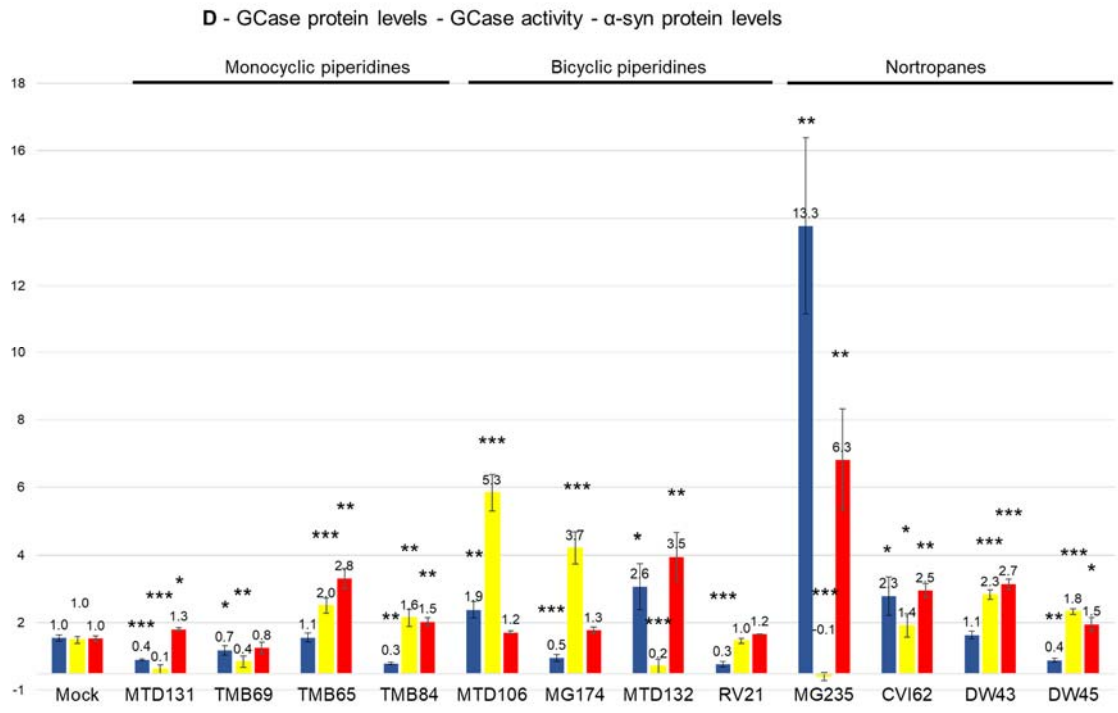

Figure 41. Chaperone effect on genotype D (L444P/G202R) – resume. GCase protein levels (blue bars), GCase activity (yellow bars) and α-syn protein levels (red bars) in terminally differentiated neurons. Protein levels and activity are normalized to the mock (no chaperone treatment) and statistically significant differences are marked as * p<0,05; ** p<0,001, *** p<0,0001.

Treatment with four chaperones resulted in statistically significant increases in protein levels (MTD106, MTD132, MG235 and CVI62). Of these, 3 were of around 2-fold, with 1.9x, 2.6x and 2.3x for MTD106, MTD132 and CVI62, respectively. MG235 increased GCase protein levels by 13.3x. Five chaperones had a deleterious effect in GCase protein levels (MTD131, TMB69, TMB84, MG174, RV21, DW45) with reductions to 0.3x

(TBM84, RV21), 0.4x (MTD131 and DW45), 0.5x (MG174) and 0.7x (TMB69) of the untreated. TMB65 and DW43 had no effect in GCase protein levels.

The results regarding GCase activity show a large chaperone dependent effect. 7 of the 12 chaperones significantly increased activity (TMB65, TMB84, MTD106, MG174, CVI62, DW43 and DW45). TMB84, CVI62 and DW45 had the lowest increases, with 1.6x, 1.4x, and 1.8x, respectively. TMB65 and DW43 had a 2-fold increase in GCase activity but the biggest increase was induced by MTD106 and MG174, with activity of 5.3x and 3.7x the mock. The increase in GCase protein levels was not accompanied by an increase in activity, but with an increase in α-syn levels, suggesting a total inhibition of the enzyme like MG235 and MTD132. Even high increases in GCase activity did not decrease synuclein levels (TMB65, TMB84, MTD106, MG174, DW43, DW45). Some cases do follow the Mazzulli's model where depletion of enzyme levels and activity has led to an increase in α-syn (MTD131). Surprisingly, enzyme activity can be enhanced despite having lower amounts and result in higher levels of α-syn (DW45).

5. Conclusion

Of the 300+ mutations described in GD, the vast majority result in conformational changes, which, although preserving the active site, lead to GCase ERAD degradation and, consequently, a decrease in GCase activity. Low levels of GCase activity lead to generalized accumulation of its substrates, mainly glucosylceramide. Although no solid genotype-phenotype correlation has been established thus far, system-wide symptoms due to GlcCer accumulation are thought to only surface when GCase activity is 50% lower than the heterozygous WT *GBA1* genotype. Current therapies are based in supplementation with recombinant tagged GCase (ERT) and lead to a decrease in GlcCer levels through upstream GlcCer synthase inhibition (SRT). Building on some of the early findings in SRT and recent discoveries in GCase 3D structure, a new class of drugs has been gaining attention – Pharmacological Chaperones (PC). Taking advantage of the fact that most GCase deficits are due to ER degradation, PC molecules aim to ease GCase's folding, helping it to escape ERAD-mediated degradation and, consequently, increasing the amount of enzyme that reaches the lysosome, maximizing enzymatic activity. Despite advances however, none of these approaches have proven to effectively decrease the neuronopathic forms of the disease, urging researchers to develop new therapeutic approaches to treat the most severe type 2 and 3 GD. Although PC are yet to prove their efficacy in delaying CNS deterioration, they have been proven to improve chaperone-assisted folding in ER, and protect against proteolytic degradation when in lysosome, effectively increasing mutated GCase total protein levels and half-life (Aymami, Barril, Rodríguez-Pascau, & Martinell, 2013; Sun et al., 2011).

In the last two decades, a series of retrospective and gene-wide association studies have irrefutably linked α-syn accumulation and PD with *GBA1* mutations. What started as sporadic case reports and genetic linkage studies of GD patients who developed PD-like symptoms, is now considered to be the biggest genetic contributor to PD cases worldwide. Moreover, GCase deficiency has been associated not only with PD, but also with α-syn accumulation, becoming a major risk factor for a group of diseases called synucleinopathies, which also include dementia with Lewy bodies and multiple system atrophy (Aflaki, Westbroek, & Sidransky, 2017; Sklerov et al., 2017). The epidemiologic data was confirmed in 2011, when Mazzulli et al reported for the first time a direct relation between decreased GCase activity a selective accumulation of α-syn in a controlled experiment. According to Mazzulli, in acidic conditions (pH=5), decreased

GCase activity levels resulted in higher levels of intracellular GlcCer, resulting in stabilization of intermediate α-syn species and consequent formation of α-syn aggregates. Simultaneously, α-syn overexpression inhibited GCase ER-Golgi trafficking, resulting in low levels of mature GCase , thus creating a pathogenic bidirectional loop (Mazzulli et al., 2011; Stojkovska, Krainc, & Mazzulli, 2018).

In the present work, we set to: I) corroborate the relationship between GCase activity and protein levels with α-syn levels in four genotypes of GD type 2 iPSc derived neurons; II) use GD iPSc derived neuronal samples to screen a group of 12 pharmacological chaperones for effect in GCase protein levels and activity; and, III) test Mazzulli's feed-forward pathogenic loop by observing how α-syn levels vary with increase in GCase activity and total protein levels. To this end, 3 genotypically independent, patient derived type II GD fibroblasts were reprogrammed to the pluripotent state through exogenous expression the Yamanaka factors (OSKM). iPSc clones of the 3 inhouse reprogrammed GD genotypes, along with previously reprogrammed GD and WT control lines, were then differentiated towards the neuronal phenotype. A combination of side-by-side chaperone treatments were then performed over 12 days after terminal differentiation, with the following results:

I) GCase level measurements align with what had been described for GD type 2 neurons, with GCase protein levels and hydrolytic activity under 20% of the WT equivalents. Concordant with the decrease in GCase parameters, we observed an increase in α-syn levels;
II) Although most chaperones influenced GCase protein levels and activity, there was no observable consistent effect within compound families or across genotypes. Chaperone effect is highly mutation-dependent, with no chaperone having a consistent effect on GCase. GCase protein levels and GCase hydrolytic activity are often assumed to be related. However, when chaperones are added, this correlation is no longer necessarily true; possibly, parameters such as inhibitory effect, affinity and resistance to the protein extraction and denaturation method used. Further studies are necessary to fully understand the effect of GlcCer-like chaperones and in which ways they can affect the intracellular environment. It would also be important to determine relevance of GCase protein levels and activity in PC testing. If, on the one hand, GCase activity reflects the relative amount of GCase protein levels and their residual hydrolytic activity, in this context, there are multiple variables that can affect activity measurements. For example, chaperone concentration on the final protein extract, chaperone-GCase affinity and compound

half-life. On the other hand, GCase protein levels can increase due to the formation of large yet inactive stabilized complexes and not present any beneficial effect (Romero et al., 2019), which could interact with α-syn, and raise its levels (T. Yap et al., 2013; T. L. Yap et al., 2011). Comparison of both parameters allowed us to reach a compromise and have an idea of the intracellular effect of each molecule at the end of the experiment, but also get a sense of the general effect for a more extended period. Notwithstanding, some chaperones showed therapeutic potential for either GD treatment or PD prevention. Clone A (L444P/L444P) had higher GCase protein levels and lower levels of α-syn in the presence of chaperones TMB69, TMB65, MTD132, RV21, MG235 and CVI62. Clone B (L444P/P415R), showed over a three-fold increase in GCase protein levels with TBM69, with a consequent reduction of 70% in α-syn. Other molecules lead to a significant α-syn decrease in this genotype. TMB65, for example, induces an over 90% decrease without any apparent effect on GCase , and chaperones RV21, DW43 and DW45, which, despite having low GCase activity levels, show normal GCase protein level and reduced α-syn. Clone C (G325R/C342G), seems to be very amenable to GCase stabilization and increases in total GCase protein levels. However, this increase never corelates to higher activity levels. It would be interesting to investigate if the GCase activity repression seen in MTD131, TMB69 and RV21 persists in other models. Chaperone MTD106 was able to simultaneously raise GCase activity levels and decrease α-syn levels by half, making it a premium candidate for a future research. Finally, chaperones do not seem to reduce α-syn Clone D (L444P/G202R). However, MTD106 increased both GCase protein levels and activity without affecting α-syn, making it a possible candidate for GD therapy.

III) Broadly speaking, our results do not support Mazzulli's feedforward loop as there was no evident and consistent correlation between either GCase protein levels or activity in total α-syn intracellular levels. Although the inverse correlation between α-syn and GCase activity has been corroborated in different contexts, the trigger and the mechanism behind it are still controversial (Stojkovska et al., 2018). Our data corroborates the inverse correlation between GCase activity and α-syn levels in neurons derived from WT or the GD genotypes used when chaperones are not used. However, for the genotypes tested in this work and 12-day treatment timeframe with our candidate chaperones at the chosen concentration (30 μM), in this particular experimental system, Mazzulli's hypothesis is not generally supported.

First, although there is some previous experimental evidence that indicates that some of the chaperones tested in this work indeed increase GCase protein levels and enzymatic activity (Table 6), this had not previously been tested in human iPSc derived neurons. In II) we tested this the behavior of a total of 48 (4 GD lines x 12 chaperones) combinations of genotype and chaperone. Regarding GCase protein levels, 15/48 (31.2 %) combinations resulted in no effect on GCase protein levels, while 23/48 (47.9%) resulted in statistically significant increases in GCase protein levels. Counter intuitively, 10/48 (20.8%), resulted in statistically significantly lower levels of GCase. At face value, this could be rationalized by saying that while most chaperones increased GCase protein levels from 1.9 to 13.3x, others had no effect on GCase protein levels. Possibly the chaperones that result in lower levels of GCase do so by altering GCase conformation in such a way that enhances ERAD mediated clearing. To our surprise, of the 23 out of 48 chaperones that increased GCase protein levels, only 1 (MTD106 on genotype L444P/G202R) increased GCase activity levels (to 5.3x). In fact, for 13 chaperones in which GCase protein levels were higher, GCase activity levels were actually lower. This suggests that these chaperones do not dissociate easily from the active site, behaving, in actual fact, as irreversible inhibitors.

While the increases in GCase measured were statistically significant, it remains to be determined whether they would have any clinical significance. So it could be concluded that the chaperones tested under this conditions do not meet the criteria of increasing both GCase protein levels and enzymatic activity. The only case in which these criteria were met were for MTD106 on genotype L444P/G202R, which increased GCase protein levels to 1,9x and activity levels to 5.3x. Measurement of α-syn levels in this treatment showed no significant variations, suggesting that the increase in GCase levels and activity afforded by this chaperone is insufficient to impact α-syn levels. A-syn accumulation is clearly a multifactorial process, with factors like LIMP2, *GBA2*, autophagy impairment and mitochondrial function playing a crucial rule (Siebert, Sidransky, & Westbroek, 2014; Stojkovska et al., 2018). Further studies are necessary to understand the effect of the tested pharmacological chaperones for longer periods of time and in more complex systems.

References

Abeliovich, A., Schmitz, Y., Fariñas, I., Choi-Lundberg, D., Ho, W.-H., Castillo, P. E., . . . Rosenthal, A. (2000). Mice Lacking α-Synuclein Display Functional Deficits in the Nigrostriatal Dopamine System. *Neuron, 25*(1), 239-252. doi: 10.1016/S0896-6273(00)80886-7

Abian, O., Alfonso, P., Velazquez-Campoy, A., Giraldo, P., Pocovi, M., & Sancho, J. (2011). Therapeutic Strategies for Gaucher Disease: Miglustat (NB-DNJ) as a Pharmacological Chaperone for Glucocerebrosidase and the Different Thermostability of Velaglucerase Alfa and Imiglucerase. *Molecular Pharmaceutics, 8*(6), 2390-2397. doi: 10.1021/mp200313e

Adegbola, A., Bury, L. A., Fu, C., Zhang, M., & Wynshaw-Boris, A. (2017). Concise Review: Induced Pluripotent Stem Cell Models for Neuropsychiatric Diseases. *STEM CELLS Translational Medicine, 6*(12), 2062-2070. doi: 10.1002/sctm.17-0150

Aflaki, E., Borger, D. K., Moaven, N., Stubblefield, B. K., Rogers, S. A., Patnaik, S., . . . Sidransky, E. (2016). A New Glucocerebrosidase Chaperone Reduces α-Synuclein and Glycolipid Levels in iPSC-Derived Dopaminergic Neurons from Patients with Gaucher Disease and Parkinsonism. *The Journal of Neuroscience, 36*(28), 7441-7452. doi: 10.1523/JNEUROSCI.0636-16.2016

Aflaki, E., Westbroek, W., & Sidransky, E. (2017). The Complicated Relationship between Gaucher Disease and Parkinsonism: Insights from a Rare Disease. *Neuron, 93*(4), 737-746. doi: 10.1016/j.neuron.2017.01.018

Aguilar-Moncayo, M., Garcia-Moreno, M. I., Trapero, A., Egido-Gabas, M., Llebaria, A., Garcia Fernandez, J. M., & Ortiz Mellet, C. (2011). Bicyclic (galacto)nojirimycin analogues as glycosidase inhibitors: Effect of structural modifications in their pharmacological chaperone potential towards [small beta]-glucocerebrosidase. *Organic & Biomolecular Chemistry, 9*(10), 3698-3713. doi: 10.1039/C1OB05234A

Aharon-Peretz , J., Rosenbaum , H., & Gershoni-Baruch , R. (2004). Mutations in the Glucocerebrosidase Gene and Parkinson's Disease in Ashkenazi Jews. *New England Journal of Medicine, 351*(19), 1972-1977. doi: doi:10.1056/NEJMoa033277

Alfonso, P., Andreu, V., Pino-Angeles, A., Moya-García, A. A., García-Moreno, M. I., Rodríguez-Rey, J. C., . . . Giraldo, P. (2013). Bicyclic Derivatives of L-Idonojirimycin as Pharmacological Chaperones for Neuronopathic Forms of Gaucher Disease. *ChemBioChem, 14*(8), 943-949. doi: 10.1002/cbic.201200708

Angot, E., Steiner, J. A., Lema Tomé, C. M., Ekström, P., Mattsson, B., Björklund, A., & Brundin, P. (2012). Alpha-Synuclein Cell-to-Cell Transfer and Seeding in Grafted Dopaminergic Neurons In Vivo. *PLOS ONE, 7*(6), e39465. doi: 10.1371/journal.pone.0039465

Association, A. s. (2015). 2015 Alzheimer's disease facts and figures. *Alzheimer's & Dementia, 11*(3), 332-384. doi: https://doi.org/10.1016/j.jalz.2015.02.003

Aureli, M., Bassi, R., Loberto, N., Regis, S., Prinetti, A., Chigorno, V., . . . Sonnino, S. (2012). Cell surface associated glycohydrolases in normal and Gaucher disease fibroblasts. *Journal of Inherited Metabolic Disease, 35*(6), 1081-1091. doi: 10.1007/s10545-012-9478-x

Awad, O., Panicker, L. M., Deranieh, R. M., Srikanth, M. P., Brown, R. A., Voit, A., . . . Feldman, R. A. (2017). Altered Differentiation Potential of Gaucher's Disease iPSC Neuronal Progenitors due to Wnt/β-Catenin Downregulation. *Stem Cell Reports, 9*. doi: 10.1016/j.stemcr.2017.10.029

Awad, O., Sarkar, C., Panicker, L. M., Miller, D., Zeng, X., Sgambato, J. A., . . . Feldman, R. A. (2015). Altered TFEB-mediated lysosomal biogenesis in Gaucher disease iPSC-derived

neuronal cells. *Human Molecular Genetics, 24*(20), 5775-5788. doi: 10.1093/hmg/ddv297

Aymami, J., Barril, X., Rodríguez-Pascau, L., & Martinell, M. (2013). Pharmacological chaperones for enzyme enhancement therapy in genetic diseases. *Pharmaceutical Patent Analyst, 2*(1), 109-124. doi: 10.4155/ppa.12.74

Baharvand, H., Mehrjardi, N.-Z., Hatami, M., Kiani, S., Rao, M., & Haghighi, M.-M. (2007). Neural differentiation from human embryonic stem cells in a defined adherent culture condition. *The International Journal of Developmental Biology, 51*(5), 371-378. doi: 10.1387/ijdb.072280hb

Beaton, B., Monzón, J. L. S., Hughes, D. A., & Pastores, G. M. (2017). Gaucher disease: risk stratification and comorbidities. *Expert Opinion on Orphan Drugs, 5*(11), 839-846. doi: 10.1080/21678707.2017.1385455

Beattie, G. M., Lopez, A. D., Bucay, N., Hinton, A., Firpo, M. T., King, C. C., & Hayek, A. (2005). Activin A Maintains Pluripotency of Human Embryonic Stem Cells in the Absence of Feeder Layers. *STEM CELLS, 23*(4), 489-495. doi: 10.1634/stemcells.2004-0279

Bekris, L. M., Mata, I. F., & Zabetian, C. P. (2010). The Genetics of Parkinson Disease. *Journal of Geriatric Psychiatry and Neurology, 23*(4), 228-242. doi: doi:10.1177/0891988710383572

Bendikov-Bar, I., & Horowitz, M. (2012). Gaucher disease paradigm: from ERAD to comorbidity. *Human mutation, 33*(10), 1398-1407. doi: 10.1002/humu.22124

Bendor, J. T., Logan, T. P., & Edwards, R. H. (2013). The Function of α-Synuclein. *Neuron, 79*(6), 1044-1066. doi: 10.1016/j.neuron.2013.09.004

Benito, J. M., García Fernández, J. M., & Mellet, C. O. (2011). Pharmacological chaperone therapy for Gaucher disease: a patent review. *Expert Opinion on Therapeutic Patents, 21*(6), 885-903. doi: 10.1517/13543776.2011.569162

Bennett, L. L., & Mohan, D. (2013). Gaucher Disease and Its Treatment Options. *Annals of Pharmacotherapy, 47*(9), 1182-1193. doi: doi:10.1177/1060028013500469

Bergeron-Brlek, M., Meanwell, M., & Britton, R. (2015). Direct synthesis of imino-C-nucleoside analogues and other biologically active iminosugars. *Nature Communications, 6*(1), 6903. doi: 10.1038/ncomms7903

Bernardo, M., & Fibbe, W. E. (2013). Mesenchymal Stromal Cells: Sensors and Switchers of Inflammation. *Cell Stem Cell, 13*(4), 392-402. doi: 10.1016/j.stem.2013.09.006

Beutler, E. (2006). Lysosomal storage diseases: Natural history and ethical and economic aspects. *Molecular Genetics and Metabolism, 88*(3), 208-215. doi: 10.1016/j.ymgme.2006.01.010

Bieri, G., Gitler, A. D., & Brahic, M. (2018). Internalization, axonal transport and release of fibrillar forms of alpha-synuclein. *Neurobiology of Disease, 109*, 219-225. doi: 10.1016/j.nbd.2017.03.007

Blanz, J., & Saftig, P. (2016). Parkinson's disease: acid-glucocerebrosidase activity and alpha-synuclein clearance. *Journal of Neurochemistry, 139*, 198-215. doi: 10.1111/jnc.13517

Bonini, N. M., Giasson, Benoit I. (2005). Snaring the Function of a-Synuclein. *Cell Biology, 123*(3), 359-361. doi: 10.1016/j.cell.2005.10.017

Brady, R. O., Kanfer, J. N., Bradley, R. M., & Shapiro, D. (1966). Demonstration of a deficiency of glucocerebroside-cleaving enzyme in Gaucher's disease. *Journal of Clinical Investigation, 45*(7), 1112-1115.

Brady, R. O., Kanfer, J. N., & Shapiro, D. (1965). Metabolism of glucocerebrosides II. Evidence of an enzymatic deficiency in Gaucher's disease. *Biochemical and Biophysical Research Communications, 18*(2), 221-225. doi: https://doi.org/10.1016/0006-291X(65)90743-6

Brady , R. O., Pentchev , P. G., Gal , A. E., Hibbert , S. R., & Dekaban , A. S. (1974). Replacement Therapy for Inherited Enzyme Deficiency. *New England Journal of Medicine, 291*(19), 989-993. doi: 10.1056/nejm197411072911901

Brundin, P., & Melki, R. (2017). Prying into the Prion Hypothesis for Parkinson's Disease. *Journal of Neuroscience, 37*(41), 9808-9818. doi: 10.1523/JNEUROSCI.1788-16.2017

Burré, J., Sharma, M., Tsetsenis, T., Buchman, V., Etherton, M. R., & Südhof, T. C. (2010). α-Synuclein Promotes SNARE-Complex Assembly in Vivo and in Vitro. *Science, 329*(5999), 1663-1667. doi: 10.1126/science.1195227

Butler, G. A. G. (2001). Glucosylceramide lipidosis–Gaucher disease. In B. A. L. Scriver C. R., Sly W.S. and Valle D (Ed.), *The metabolic and molecular bases of inherited diseases* (8 ed., pp. 3635–3668). New York: McGraw-Hill.

Campeau, P. M., Rafei, M., Boivin, M.-N., Sun, Y., Grabowski, G. A., & Galipeau, J. (2009). Characterization of Gaucher disease bone marrow mesenchymal stromal cells reveals an altered inflammatory secretome. *Blood, 114*(15), 3181-3190. doi: 10.1182/blood-2009-02-205708

Chambers, S. M., Fasano, C. A., Papapetrou, E. P., Tomishima, M., Sadelain, M., & Studer, L. (2009). Highly efficient neural conversion of human ES and iPS cells by dual inhibition of SMAD signaling. *Nature Biotechnology, 27*(3). doi: 10.1038/nbt.1529

Choi, J. H., Stubblefield, B., Cookson, M. R., Goldin, E., Velayati, A., Tayebi, N., & Sidransky, E. (2011). Aggregation of α-synuclein in brain samples from subjects with glucocerebrosidase mutations. *Molecular Genetics and Metabolism, 104*(1–2), 185-188. doi: doi.org/10.1016/j.ymgme.2011.06.008

Codolo, G., Plotegher, N., Pozzobon, T., Brucale, M., Tessari, I., Bubacco, L., & de Bernard, M. (2013). Triggering of Inflammasome by Aggregated α–Synuclein, an Inflammatory Response in Synucleinopathies. *PLOS ONE, 8*(1), e55375. doi: 10.1371/journal.pone.0055375

Cohen, P., & Knebel, A. (2006). KESTREL: a powerful method for identifying the physiological substrates of protein kinases. *Biochemical Journal, 393*(1), 1-6. doi: 10.1042/BJ20051545

Cooper, A. A., Gitler, A. D., Cashikar, A., Haynes, C. M., Hill, K. J., Bhullar, B., . . . Lindquist, S. (2006). α-Synuclein Blocks ER-Golgi Traffic and Rab1 Rescues Neuron Loss in Parkinson's Models. *Science, 313*(5785), 324-328. doi: 10.1126/science.1129462

Costanzo, M., & Zurzolo, C. (2013). The cell biology of prion-like spread of protein aggregates: mechanisms and implication in neurodegeneration. *Biochemical Journal, 452*(1), 1.

Cuny, G. D., Yu, P. B., Laha, J. K., Xing, X., Liu, J.-F., Lai, C. S., . . . Peterson, R. T. (2008). Structure-activity relationship study of bone morphogenetic protein (BMP) signaling inhibitors. *Bioorganic & medicinal chemistry letters, 18*(15), 4388-4392. doi: 10.1016/j.bmcl.2008.06.052

de la Mata, M., Cotán, D., Oropesa-Ávila, M., Garrido-Maraver, J., Cordero, M. D., Paz, M., . . . Sánchez-Alcázar, J. A. (2015). Pharmacological Chaperones and Coenzyme Q10 Treatment Improves Mutant β-Glucocerebrosidase Activity and Mitochondrial Function in Neuronopathic Forms of Gaucher Disease. *Scientific Reports, 5*(1), 10903. doi: 10.1038/srep10903

Dhara, S. K., & Stice, S. L. (2008). Neural differentiation of human embryonic stem cells. *Journal of Cellular Biochemistry, 105*(3), 633-640. doi: 10.1002/jcb.21891

Diao, J., Burré, J., Vivona, S., Cipriano, D. J., Sharma, M., Kyoung, M., . . . Brunger, A. T. (2013). Native α-synuclein induces clustering of synaptic-vesicle mimics via binding to phospholipids and synaptobrevin-2/VAMP2. *eLife, 2*, e00592. doi: 10.7554/eLife.00592

Du, Z.-W. W., & Zhang, S.-C. C. (2004). Neural differentiation from embryonic stem cells: which way? *Stem cells and development, 13*(4), 372-381. doi: 10.1089/scd.2004.13.372

Dvir, H., Harel, M., McCarthy, A. A., Toker, L., Silman, I., Futerman, A. H., & Sussman, J. L. (2003). X-ray structure of human acid-β-glucosidase, the defective enzyme in Gaucher disease. *EMBO Reports, 4*(7), 704-709. doi: 10.1038/sj.embor.embor873

Elleder, M. (2006). Glucosylceramide transfer from lysosomes—the missing link in molecular pathology of glucosylceramidase deficiency: A hypothesis based on existing data. *Journal of Inherited Metabolic Disease, 29*(6), 707-715. doi: 10.1007/s10545-006-0411-z

Enquist, I., Bianco, C., Ooka, A., Nilsson, E., Månsson, J.-E., Ehinger, M., . . . Karlsson, S. (2007). Murine models of acute neuronopathic Gaucher disease. *Proceedings of the National*

Academy of Sciences of the United States of America, 104(44), 17483-17488. doi: 10.1073/pnas.0708086104

Fan, J.-Q., Ishii, S., Asano, N., & Suzuki, Y. (1999). Accelerated transport and maturation of lysosomal α–galactosidase A in Fabry lymphoblasts by an enzyme inhibitor. *Nature medicine, 5*(1), 112-115. doi: 10.1038/4801

Flagmeier, P., Meisl, G., Vendruscolo, M., Knowles, T. P. J., Dobson, C. M., Buell, A. K., & Galvagnion, C. (2016). Mutations associated with familial Parkinson's disease alter the initiation and amplification steps of α-synuclein aggregation. *Proceedings of the National Academy of Sciences, 113*(37), 10328-10333. doi: 10.1073/pnas.1604645113

Fog, C., Zago, P., Malini, E., Solanko, L., Peruzzo, P., Bornæs, C., . . . Kirkegaard, T. (2018). The heat shock protein amplifier arimoclomol improves refolding, maturation and lysosomal activity of glucocerebrosidase. *EBioMedicine, 38*. doi: 10.1016/j.ebiom.2018.11.037

Freundt, E. C., Maynard, N., Clancy, E. K., Roy, S., Bousset, L., Sourigues, Y., . . . Brahic, M. (2012). Neuron-to-neuron transmission of α-synuclein fibrils through axonal transport. *Annals of Neurology, 72*(4), 517-524. doi: 10.1002/ana.23747

Gallegos, S., Pacheco, C., Peters, C., Opazo, C. M., & Aguayo, L. G. (2015). Features of alpha-synuclein that could explain the progression and irreversibility of Parkinson's disease. *Frontiers in Neuroscience, 9*, 59. doi: 10.3389/fnins.2015.00059

Galvagnion, C. (2017). The Role of Lipids Interacting with α-Synuclein in the Pathogenesis of Parkinson's Disease. *Journal of Parkinson's Disease, Preprint*(Preprint), 1-18. doi: 10.3233/JPD-171103

Galvin, J. E., Lee, V., & Trojanowski, J. Q. (2001). Synucleinopathies: Clinical and Pathological Implications. *Archives of Neurology, 58*(2), 186-190. doi: 10.1001/archneur.58.2.186

García-Sanz, P., Orgaz, L., Fuentes, J. M., Vicario, C., & Moratalla, R. (2018). Cholesterol and multilamellar bodies: Lysosomal dysfunction in GBA-Parkinson disease. *Autophagy, 14*(4), 717-718. doi: 10.1080/15548627.2018.1427396

Gegg, M. E., & Schapira, A. (2016). Mitochondrial dysfunction associated with glucocerebrosidase deficiency. *Neurobiology of Disease, 90*, 43-50. doi: 10.1016/j.nbd.2015.09.006

Ginns, E. I., Choudary, P. V., Martin, B. M., Winfield, S., Stubblefield, B., Mayor, J., . . . Barranger, J. A. (1984). Isolation of cDNA clones for human beta-glucocerebrosidase using the lambda gt11 expression system. *Biochemical and Biophysical Research Communications, 123*(2), 574-580. doi: 10.1016/0006-291x(84)90268-7

Ginzburg, L., Kacher, Y., & Futerman, A. H. (2004). The pathogenesis of glycosphingolipid storage disorders. *Seminars in Cell & Developmental Biology, 15*(4), 417-431. doi: 10.1016/j.semcdb.2004.03.003

Goker-Alpan, O., Hruska, K. S., Orvisky, E., Kishnani, P. S., Stubblefield, B. K., Schiffmann, R., & Sidransky, E. (2005). Divergent phenotypes in Gaucher disease implicate the role of modifiers. *Journal of Medical Genetics, 42*(6). doi: 10.1136/jmg.2004.028019

Goker-Alpan, O., Schiffmann, R., Park, J. K., Stubblefield, B. K., Tayebi, N., & Sidransky, E. (2003). Phenotypic continuum in neuronopathic gaucher disease: an intermediate phenotype between type 2 and type 3. *The Journal of Pediatrics, 143*(2), 273-276. doi: http://dx.doi.org/10.1067/S0022-3476(03)00302-0

Gordon, J., Amini, S., & White, M. K. (2013). General Overview of Neuronal Cell Culture. *General Overview of Neuronal Cell Culture, 1078*, 1-8. doi: 10.1007/978-1-62703-640-5_1

Grabowski, G. A. (2008). Phenotype, diagnosis, and treatment of Gaucher's disease. *The Lancet, 372*(9645), 1263-1271. doi: http://dx.doi.org/10.1016/S0140-6736(08)61522-6

Grabowski, G. A., Bendikov-Bar, I., Maor, G., & Horowitz, M. (2013). Gaucher Disease: Basic and Clinical Perspectives. *Gaucher Disease: Basic and Clinical Perspectives*, 140-157. doi: 10.2217/ebo.12.298

Grabowski, G. A., Zimran, A., & Ida, H. (2015). Gaucher disease types 1 and 3: Phenotypic characterization of large populations from the ICGG Gaucher Registry. *American Journal of Hematology, 90*(S1). doi: 10.1002/ajh.24063

Gruschus, J. M., Jiang, Z., Yap, T., Hill, S. A., Grishaev, A., Piszczek, G., . . . Lee, J. C. (2015). Dissociation of glucocerebrosidase dimer in solution by its co-factor, saposin C. *Biochemical and Biophysical Research Communications, 457*(4), 561-566. doi: 10.1016/j.bbrc.2015.01.024

Hein, L. K., Meikle, P. J., Hopwood, J. J., & Fuller, M. (2007). Secondary sphingolipid accumulation in a macrophage model of Gaucher disease. *Molecular Genetics and Metabolism, 92*(4), 336-345. doi: 10.1016/j.ymgme.2007.08.001

Hirabayashi, Y., Itoh, Y., Tabata, H., Nakajima, K., Akiyama, T., Masuyama, N., & Gotoh, Y. (2004). The Wnt/β-catenin pathway directs neuronal differentiation of cortical neural precursor cells. *Development, 131*(12), 2791-2801. doi: 10.1242/dev.01165

Hollak, C. E., van Weely, S., van Oers, M. H., & Aerts, J. M. (1994). Marked elevation of plasma chitotriosidase activity. A novel hallmark of Gaucher disease. *Journal of Clinical Investigation, 93*(3), 1288-1292.

Horowitz, M., Wilder, S., Horowitz, Z., Reiner, O., Gelbart, T., & Beutler, E. (1989). The human glucocerebrosidase gene and pseudogene: Structure and evolution. *Genomics, 4*(1), 87-96. doi: https://doi.org/10.1016/0888-7543(89)90319-4

Hruska, K. S., LaMarca, M. E., Scott, C. R., & Sidransky, E. (2008). Gaucher disease: mutation and polymorphism spectrum in the glucocerebrosidase gene (GBA). *Human Mutation, 29*(5), 567-583. doi: 10.1002/humu.20676

Inman, G. J., Nicolás, F. J., Callahan, J. F., Harling, J. D., Gaster, L. M., Reith, A. D., . . . Hill, C. S. (2002). SB-431542 is a potent and specific inhibitor of transforming growth factor-beta superfamily type I activin receptor-like kinase (ALK) receptors ALK4, ALK5, and ALK7. *Molecular pharmacology, 62*(1), 65-74.

Itskovitz-Eldor, J. (2018). 20th Anniversary of Isolation of Human Embryonic Stem Cells: A Personal Perspective. *Stem cell reports, 10*(5), 1439-1441. doi: 10.1016/j.stemcr.2018.04.011

Itsykson, P., Ilouz, N., Turetsky, T., Goldstein, R. S., Pera, M. F., Fishbein, I., . . . Reubinoff, B. E. (2005). Derivation of neural precursors from human embryonic stem cells in the presence of noggin. *Molecular and cellular neurosciences, 30*(1), 24-36. doi: 10.1016/j.mcn.2005.05.004

James, D., Levine, A. J., Besser, D., & Hemmati-Brivanlou, A. (2005). TGFβ/activin/nodal signaling is necessary for the maintenance of pluripotency in human embryonic stem cells. *Development, 132*(6), 1273-1282. doi: 10.1242/dev.01706

Kadali, S., Kolusu, A., Sunkara, S., Gummadi, M., & Undamatla, J. (2016). Clinical evaluation of chitotriosidase enzyme activity in Gaucher and Niemann Pick A/B diseases: A retrospective study from India. *Clinica Chimica Acta, 457*, 8-11. doi: 10.1016/j.cca.2016.03.004

Kang, L., Zhan, X., Ye, J., Han, L., Qiu, W., Gu, X., & Zhang, H. (2018). A rare form of Gaucher disease resulting from saposin C deficiency. *Blood Cells, Molecules, and Diseases, 68*, 60-65. doi: 10.1016/j.bcmd.2017.04.001

Klein, A. D. D., & Futerman, A. H. (2013). Lysosomal storage disorders: old diseases, present and future challenges. *Pediatric endocrinology reviews : PER, 11 Suppl 1*, 59-63.

Koprivica, V., Stone, D. L., Park, J. K., Callahan, M., Frisch, A., Cohen, I. J., . . . Sidransky, E. (2000). Analysis and Classification of 304 Mutant Alleles in Patients with Type 1 and Type 3 Gaucher Disease. *The American Journal of Human Genetics, 66*(6), 1777-1786. doi: http://dx.doi.org/10.1086/302925

Korhonen, P., Malm, T., & White, A. R. (2018). 3D human brain cell models: New frontiers in disease understanding and drug discovery for neurodegenerative diseases. *Neurochemistry International*. doi: 10.1016/j.neuint.2018.08.012

Lange, M. C., Teive, H. A. G., Troiano, A. R., Bitencourt, M., Funke, V. A. M., Setúbal, D. C., . . . do Paraná, B. (2006). Bone marrow transplantation in patients with storage diseases: a developing country experience. *Arquivos de Neuro-Psiquiatria, 64*(1), 1-4. doi: 10.1590/S0004-282X2006000100001

Laping, N. J., Grygielko, E., Mathur, A., Butter, S., Bomberger, J., Tweed, C., . . . Olson, B. A. (2002). Inhibition of Transforming Growth Factor (TGF)-β1–Induced Extracellular Matrix with a Novel Inhibitor of the TGF-β Type I Receptor Kinase Activity: SB-431542. *Molecular pharmacology, 62*(1), 58-64. doi: 10.1124/mol.62.1.58

Li, X.-J., Du, Z.-W., Zarnowska, E. D., Pankratz, M., Hansen, L. O., Pearce, R. A., & Zhang, S.-C. (2005). Specification of motoneurons from human embryonic stem cells. *Nature Biotechnology, 23*(2), 215-221. doi: 10.1038/nbt1063

Lopez, G., Monestime, G., & Sidransky, E. (2016). Clinical studies of GBA1-associated parkinsonism: progress and challenges. *Neurodegenerative Disease Management, 6*(1), 1-4. doi: 10.2217/nmt.15.68

Lu, J., Chiang, J., Iyer, R. R., Thompson, E., Kaneski, C. R., Xu, D. S., . . . Zhuang, Z. (2010). Decreased glucocerebrosidase activity in Gaucher disease parallels quantitative enzyme loss due to abnormal interaction with TCP1 and c-Cbl. *Proceedings of the National Academy of Sciences, 107*(50), 21665-21670. doi: 10.1073/pnas.1014376107

Luan, Z., Higaki, K., Aguilar-Moncayo, M., Ninomiya, H., Ohno, K., García-Moreno, I. M., . . . Suzuki, Y. (2009). Chaperone Activity of Bicyclic Nojirimycin Analogues for Gaucher Mutations in Comparison with N-(n-nonyl)Deoxynojirimycin. *ChemBioChem, 10*(17), 2780-2792. doi: 10.1002/cbic.200900442

Luan, Z., Li, L., Higaki, K., Nanba, E., Suzuki, Y., & Ohno, K. (2013). The chaperone activity and toxicity of ambroxol on Gaucher cells and normal mice. *Brain and Development, 35*(4), 317-322. doi: 10.1016/j.braindev.2012.05.008

Macedo, D., Jardim, C., Figueira, I., Almeida, F. A., McDougall, G. J., Stewart, D., . . . Santos, C. N. (2018). (Poly)phenol-digested metabolites modulate alpha-synuclein toxicity by regulating proteostasis. *Scientific Reports, 8*(1), 6965. doi: 10.1038/s41598-018-25118-z

Maden, M. (2007). Retinoic acid in the development, regeneration and maintenance of the nervous system. *Nature Reviews Neuroscience, 8*(10), 755-765. doi: 10.1038/nrn2212

Madhu, V., Dighe, A. S., Cui, Q., & Deal, N. D. (2016). Dual Inhibition of Activin/Nodal/TGF-β and BMP Signaling Pathways by SB431542 and Dorsomorphin Induces Neuronal Differentiation of Human Adipose Derived Stem Cells. *Stem Cells International, 2016*, 1-13. doi: 10.1155/2016/1035374

Maor, G., Filocamo, M., & Horowitz, M. (2013). ITCH regulates degradation of mutant glucocerebrosidase: implications to Gaucher disease. *Human Molecular Genetics, 22*(7), 1316-1327. doi: 10.1093/hmg/dds535

Marques, O., & Outeiro, T. F. (2012). Alpha-synuclein: from secretion to dysfunction and death. *Cell Death & Disease, 3*(7). doi: 10.1038/cddis.2012.94

Martins, A. R. F. (2013). *Differentiation of Human Pluripotent Stem Cells to the Neuronal Dopaminergic Fate.* (Master), UAlg, Universidade do Algarve. Retrieved from http://hdl.handle.net/10400.1/8351 Sapientia database. (10400.1/8351)

Mason, I. (2007). Initiation to end point: the multiple roles of fibroblast growth factors in neural development. *Nature Reviews Neuroscience, 8*(8), 583-596. doi: 10.1038/nrn2189

Mazzulli, J. R., Xu, Y.-H., Sun, Y., Knight, A. L., McLean, P. J., Caldwell, G. A., . . . Krainc, D. (2011). Gaucher Disease Glucocerebrosidase and α-Synuclein Form a Bidirectional Pathogenic Loop in Synucleinopathies. *Cell, 146*(1), 37-52. doi: 10.1016/j.cell.2011.06.001

McEachern, K. A., Fung, J., Komarnitsky, S., Siegel, C. S., Chuang, W.-L., Hutto, E., . . . Marshall, J. (2007). A specific and potent inhibitor of glucosylceramide synthase for substrate inhibition therapy of Gaucher disease. *Molecular Genetics and Metabolism, 91*(3), 259-267. doi: 10.1016/j.ymgme.2007.04.001

McNeill, A., Duran, R., Proukakis, C., Bras, J., Hughes, D., Mehta, A., . . . Schapira, A. H. V. (2012). Hyposmia and Cognitive Impairment in Gaucher Disease Patients and Carriers. *Movement disorders : official journal of the Movement Disorder Society, 27*(4), 526-532. doi: 10.1002/mds.24945

Meijer, L., Skaltsounis, A.-L., Magiatis, P., Polychronopoulos, P., Knockaert, M., Leost, M., . . . Greengard, P. (2003). GSK-3-Selective Inhibitors Derived from Tyrian Purple Indirubins. *Chemistry & Biology, 10*(12), 1255-1266. doi: 10.1016/j.chembiol.2003.11.010

Mena-Barragán, T., Narita, A., Matias, D., Tiscornia, G., Nanba, E., Ohno, K., . . . Ortiz Mellet, C. (2015). pH-Responsive Pharmacological Chaperones for Rescuing Mutant Glycosidases. *Angewandte Chemie International Edition, 54*(40), 11696-11700. doi: 10.1002/anie.201505147

Mencarelli, C., & Martinez–Martinez, P. (2013). Ceramide function in the brain: when a slight tilt is enough. *Cellular and Molecular Life Sciences, 70*(2), 181-203. doi: 10.1007/s00018-012-1038-x

Menges, S., Minakaki, G., Schaefer, P. M., Meixner, H., Prots, I., Schlötzer-Schrehardt, U., . . . Klucken, J. (2017). Alpha-synuclein prevents the formation of spherical mitochondria and apoptosis under oxidative stress. *Scientific Reports, 7*(1). doi: 10.1038/srep42942

Mercado, G., Valdés, P., & Hetz, C. (2013). An ERcentric view of Parkinson's disease. *Trends in Molecular Medicine, 19*(3), 165-175. doi: 10.1016/j.molmed.2012.12.005

Mistry, P. K., Lopez, G., Schiffmann, R., Barton, N. W., Weinreb, N. J., & Sidransky, E. (2017). Gaucher disease: Progress and ongoing challenges. *Molecular Genetics and Metabolism, 120*(1-2), 8-21. doi: 10.1016/j.ymgme.2016.11.006

Mizuseki, K., Sakamoto, T., Watanabe, K., Muguruma, K., Ikeya, M., Nishiyama, A., . . . Sasai, Y. (2003). Generation of neural crest-derived peripheral neurons and floor plate cells from mouse and primate embryonic stem cells. *Proceedings of the National Academy of Sciences, 100*(10), 5828-5833. doi: 10.1073/pnas.1037282100

Monteiro, F. D. R. (2016). *Using induced pluripotent stem cells to investigate the mechanistic link between Gaucher disease and Parkinson related synucleinopathies.* (Master Scientific), Universidade do Algarve, Universidade do Algarve. Retrieved from http://hdl.handle.net/10400.1/8411 (10400.1/8411)

Mulligan, K. A., & Cheyette, B. N. R. (2012). Wnt Signaling in Vertebrate Neural Development and Function. *Journal of Neuroimmune Pharmacology, 7*(4), 774-787. doi: 10.1007/s11481-012-9404-x

Mullin, S., & Schapira, A. (2015). The genetics of Parkinson's disease. *British Medical Bulletin, 114*(1), 39-52. doi: 10.1093/bmb/ldv022

Murray, J. T., Campbell, D. G., Morrice, N., Auld, G. C., Shpiro, N., Marquez, R., . . . Cohen, P. (2004). Exploitation of KESTREL to identify NDRG family members as physiological substrates for SGK1 and GSK3. *Biochemical Journal, 384*(3), 477-488. doi: 10.1042/bj20041057

Nagral, A. (2014). Gaucher Disease. *Journal of Clinical and Experimental Hepatology, 4*(1), 37-50. doi: 10.1016/j.jceh.2014.02.005

Nalysnyk, L., Rotella, P., Simeone, J. C., Hamed, A., & Weinreb, N. (2017). Gaucher disease epidemiology and natural history: a comprehensive review of the literature. *Hematology, 22*(2), 65-73. doi: 10.1080/10245332.2016.1240391

Norris, E. H., Giasson, B. I., & Lee, V. M. Y. (2004). α-Synuclein: Normal Function and Role in Neurodegenerative Diseases *Current Topics in Developmental Biology* (Vol. 60, pp. 17-54): Academic Press.

Okabe, S., Forsberg-Nilsson, K., Spiro, A. C., Segal, M., & McKay, R. D. G. (1996). Development of neuronal precursor cells and functional postmitotic neurons from embryonic stem cells in vitro. *Mechanisms of Development, 59*(1), 89-102. doi: https://doi.org/10.1016/0925-4773(96)00572-2

Pandey, M. K., Burrow, T. A., Rani, R., Martin, L. J., Witte, D., Setchell, K. D., . . . Grabowski, G. A. (2017). Complement drives glucosylceramide accumulation and tissue inflammation in Gaucher disease. *Nature, 543*(7643), 108. doi: 10.1038/nature21368

Pandey, M. K., & Grabowski, G. A. (2013). Immunological cells and functions in Gaucher disease. *Critical reviews in oncogenesis, 18*(3), 197-220.

Pandey, M. K., Rani, R., Zhang, W., Setchell, K., & Grabowski, G. A. (2012). Immunological cell type characterization and Th1–Th17 cytokine production in a mouse model of Gaucher disease. *Molecular Genetics and Metabolism, 106*(3), 310-322. doi: 10.1016/j.ymgme.2012.04.020

Panicker, L. M., Miller, D., Park, T., Patel, B., Azevedo, J. L., Awad, O., . . . Feldman, R. A. (2012). Induced pluripotent stem cell model recapitulates pathologic hallmarks of Gaucher disease. *Proceedings of the National Academy of Sciences, 109*(44), 18054-18059. doi: 10.1073/pnas.1207889109

Parenti, G., Andria, G., & Valenzano, K. J. (2015). Pharmacological Chaperone Therapy: Preclinical Development, Clinical Translation, and Prospects for the Treatment of Lysosomal Storage Disorders. *Molecular Therapy, 23*(7), 1138-1148. doi: 10.1038/mt.2015.62

Parihar, M. S., Parihar, A., Fujita, M., Hashimoto, M., & Ghafourifar, P. (2008). Mitochondrial association of alpha-synuclein causes oxidative stress. *Cellular and Molecular Life Sciences, 65*(7), 1272-1284. doi: 10.1007/s00018-008-7589-1

Patani, R., Compston, A., Puddifoot, C. A., Wyllie, D. J. A., Hardingham, G. E., Allen, N. D., & Chandran, S. (2009). Activin/Nodal Inhibition Alone Accelerates Highly Efficient Neural Conversion from Human Embryonic Stem Cells and Imposes a Caudal Positional Identity. *PLOS ONE, 4*(10), e7327. doi: 10.1371/journal.pone.0007327

Patel, D., & Witt, S. N. (2018). Sorting Out the Role of α-Synuclein in Retromer-Mediated Endosomal Protein Sorting. *Journal of Experimental Neuroscience, 12*, 1179069518796215. doi: 10.1177/1179069518796215

Patnaik, S., Zheng, W., Choi, J. H., Motabar, O., Southall, N., Westbroek, W., . . . Marugan, J. J. (2012). Discovery, Structure–Activity Relationship, and Biological Evaluation of Noninhibitory Small Molecule Chaperones of Glucocerebrosidase. *Journal of Medicinal Chemistry, 55*(12), 5734-5748. doi: 10.1021/jm300063b

Perrier, A. L., Tabar, V., Barberi, T., Rubio, M. E., Bruses, J., Topf, N., . . . Studer, L. (2004). Derivation of midbrain dopamine neurons from human embryonic stem cells. *Proceedings of the National Academy of Sciences, 101*(34), 12543-12548. doi: 10.1073/pnas.0404700101

Platt, F. M., & Jeyakumar, M. (2008). Substrate reduction therapy. *Acta Paediatrica, 97*(s457), 88-93. doi: 10.1111/j.1651-2227.2008.00656.x

Poewe, W., Seppi, K., Tanner, C. M., Halliday, G. M., Brundin, P., Volkmann, J., . . . Lang, A. E. (2017). Parkinson disease. *Nature Reviews Disease Primers, 3*, 17013. doi: 10.1038/nrdp.2017.13

R Kornfeld, a., & Kornfeld, S. (1985). Assembly of Asparagine-Linked Oligosaccharides. *Annual Review of Biochemistry, 54*(1), 631-664. doi: 10.1146/annurev.bi.54.070185.003215

Radin, N. S. (1996). Treatment of Gaucher disease with an enzyme inhibitor. *Glycoconjugate Journal, 13*(2), 153-157. doi: 10.1007/BF00731489

Rao Vunnam, R., & Radin, N. S. (1980). Analogs of ceramide that inhibit glucocerebroside synthetase in mouse brain. *Chemistry and Physics of Lipids, 26*(3), 265-278. doi: https://doi.org/10.1016/0009-3084(80)90057-2

Reczek, D., Schwake, M., Schröder, J., Hughes, H., Blanz, J., Jin, X., . . . Saftig, P. (2007). LIMP-2 Is a Receptor for Lysosomal Mannose-6-Phosphate-Independent Targeting of β-Glucocerebrosidase. *Cell, 131*(4), 770-783. doi: 10.1016/j.cell.2007.10.018

Reeve, A., Simcox, E., & Turnbull, D. (2014). Ageing and Parkinson's disease: Why is advancing age the biggest risk factor? *Ageing Research Reviews, 14*, 19-30. doi: 10.1016/j.arr.2014.01.004

Romero, R., Ramanathan, A., Yuen, T., Bhowmik, D., Mathew, M., Munshi, L. B., . . . Zaidi, M. (2019). Mechanism of glucocerebrosidase activation and dysfunction in Gaucher disease unraveled by molecular dynamics and deep learning. *Proceedings of the National Academy of Sciences, 116*(11), 5086-5095. doi: 10.1073/pnas.1818411116

Ron, I., & Horowitz, M. (2005). ER retention and degradation as the molecular basis underlying Gaucher disease heterogeneity. *Human Molecular Genetics, 14*(16), 2387-2398. doi: 10.1093/hmg/ddi240

Rosenbloom, B., Balwani, M., Bronstein, J. M., Kolodny, E., Sathe, S., Gwosdow, A. R., . . . Weinreb, N. J. (2011). The incidence of Parkinsonism in patients with type 1 Gaucher disease: Data from the ICGG Gaucher Registry. *Blood cells, molecules & diseases, 46*(1), 95-102. doi: 10.1016/j.bcmd.2010.10.006

Rostami, J., Holmqvist, S., Lindström, V., Sigvardson, J., Westermark, G. T., Ingelsson, M., . . . Erlandsson, A. (2017). Human Astrocytes Transfer Aggregated Alpha-Synuclein via Tunneling Nanotubes. *Journal of Neuroscience, 37*(49), 11835-11853. doi: 10.1523/JNEUROSCI.0983-17.2017

Santos, D., & Tiscornia, G. (2017). Induced Pluripotent Stem Cell Modeling of Gaucher's Disease: What Have We Learned? *International Journal of Molecular Sciences, 18*(4), 888. doi: 10.3390/ijms18040888

Sardi, S. P., Clarke, J., Kinnecom, C., Tamsett, T. J., Li, L., Stanek, L. M., . . . Shihabuddin, L. S. (2011). CNS expression of glucocerebrosidase corrects α-synuclein pathology and memory in a mouse model of Gaucher-related synucleinopathy. *Proceedings of the National Academy of Sciences of the United States of America, 108*(29), 12101-12106. doi: 10.1073/pnas.1108197108

Sato, C., Morgan, A., Lang, A. E., Salehi-Rad, S., Kawarai, T., Meng, Y., . . . Rogaeva, E. (2005). Analysis of the glucocerebrosidase gene in Parkinson's disease. *Movement Disorders, 20*(3), 367-370. doi: 10.1002/mds.20319

Schöndorf, D. C., Aureli, M., McAllister, F. E., Hindley, C. J., Mayer, F., Schmid, B., . . . Deleidi, M. (2014). iPSC-derived neurons from GBA1-associated Parkinson's disease patients show autophagic defects and impaired calcium homeostasis. *Nature Communications, 5*. doi: 10.1038/ncomms5028

Scudamore, O., & Ciossek, T. (2018). Increased Oxidative Stress Exacerbates α-Synuclein Aggregation In Vivo. *Journal of Neuropathology & Experimental Neurology*. doi: 10.1093/jnen/nly024

Shahmoradian, S. H., Genoud, C., Graff-Meyer, A., Hench, J., Moors, T., Schweighauser, G., . . . Lauer, M. E. (2017). Lewy pathology in Parkinson's disease consists of a crowded organellar membranous medley. *bioRxiv*. doi: 10.1101/137976

Shawky, R. M., & Elsayed, S. M. (2016). Treatment options for patients with Gaucher disease. *Egyptian Journal of Medical Human Genetics, 17*(3), 281-285. doi: 10.1016/j.ejmhg.2016.02.001

Shayman, J. A. (2010). Eliglustat tartrate: Glucosylceramide Synthase Inhibitor Treatment of Type 1 Gaucher Disease. *Drugs of the future, 35*(8), 613-620.

Sidransky, E. (2012). Gaucher Disease: Insights from a Rare Mendelian Disorder. *Discovery medicine, 14*(77), 273-281.

Sidransky, E., & Hart, P. S. (2012). Penetrance of PD in Glucocerebrosidase Gene Mutation Carriers. *Neurology, 79*(1), 106-107. doi: 10.1212/01.wnl.0000416261.29035.4c

Sidransky, E., & Lopez, G. (2012). The link between the GBA gene and parkinsonism. *The Lancet. Neurology, 11*(11), 986-998. doi: 10.1016/S1474-4422(12)70190-4

Siebert, M., Sidransky, E., & Westbroek, W. (2014). Glucocerebrosidase is shaking up the synucleinopathies. *Brain, 137*(5), 1304-1322. doi: 10.1093/brain/awu002

Sklerov, M., Kang, U. J., Liong, C., Clark, L., Marder, K., Pauciulo, M., . . . Alcalay, R. N. (2017). Frequency of GBA Variants in Autopsy-proven Multiple System Atrophy. *Movement Disorders Clinical Practice, 4*(4), 574-581. doi: 10.1002/mdc3.12481

Smith, L., Mullin, S., & Schapira, A. (2017). Insights into the structural biology of Gaucher disease. *Experimental Neurology, 298*, 180-190. doi: 10.1016/j.expneurol.2017.09.010

Sorge, J., West, C., Westwood, B., & Beutler, E. (1985). Molecular cloning and nucleotide sequence of human glucocerebrosidase cDNA. *Proceedings of the National Academy of Sciences of the United States of America, 82*(21), 7289-7293.

Stojkovska, I., Krainc, D., & Mazzulli, J. R. (2018). Molecular mechanisms of α-synuclein and GBA1 in Parkinson's disease. *Cell and Tissue Research, 373*(1), 51-60. doi: 10.1007/s00441-017-2704-y

Straniero, L., Rimoldi, V., Samarani, M., Goldwurm, S., Fonzo, A., Krüger, R., . . . Asselta, R. (2017). The GBAP1 pseudogene acts as a ceRNA for the glucocerebrosidase gene GBA by sponging miR-22-3p. *Scientific Reports, 7*(1), 12702. doi: 10.1038/s41598-017-12973-5

Sun, Y., Florer, J., Mayhew, C. N., Jia, Z., Zhao, Z., Xu, K., . . . Grabowski, G. A. (2015). Properties of Neurons Derived from Induced Pluripotent Stem Cells of Gaucher Disease Type 2 Patient Fibroblasts: Potential Role in Neuropathology. *PLOS ONE, 10*(3). doi: 10.1371/journal.pone.0118771

Sun, Y., Ran, H., Liou, B., Quinn, B., Zamzow, M., Zhang, W., . . . Grabowski, G. A. (2011). Isofagomine In Vivo Effects in a Neuronopathic Gaucher Disease Mouse. *PLOS ONE, 6*(4). doi: 10.1371/journal.pone.0019037

Surmacz, B., Fox, H., Gutteridge, A., Lubitz, S., & Whiting, P. (2012). Directing Differentiation of Human Embryonic Stem Cells Toward Anterior Neural Ectoderm Using Small Molecules. *STEM CELLS, 30*(9), 1875-1884. doi: 10.1002/stem.1166

Takahashi, K., Tanabe, K., Ohnuki, M., Narita, M., Ichisaka, T., Tomoda, K., & Yamanaka, S. (2007). Induction of Pluripotent Stem Cells from Adult Human Fibroblasts by Defined Factors. *Cell, 131*(5), 861-872. doi: 10.1016/j.cell.2007.11.019

Takahashi, K., & Yamanaka, S. (2006). Induction of Pluripotent Stem Cells from Mouse Embryonic and Adult Fibroblast Cultures by Defined Factors. *Cell, 126*(4), 663-676. doi: http://dx.doi.org/10.1016/j.cell.2006.07.024

Tantawy, A. (2015). Cytokines in Gaucher disease: Role in the pathogenesis of bone and pulmonary disease. *Egyptian Journal of Medical Human Genetics, 16*(3), 207-213. doi: 10.1016/j.ejmhg.2015.02.001

Tenreiro, S., Rosado-Ramos, R., Gerhardt, E., Favretto, F., Magalhães, F., Popova, B., . . . Outeiro, T. (2016). Yeast reveals similar molecular mechanisms underlying alpha- and beta-synuclein toxicity. *Human Molecular Genetics, 25*(2), 275-290. doi: 10.1093/hmg/ddv470

Tiscornia, G., Singer, O., & Verma, I. M. (2006). Production and purification of lentiviral vectors. *Nature Protocols, 1*(1), 241-245. doi: 10.1038/nprot.2006.37

Tiscornia, G., Vivas, E., & Belmonte, J. (2011). Diseases in a dish: modeling human genetic disorders using induced pluripotent cells. *Nature medicine*, 1570-1576. doi: 10.1038/nm.2504

Tiscornia, G., Vivas, E., Matalonga, L., Berniakovich, I., Monasterio, M., Eguizábal, C., . . . Belmonte, J. (2013). Neuronopathic Gaucher's disease: induced pluripotent stem cells for disease modelling and testing chaperone activity of small compounds. *Human Molecular Genetics, 22*(4), 633-645. doi: 10.1093/hmg/dds471

Toft, M., Pielsticker, L., Ross, O. A., Aasly, J. O., & Farrer, M. J. (2006). Glucocerebrosidase gene mutations and Parkinson disease in the Norwegian population. *Neurology, 66*(3), 415-417. doi: 10.1212/01.wnl.0000196492.80676.7c

Torralba, M. A., Olivera, S., Bureo, J. C., Dalmau, J., Nuñez, R., León, P., & Villarrubia, J. (2016). Residual enzymatic activity as a prognostic factor in patients with Gaucher disease type 1: correlation with Zimran and GAUSS-I index and the severity of bone disease. *QJM: An International Journal of Medicine, 109*(7), 449-452. doi: 10.1093/qjmed/hcw002

Torrent, R., De Angelis Rigotti, F., Dell, #039, Era, P., Memo, M., . . . Consiglio, A. (2015). Using iPS Cells toward the Understanding of Parkinson's Disease. *Journal of Clinical Medicine, 4*(4), 548.

Tosatto, L., Andrighetti, A. O., Plotegher, N., Antonini, V., Tessari, I., Ricci, L., . . . Dalla Serra, M. (2012). Alpha-synuclein pore forming activity upon membrane association. *Biochimica et Biophysica Acta (BBA) - Biomembranes, 1818*(11), 2876-2883. doi: https://doi.org/10.1016/j.bbamem.2012.07.007

Trapero, A., González-Bulnes, P., Butters, T. D., & Llebaria, A. (2012). Potent Aminocyclitol Glucocerebrosidase Inhibitors are Subnanomolar Pharmacological Chaperones for Treating Gaucher Disease. *Journal of Medicinal Chemistry, 55*(9), 4479-4488. doi: 10.1021/jm300342q

Tsigelny, I. F., Sharikov, Y., Wrasidlo, W., Gonzalez, T., Desplats, P. A., Crews, L., . . . Masliah, E. (2012). Role of α-synuclein penetration into the membrane in the mechanisms of oligomer pore formation. *FEBS Journal, 279*(6), 1000-1013. doi: 10.1111/j.1742-4658.2012.08489.x

Vitner, E. B., Dekel, H., Zigdon, H., Shachar, T., Farfel-Becker, T., Eilam, R., . . . Futerman, A. H. (2010). Altered expression and distribution of cathepsins in neuronopathic forms of Gaucher disease and in other sphingolipidoses. *Human Molecular Genetics, 19*(18), 3583-3590. doi: 10.1093/hmg/ddq273

Vitner, E. B., Farfel-Becker, T., Eilam, R., Biton, I., & Futerman, A. H. (2012). Contribution of brain inflammation to neuronal cell death in neuronopathic forms of Gaucher's disease. *Brain, 135*(6), 1724-1735. doi: 10.1093/brain/aws095

Vitner, E. B., Salomon, R., Farfel-Becker, T., Meshcheriakova, A., Ali, M., Klein, A. D., . . . Futerman, A. H. (2014). RIPK3 as a potential therapeutic target for Gaucher´s disease. *Nature medicine, 20*, 204. doi: 10.1038/nm.3449

Watson, C. L., Mahe, M. M., Múnera, J., Howell, J. C., Sundaram, N., Poling, H. M., . . . Helmrath, M. A. (2014). An in vivo model of human small intestine using pluripotent stem cells. *Nature medicine, 20*(11), 1310-1314. doi: 10.1038/nm.3737

Weil, R., Lashley, T., Bras, J., Schrag, A., & Schott, J. (2017). Current concepts and controversies in the pathogenesis of Parkinson?s disease dementia and Dementia with Lewy Bodies [version 1; referees: 2 approved]. *F1000Research, 6*(1604). doi: 10.12688/f1000research.11725.1

Wenstrup, R. J., Roca-Espiau, M., Weinreb, N. J., & Bembi, B. (2002). Skeletal aspects of Gaucher disease: a review. *The British Journal of Radiology, 75*(suppl_1), A2-A12. doi: 10.1259/bjr.75.suppl_1.750002

Westbroek, W., Gustafson, A., & Sidransky, E. (2011). Exploring the link between glucocerebrosidase mutations and parkinsonism. *Trends in Molecular Medicine, 17*(9), 485-493. doi: 10.1016/j.molmed.2011.05.003

White, G. E., Iqbal, A. J., & Greaves, D. R. (2012). CC Chemokine Receptors and Chronic Inflammation--Therapeutic Opportunities and Pharmacological Challenges. *Pharmacological Reviews, 65*(1), 47-89. doi: 10.1124/pr.111.005074

Willemsen, R., Tybulewicz, V., Sidransky, E., Eliason, W. K., Martin, B. M., LaMarca, M. E., . . . Ginns, E. I. (1995). A biochemical and ultrastructural evaluation of the type 2 Gaucher mouse. *Molecular and Chemical Neuropathology, 24*(2), 179. doi: 10.1007/bf02962142

Woo, S.-M., Kim, J., Han, H.-W., Chae, J.-I., Son, M.-Y., Cho, S., . . . Kang, Y.-K. (2009). Notch signaling is required for maintaining stem-cell features of neuroprogenitor cells derived from human embryonic stem cells. *BMC neuroscience, 10*, 97-97. doi: 10.1186/1471-2202-10-97

Wu, Z., Zhang, W., Chen, G., Cheng, L., Liao, J., Jia, N., . . . Xiao, L. (2008). Combinatorial Signals of Activin/Nodal and Bone Morphogenic Protein Regulate the Early Lineage Segregation of Human Embryonic Stem Cells. *Journal of Biological Chemistry, 283*(36), 24991-25002. doi: 10.1074/jbc.M803893200

Xiao, L., Yuan, X., & Sharkis, S. J. (2006). Activin A Maintains Self-Renewal and Regulates Fibroblast Growth Factor, Wnt, and Bone Morphogenic Protein Pathways in Human Embryonic Stem Cells. *STEM CELLS, 24*(6), 1476-1486. doi: 10.1634/stemcells.2005-0299

Xu, X.-h., & Zhong, Z. (2013). Disease modeling and drug screening for neurological diseases using human induced pluripotent stem cells. *Acta Pharmacologica Sinica, 34*(6). doi: 10.1038/aps.2013.63

Yang, N.-Y., Lee, Y.-N., Lee, H.-J., Kim, Y., & Lee, S.-J. (2013). Glucocerebrosidase, a new player changing the old rules in Lewy body diseases. *Biological Chemistry, 394*(7), 807-818. doi: 10.1515/hsz-2012-0322

Yap, T., Jiang, Z., Heinrich, F., Gruschus, J. M., Pfefferkorn, C. M., Barros, M., . . . Lee, J. C. (2015). Structural Features of Membrane-bound Glucocerebrosidase and α-Synuclein Probed by Neutron Reflectometry and Fluorescence Spectroscopy. *Journal of Biological Chemistry, 290*(2), 744-754. doi: 10.1074/jbc.M114.610584

Yap, T., Velayati, A., Sidransky, E., & Lee, J. C. (2013). Membrane-bound α-synuclein interacts with glucocerebrosidase and inhibits enzyme activity. *Molecular Genetics and Metabolism, 108*(1), 56-64. doi: 10.1016/j.ymgme.2012.11.010

Yap, T. L., Gruschus, J. M., Velayati, A., Westbroek, W., Goldin, E., Moaven, N., . . . Lee, J. C. (2011). Alpha-synuclein interacts with Glucocerebrosidase providing a molecular link between Parkinson and Gaucher diseases. *The Journal of biological chemistry, 286*(32), 28080-28088. doi: 10.1074/jbc.M111.237859

Ysselstein, D., Joshi, M., Mishra, V., Griggs, A. M., Asiago, J. M., McCabe, G. P., . . . Rochet, J.-C. (2015). Effects of impaired membrane interactions on α-synuclein aggregation and neurotoxicity. *Neurobiology of Disease, 79*, 150-163. doi: 10.1016/j.nbd.2015.04.007

Zaltieri, M., Grigoletto, J., Longhena, F., Navarria, L., Favero, G., Castrezzati, S., . . . Bellucci, A. (2015). α-synuclein and synapsin III cooperatively regulate synaptic function in dopamine neurons. *Journal of Cell Science, 128*(13), 2231-2243. doi: 10.1242/jcs.157867

Zeng, X.-S., Geng, W.-S., Jia, J.-J., Chen, L., & Zhang, P.-P. (2018). Cellular and Molecular Basis of Neurodegeneration in Parkinson Disease. *Frontiers in Aging Neuroscience, 10*(109). doi: 10.3389/fnagi.2018.00109

Zhang, S.-C., Wernig, M., Duncan, I. D., Brüstle, O., & Thomson, J. A. (2001). In vitro differentiation of transplantable neural precursors from human embryonic stem cells. *Nature Biotechnology, 19*, 1129. doi: 10.1038/nbt1201-1129

Zhao, Y., Ren, J., Padilla-Parra, S., Fry, E. E., & Stuart, D. I. (2014). Lysosome sorting of β-glucocerebrosidase by LIMP-2 is targeted by the mannose 6-phosphate receptor. *Nature Communications, 5*. doi: 10.1038/ncomms5321

Zhou, J., Su, P., Li, D., Tsang, S., Duan, E., & Wang, F. (2010). High-Efficiency Induction of Neural Conversion in Human ESCs and Human Induced Pluripotent Stem Cells with a Single Chemical Inhibitor of Transforming Growth Factor Beta Superfamily Receptors. *STEM CELLS, 28*(10), 1741-1750. doi: 10.1002/stem.504